U.S. Department
of Transportation
National Highway
Traffic Safety
Administration

www.nhtsa.gov

DOT HS 811 816 October 2013

Post-Crash Hydrogen Leakage Limits and Fire Safety Research

DISCLAIMER

Technical Report Documentation Page

1. Report No.	2. Government Accession No.	3. Recipient's Catalog No.
DOT HS 811 816		

4. Title and Subtitle Post-Crash Hydrogen Leakage Limits and Fire Safety Research	5. Report Date October 2013
	6. Performing Organization
7. Author(s) Reuther, J. J., John, J. S., Shawcross, P. E., Kimmel, G.	8. Performing Organization
9. Performing Organization Name and Address Battelle Memorial Institute 505 King Avenue Columbus, OH 43201	10. Work Unit No. (TRAIS)
	11. Contract or Grant No. DTNH22-08-D-00080
12. Sponsoring Agency Name and Address National Highway Traffic Safety Administration Office of Vehicle Crashworthiness Research 1200 New Jersey Avenue, SE Washington, DC 20590	13. Type of Report and Period Final Report
	14. Sponsoring Agency Code

15. Supplementary Notes

Barbara Hennessey was the Contracting Officer's Technical Representative (COTR) for this project.

16. Abstract

Federal Motor Vehicle Safety Standards (FMVSS) for fuel system integrity set limits for fuel spillage during and after crashes to reduce the occurrence of deaths and injuries from fire. FMVSS 301 and 303 respectively specify post-crash limits for liquid fuels and compressed natural gas (CNG). These limits have been used as a benchmark for setting leakage limits for hydrogen, based on energy equivalence, in industry standards and proposed or enacted international regulations. However the properties of hydrogen with regard to leak behavior and combustion are very different from those of liquid fuels or CNG. Gasoline will pool and dissipate slowly. CNG and hydrogen will rise and dissipate more rapidly. Hydrogen has a much wider range of flammability in air than most fuels, including CNG: 4% to 75% for hydrogen versus 5% to 15% for CNG. Therefore, a research program was developed and executed to assess the safety of the proposed allowable leak rate for hydrogen, through leak and ignition experiments in and around vehicles and vehicle compartment simulators.

17. Key Words	18. Distribution Statement
Hydrogen safety, fuel cell vehicle, fuel system integrity, alternative fuels	Document is available to the public from the National Technical Information Service www.ntis.gov

19. Security Classif. (of this report)	20. Security Classif. (of this page)	21. No. of Pages	22. Price
Unclassified		160	

Form DOT F 1700.7 (8-72) Reproduction of completed page authorized

EXECUTIVE SUMMARY

The objective of Task Order 3 was to conduct research on the fire safety of hydrogen leakage limits proposed by the Society of Automotive Engineers (SAE J2578, 2008), including calculations and experimental verification. The result is this report, *Post-Crash Hydrogen Leakage Limits and Fire Safety Research*. This assessment supports safety policy objectives to adopt post-crash pass/fail leakage criteria for hydrogen-powered motor vehicles. This research reviews the safety of hydrogen fuel system leak rates to the accumulation of ignitable mixtures of hydrogen in enclosed trunk, passenger, and engine compartments.

The three tasks completed as part of Task Order 3 are:

Task 2a: Leak Rate vs. Hydrogen Concentration Tests on Intact Automobile;
Task 2b: Ignition and Combustion Tests on Simulated Automobile Compartments; and
Task 2c: Full-Scale Leak, Ignition, and Fire Tests on Intact and Crashed Automobiles.

In Task 2a, a series of tests were conducted in which hydrogen concentration data was recorded in different vehicle compartments to determine the effect of leak rate on the creation of worst-case conditions, defined as stoichiometric hydrogen in air (~30%). Hydrogen flow originated from specific locations directly into or underneath the vehicle. Hydrogen leak rates were varied between 59 and 239 liters per minute (lpm), corresponding to half or double the energy equivalent of leakage limits specified in Federal Motor Vehicle Safety Standard (FMVSS) 301 for liquid fuels and FMVSS 303 for compressed natural gas (CNG). Test duration was not to exceed one hour, the maximum time required from FMVSS 303, or until hydrogen concentration essentially achieved steady-state conditions. Several other tests were conducted to measure the decay rate of hydrogen concentration inside the vehicle after the leak had ceased. The work performed and results produced under Task 2a comprise Volume I of this Final Report.

In Task 2b, a series of tests measured the heat flux and overpressure created upon ignition and combustion of flammable levels of hydrogen accumulating in trunk and passenger compartments following plausible leak rates from a post-crash hydrogen fuel system. The objective was to quantify hydrogen combustion effects and to relate them to predictions on the extent of personal injury. These tests were conducted in an automobile compartment simulator (ACS) that reconstructed the volumes of the trunk, rear, and front passenger compartments of the 2008 Mitsubishi Lancer used as a test vehicle in Task 2a. The ACS allowed multiple ignition tests to be conducted on the same system in a relatively short period of time via the use of replaceable compartment panels. The work performed and results produced under Task 2b comprise Volume II of this Final Report.

In Task 2c, a series of tests were conducted to quantify the effects of crash damage on hydrogen accumulation and hydrogen combustion characteristics for three leak parameters (location, rate, and duration); relate them to the extent of personal injury (physical trauma and burns); and assess the establishment of a minimum allowable post-crash hydrogen leak rate. Task 2c tests were conducted on four vehicles: intact and front-impact-damaged 2008 Mitsubishi Lancers; a side-impact-damaged 2009 Mazda6 Sedan; and a rear-impact-damaged 2008 Ford Taurus. The work performed and results produced under Task 2c comprise Volume III of this Final Report.

Altogether, 88 tests were conducted in Tasks 2a, 2b, and 2c. Task 2a consisted of 15 tests: 14 were hydrogen accumulation tests with an intact vehicle and 1 was a sensor response test. Task 2b consisted of 19 tests with the ACS: 11 were hydrogen accumulation tests and 8 were ignition tests. Task 2c consisted of 54 tests with intact, front-impact-damaged, side-impact-damaged, and rear-impact damaged vehicles. Of the 54 tests, 39 were on accumulation, 8 on ignition, and 7 on the measurement of sensor response time.

With regard to achieving the objective of determining a *minimum allowable* *post-crash leak rate*, tests indicated that leak rate is not a defining metric. Instead, the critical information was whether hydrogen, if allowed to leak into a car compartment, could accumulate anywhere *locally* to ~5 percent, just above the lower flammability limit of hydrogen (~4%). Tests indicated that flammable concentrations of hydrogen could accumulate in different locations within passenger compartments, either at low leak rates after long times or at high leak rates after short times.

Ignition effects varied in terms of peak thermal flux, overpressure, and internal vehicular damage. Aftereffects ranged from window fogging (condensation from hydrogen combustion) to structural damage (deformation of doors and broken windows) to second-degree burns and 50 percent eardrum rupture.

One additional significant finding was a propensity for secondary fire after sparking and hydrogen ignition, which was replicated. These secondary fires, which consumed flammable material inside the vehicles, occurred in the intact and in front-impact and side-impact cars. The origin of these secondary fires, which erupted within minutes after initial sparking and severely damaged the vehicles, appeared to be combustible material inside the trunk (spare tire) or cabin (headliner).

Significant overall observations and recommendations from Task 2c tests were as follows:

- All accumulation of hydrogen should be avoided in passenger compartments.
- More than one sensor in various locations is needed for passenger-alarm purposes.
- Vehicle devices that vent passenger compartments upon impact may be warranted.
- New flammability tests on fabrics exposed to hydrogen (not air) have merit.
- On-board vehicle fire-suppression systems could be revisited.

Table of Contents

Page

List of Appendices

Table of Contents (Cont.)

Page

List of Tables

Table of Contents (Cont.)

Page

List of Figures

Table of Contents (Cont.)

Page

List of Figures (Cont.)

Table of Contents (Cont.)

Page

List of Figures (Cont.)

Table of Contents (Cont.)

Page

List of Figures (Cont.)

Table of Contents (Cont.)

Page

List of Figures (Cont.)

INTRODUCTION

To address safety requirements, the National Highway Traffic Safety Administration needs data and information to characterize and quantify hazards posed by post-crash hydrogen leakage to occupants, first responders, and the public.

The Society of Automotive Engineers (SAE) recommended practice for general fuel cell safety is rule SAE J2578 (2008), and is similar to Japanese fuel cell development regulations for post-crash fuel system integrity, specifically leakage interim limits. The suggested limits for hydrogen were associated with a 60-minute period following front-, side-, or rear-impact crash tests. These limits were based on the energy equivalence to leakage limits specified in Federal Motor Vehicle Safety Standard (FMVSS) 301 for liquid fuels and in FMVSS 303 for compressed natural gas (CNG).

However, the properties of hydrogen are different from these fuels and can pose a lesser or greater risk from post-crash fire. Gasoline pools and dissipates slowly. CNG, like hydrogen, is lighter than air and rises and dissipates. Hydrogen dissipates more rapidly than CNG when not confined and can enter into vehicle compartments more easily than liquid fuel vapors or CNG. Hydrogen also has a much wider range of flammability in air than most fuels, including CNG (4% to 75% for hydrogen versus 5% to 15% for CNG).

The objective of Task Order 3, *Post-Crash Hydrogen Leakage Limits and Fire Safety Research*, was to conduct tests on the veracity of proposed hydrogen leakage limits (SAE J2578, FMVSS 301, and FMVSS 303), including calculations and experimental verification. This assessment provides technical data that correlates hydrogen fuel system leak rates to the accumulation of ignitable mixtures of hydrogen in enclosed trunk, passenger, and engine compartments, and quantifies hydrogen combustion effects, including the potential for personal injury.

A total of 88 tests were conducted in Tasks 2a, 2b, and 2c. Task 2a consisted of 15 tests: 14 were accumulation tests with the intact vehicle, and 1 was a sensor response test. Task 2b consisted of 19 tests with the automobile compartment simulator (ACS): 11 were accumulation tests and 9 were ignition tests. Task 2c consisted of 54 tests with intact, front-impact, side-impact, and rear-impact vehicles. Of the 54 tests, 39 were on accumulation, 8 on ignition, and 7 on sensor response time. The overall matrix for tests on Task Order 3 Tasks 2a, 2b, and 2c is shown in Table 1.

Table 1. Test matrix for Task Order 3 Tasks 2a, 2b, and 2c.

Test #	Task #	Vehicle	Leakage Location	Leak Rate (lpm)	Test Type	Test Result
1	2a	Intact	Trunk	118	60 min accumulation	Ignitable H_2 levels detected.
2	2a	Intact	Under vehicle, up	118	60 min accumulation	Ignitable H_2 levels not detected.
3	2a	Intact	Under vehicle, 45^o forward	118	30 min accumulation	Ignitable H_2 levels not detected.
4	2a	Intact	Trunk	118	60 min duration	Ignitable H_2 levels detected.
5	2a	Intact	Passenger compartment	118	60 min accumulation	Ignitable H_2 levels detected.
6	2a	Intact	Under vehicle, down	118	60 min accumulation	Ignitable H_2 levels not detected.
7	2a	Intact	Under vehicle, 45^o rearward	118	30 min accumulation	Ignitable H_2 levels not detected.
8	2a	Intact	Under vehicle, up	58	30 min accumulation	Ignitable H_2 levels not detected.
9	2a	Intact	Under vehicle, up	239	60 min accumulation	Ignitable H_2 levels not detected.
10	2a	Intact	Under vehicle, up	118	60 min accumulation	Ignitable H_2 levels not detected.
11	2a	Intact	Trunk	58	60 min accumulation	Ignitable H_2 levels detected.
12	2a	Intact	Trunk	239	60 min accumulation	Ignitable H_2 levels detected.
13	2a	Intact	Passenger compartment	118	60 min accumulation	Ignitable H_2 levels detected.
14	2a	Intact	Under vehicle engine	239	60 min duration	Ignitable H_2 levels briefly detected at one engine sensor.
15	2a	···	···	···	Sensor response	All sensors responded.
16	2b	ACS	Trunk	118	10 min accumulation	Ignitable H_2 levels detected.
17	2b	ACS	Trunk	118	10 min accumulation	Ignitable H_2 levels detected.
18	2b	ACS	Trunk	118	37 min, 35 sec accumulation	Ignitable H_2 levels detected.
19	2b	ACS	Trunk	118	20 min accumulation	Ignitable H_2 levels detected.
20	2b	ACS	Trunk	118	15 min accumulation	Ignitable H_2 levels detected.
21	2b	ACS	Trunk	118	30 min accumulation	Ignitable H_2 levels detected.
22	2b	ACS	Passenger compartment	118	30 min accumulation	Ignitable H_2 levels detected.
23	2b	ACS	Passenger compartment	118	30 min accumulation	Ignitable H_2 levels detected.
24	2b	ACS	Passenger compartment	118	Ignition	Ignition; heat flux and overpressure data captured.

Table 1. Test matrix for Task Order 3 Tasks 2a, 2b, and 2c. (Cont.)

Test #	Task #	Vehicle	Leakage Location	Leak Rate (lpm)	Test Type	Test Result
25	2b	ACS	Passenger compartment	118	Ignition	Ignition; heat flux and overpressure data captured.
26	2b	ACS	Passenger compartment	118	Ignition	Ignition; heat flux and overpressure data captured.
27	2b	ACS	Passenger compartment	118	60 min accumulation	Ignitable H_2 levels detected.
28	2b	ACS	Passenger compartment	118	Ignition	Ignition; heat flux and overpressure data captured.
29	2b	ACS	Passenger compartment	118	Ignition	Ignition; heat flux and overpressure data captured.
30	2b	ACS	Trunk	118	60 min accumulation	Errant test.
31	2b	ACS	Trunk	118	30 min accumulation	Ignitable H_2 levels detected.
32	2b	ACS	Trunk	118	Ignition	Ignition; heat flux and overpressure data captured.
33	2b	ACS	Trunk	118	Ignition	Ignition; heat flux and overpressure data captured.
34	2b	ACS	Trunk	118	Ignition	Ignition; heat flux and overpressure data captured.
35	2c	Front-impact	Passenger compartment	118	60 min accumulation	Ignitable H_2 levels detected.
36	2c	Front-impact	Trunk	118	60 min accumulation	Ignitable H_2 levels detected.
37	2c	Front-impact	Trunk	59	60 min accumulation	Ignitable H_2 levels detected.
38	2c	Front-impact	Trunk	236	60 min accumulation	Ignitable H_2 levels detected.
39	2c	Front-impact	Passenger compartment	59	60 min accumulation	Ignitable H_2 levels detected.
40	2c	Front-impact	Passenger compartment	236	60 min accumulation	Ignitable H_2 levels detected.
41	2c	Front-impact	Passenger compartment	30	60 min accumulation	Ignitable H_2 levels detected.
42	2c	Front-impact	Trunk	30	60 min accumulation	Ignitable H_2 levels detected.
43	2c	Front-impact	Under vehicle, up	30	60 min accumulation	Ignitable H_2 levels not detected.
44	2c	Front-impact	Under vehicle, up	59	60 min accumulation	Ignitable H_2 levels not detected.
45	2c	Front-impact	Under vehicle, up	118	60 min accumulation	Ignitable H_2 levels not detected.

Table 1. Test matrix for Task Order 3 Tasks 2a, 2b, and 2c. (Cont.)

Test #	Task #	Vehicle	Leakage Location	Leak Rate (lpm)	Test Type	Test Result
46	2c	Front-impact	Under vehicle, up	236	60 min accumulation	Ignitable H_2 levels not detected.
47	2c	Rear-impact	Passenger compartment	118	60 min accumulation	Ignitable H_2 levels detected.
48	2c	Rear-impact	Passenger compartment	59	60 min accumulation	Ignitable H_2 levels detected.
49	2c	Rear-impact	Passenger compartment	30	60 min accumulation	Ignitable H_2 levels detected.
50	2c	Rear-impact	Under vehicle, up	30	60 min accumulation	Ignitable H_2 levels not detected.
51	2c	Rear-impact	Under vehicle, up	59	60 min accumulation	Ignitable H_2 levels not detected.
52	2c	Rear-impact	Under vehicle, up	118	60 min accumulation	Ignitable H_2 levels not detected.
53	2c	Rear-impact	Under vehicle, up	236	60 min accumulation	Ignitable H_2 levels not detected.
54	2c	Rear-impact	Passenger compartment	236	60 min accumulation	Ignitable H_2 levels detected.
55	2c	…	…	…	Sensor response	All sensors responded.
56	2c	Side-impact	Passenger compartment	118	60 min accumulation	Ignitable H_2 levels detected.
57	2c	Side-impact	Passenger compartment	59	60 min accumulation	Ignitable H_2 levels detected.
58	2c	Side-impact	Passenger compartment	30	60 min accumulation	Ignitable H_2 levels not detected.
59	2c	Side-impact	Trunk	59	60 min accumulation	Ignitable H_2 levels not detected.
60	2c	Side-impact	Trunk	30	60 min accumulation	Ignitable H_2 levels not detected.
61	2c	Side-impact	Under vehicle, up	30	60 min accumulation	Ignitable H_2 levels not detected.
62	2c	Side-impact	Under vehicle, up	118	60 min accumulation	Ignitable H_2 levels not detected.
63	2c	Side-impact	Under vehicle, up	236	60 min accumulation	Ignitable H_2 levels not detected.
64	2c	Side-impact	Trunk	236	60 min accumulation	Ignitable H_2 levels not detected.
65	2c	Side-impact	Trunk	118	60 min accumulation	Ignitable H_2 levels not detected.
66	2c	Side-impact	Passenger compartment	236	60 min accumulation	Ignitable H_2 levels detected.
67	2c	Side-impact	Under vehicle, up	59	60 min accumulation	Ignitable H_2 levels not detected.
68	2c	Front-impact	Trunk	118	Ignition; 1.5 min leak duration	Ignition and secondary fire; heat flux and overpressure data captured.
69	2c	”	…	…	Sensor response	All sensors responded.
70	2c	…	…	…	Sensor response	All sensors responded.
71	2c	…	…	…	Sensor response	All sensors responded.

Table 1. Test matrix for Task Order 3 Tasks 2a, 2b, and 2c. (Cont.)

Test #	Task #	Vehicle	Leakage Location	Leak Rate (lpm)	Test Type	Test Result
72	2c	Intact	Trunk	3	60 min accumulation followed by 30 min settling	Ignitable H_2 levels not detected.
73	2c	Intact	Trunk	3	60 min accumulation followed by 30 min settling	Ignitable H_2 levels not detected.
74	2c	Intact	Passenger compartment	3	60 min accumulation followed by 30 min settling	Ignitable H_2 levels not detected.
75	2c	Intact	Passenger compartment	3	60 min accumulation followed by 30 min settling	Ignitable H_2 levels not detected.
76	2c	...	...	...	Sensor response	All sensors responded.
77	2c	Intact	Trunk	3	60 min accumulation followed by 30 min settling	Ignitable H_2 levels not detected.
78	2c	Intact	Trunk	6	60 min accumulation followed by 30 min settling	Ignitable H_2 levels detected.
79	2c	Intact	Trunk	15	60 min accumulation followed by 30 min settling	Ignitable H_2 levels detected.
80	2c	...	...	...	Sensor response	All sensors responded.
81	2c	...	...	...	Sensor response	All sensors responded.
82	2c	Intact	Trunk	3	Ignition; 60 min leak duration	No ignition.
83	2c	Intact	Trunk	6	Ignition; 60 min leak duration	Ignition and secondary fire; heat flux and overpressure data captured.
84	2c	Rear-impact	Passenger compartment	6	Ignition; 60 min leak	No ignition.

Table 1. Test matrix for Task Order 3 Tasks 2a, 2b, and 2c. (Cont.)

Test #	Task #	Vehicle	Leakage Location	Leak Rate (lpm)	Test Type	Test Result
					duration	
85	2c	Rear-impact	Passenger compartment	12	Ignition; 60 min leak duration	No ignition.
86	2c	Rear-impact	Passenger compartment	24	Ignition; 60 min leak duration	Ignition; no secondary fire; heat flux and overpressure data captured.
87	2c	Rear-impact	Passenger compartment	48	Ignition; 60 min leak duration	Ignition, no secondary fire; heat flux and overpressure data captured.
88	2c	Side-impact	Trunk	60	Ignition; 60 min leak duration	Ignition and secondary fire; heat flux and overpressure data captured.

VOLUME I: TASK 2A

A series of tests was conducted in which hydrogen concentration data was recorded in different compartments within a vehicle to determine the effect of leak rate on the creation of worst-case conditions, defined as stoichiometric hydrogen, 30 percent in air. The flow of hydrogen originated from specific locations directly into or underneath the vehicle. Hydrogen leakage flowrates varied from 59 to 239 liters per minute (lpm), corresponding to half or double the energy equivalence to leakage limits specified in FMVSS 301 for liquid fuels and FMVSS 303 for CNG. The test duration was not to exceed one hour, the required time duration time in FMVSS 303, or until hydrogen concentrations essentially achieved steady-state conditions. Additionally, several tests were conducted to measure the decay rate of hydrogen concentration inside the vehicle after the leak had ceased.

Results are summarized in a series of graphs that show when hydrogen concentrations in the trunk, rear-passenger, front-passenger, and engine compartments are within the flammability range (4%-75%), with an emphasis on when the concentrations are in the near-stoichiometric range (28%-32%). This data will be used to assess the potential hazard posed to passengers in Tasks 2b and 2c of test and evaluation.

The data showed that leaks located underneath the vehicle did not significantly increase the concentration of hydrogen in any vehicle compartment. The sensor arrays located in the trunk, rear passenger, front passenger, and engine compartments consistently showed no appreciable accumulation of hydrogen. However, the same cannot be reported for leaks directly into the trunk or passenger compartments. In these scenarios, hydrogen concentrations achieved the stoichiometric regime for all the leakage rates tested. Under the pseudo standard leakage rate (118 lpm), a leak into the trunk compartment created hydrogen concentrations in the 50% to 60 percent range at the higher sensor positions. Sensors located at occupant waist-level measured around 30 percent. The same leak rate into the passenger compartment yielded steady-state hydrogen concentrations in the 40% to 50 percent range.

Decreasing the flowrate to 58 lpm did not render the leak less hazardous; on the contrary, at this flowrate the trunk compartment leak resulted in steady-state concentrations closer to 30 percent at all sensor locations inside the vehicle, establishing longer dwell times in the 30 percent regime. Increasing the flowrate to 239 lpm also did not assuage the danger of leaks in the trunk. Although at this flowrate, the hydrogen concentrations spent less time in the 30 percent regime; the final steady-state values were closer to 75 percent. At this level, asphyxiation becomes a serious concern. Similar results were observed for lower and higher rate leaks into the passenger compartment.

TASK SCOPE AND OBJECTIVE

This report explains the work performed and results developed under Task Order 3 Task 2a: Conduct Leak Rate Versus Hydrogen Concentration Tests on Intact Automobiles. The scope of Task 2a is the determination of the relationship between plausible leak rates from a post-crash hydrogen fuel system and the level of accumulation of hydrogen in the trunk, passenger, and engine compartments. The objective of Task 2a is to conduct a series of tests during which hydrogen is released purposely into and underneath a vehicle while measuring hydrogen concentration as a function of time at multiple in-vehicle locations. The resulting data is intended to show, for the conditions tested, when and where a potentially combustible mixture of hydrogen, 4 percent to 75 percent in air, is formed inside a vehicle compartment.

Automobile operating conditions would affect hydrogen accumulation directly, specifically vent fan speed (zero, slow, or fast) and window position (up or down), in the passenger compartment. Fan speed was selected to be zero (fans off). This speed was justified due to typical post-crash conditions in which electrical power is lost. The selected window position was closed and is supported by investigative evidence; in approximately 70 percent of crashes, windows are closed and intact. Having the windows closed promotes the accumulation of hydrogen in the passenger compartment. Specification of these variables, that affect how quickly and to what levels hydrogen accumulates, was biased toward creating a worst-case scenario.

The hydrogen leak rate used was 118 lpm, a benchmark derived in SAE J2578 by analogy from the energy equivalence of gasoline leakage in FMVSS 301. Subsequent tests used the traditional Bruceton "up-and-down method," wherein leak tests were conducted at half or double the reference flowrate. The intent was to determine the role of the flowrate in creating hazardous conditions. Perhaps certain rates resulted in safer (nonflammable) or lower-danger (~4-25% or ~50-75%) mixtures of hydrogen in air, corresponding to a slow burning flame which creates a low overpressure. The worst-case scenario would be when leaking and mixing produced a stoichiometric concentration of hydrogen (~30% hydrogen in air) uniformly throughout a compartment.

Hydrogen concentration data was recorded from the time the leak was initiated to either 60 min (the maximum time required for leak limits in FMVSS 303) or when a steady-state concentration of hydrogen was achieved. Additionally, after several leak tests, the concentration decay time for the hydrogen that remained in the vehicle was recorded. This decay time was essentially a function of how well hydrogen escaped through various routes out of the vehicle compartments.

TEST FACILITY, INSTRUMENTATION, AND HARDWARE

Test Facility. Tests were conducted at the Battelle High Energy Research Laboratory Area (HERLA) inside JS-10, a 42-ft diameter, steel-reinforced concrete, domed chamber capable of containing the blast from up to 50 lbs of TNT explosive or the equivalent energy of other flammable materials, including hydrogen and CNG. Conducting tests inside this large blast containment chamber precluded the influence of variable meteorological conditions, which could affect the dispersion and ignition properties of the hydrogen. Factors such as ventilation, temperature, and relative humidity were recorded during the testing (quiescent and within a controllable range). JS-10, shown in Figure I-1, is large enough to accommodate a vehicle and allows leak and ignition-fire tests to be conducted with flammable hydrogen-air mixtures.

Figure I-1. JS-10 blast chamber/dome used for indoor testing of leak rates with car.

Vehicle. The automobile employed for evaluation was a 2008 Mitsubishi Lancer C85603, Vehicle No. JA3AU16U08U036749, acquired by Battelle as "government-furnished equipment" (GFE).

Sensors. Two types of hydrogen sensors were used during testing. Neodym's Panterra hydrogen sensors can measure hydrogen concentrations from 0 to 100 percent and were positioned at 12 specific locations within the trunk, passenger, and engine compartments to monitor concentrations as a function of time. These sensors displayed a rise time, discussed in detail later, of approximately 1.5 sec and were configured with the sensing unit remote from the supporting electronics. A Panterra sensor also was placed on the ceiling of the blast chamber to monitor hydrogen accumulation and to assist in exhausting the chamber post-test.

Neodym HydroKnowz sensors equipped with alarms were the second type of sensor. These sensors were placed on the ceiling in the blast chamber and in the control room to monitor the presence of hydrogen during testing in order to safeguard against the accumulation of potentially dangerous (flammable) hydrogen in either location while personnel were present. These sensors have higher resolutions, but can measure only up to 4 percent hydrogen concentrations. The alarms were set to activate when hydrogen concentrations reached 1 percent (10,000 ppm) in air. Figure I-2 shows the two sensor types in their respective housings.

Figure I-2. Neodym Panterra (left) and HydroKnowz (right) sensors.

Sensor Locations. The test vehicle was instrumented with sensors to measure hydrogen concentration in its three main compartments, trunk, passenger, and engine. Each compartment contained a suite of hydrogen sensors:

- 3 in the trunk compartment;
- 3 in the rear of the passenger compartment;
- 3 in the front of the passenger compartment; and
- 3 sensors in the engine compartment.

Each compartment contained sensors positioned at 10 percent, 50 percent, and 90 percent of the vertical dimension. The sensor suites were located along the centerline of the vehicle, except in the engine compartment due to free space constraints. The sensor positions also were referenced to the leading edge of the front bumper subsequently referred to as the sensor reference point. The face of each sensor was oriented downward to aid in the detection of the rising hydrogen.

Trunk compartment sensors were located approximately 155 in. back from the sensor reference point, Figure I-3. Sensors were mounted along a vertical pole that extended from the trunk bottom inside surface to the top inside surface, covering a vertical dimension of approximately 32 in. This sensor array was positioned above the spare tire location.

Figure I-3. Positioning of trunk compartment sensor suite at 10 percent, 50 percent, and 90 percent heights.

The rear-passenger compartment sensors were mounted in a similar fashion, shown in Figure I-4, and were located approximately 122 in. from the vehicle sensor reference point. The height, approximately 37 in., was defined by the roof liner and the top center of the rear-passenger seat. This arrangement again shown some symmetry for concentration measurements, and approximately represented the locations of an occupant's waist, chest and head.

Figure I-4. Positioning of rear-passenger compartment sensor suite at 10 percent, 50 percent, and 90 percent heights.

The front passenger compartment sensors were placed approximately 90 in. back from the reference point. The sensors, shown in Figure I-5, were mounted on a pole placed in the front passenger cup-holder console and extended to the roof liner, approximately 34 in.

Figure I-5. Positioning of front passenger compartment sensor suite at 10 percent, 50 percent, and 90 percent heights.

The engine compartment sensors, shown in Figure I-6, were located approximately 44 in. back from the reference point, between the engine and firewall. Magnetic mounting bases with adjustable holders were used to mount sensors at 10 percent, 50 percent, and 90 percent of the total compartment height, approximately 26.5 in. These sensor faces were not vertically in-line with one another due to the free volume restrictions imposed by engine components, tubing, hoses, and fluid reservoirs. These components were left in place and the sensors were positioned around them, keeping potential hydrogen flow paths intact. As with the other suites, each sensor face was oriented downward to promote detection of the rising hydrogen.

Figure I-6. Positioning of engine compartment sensor suite at 10 percent, 50 percent, and 90 percent heights.

Hydrogen Leak Locations. The flow of hydrogen originated from specific locations directly into or underneath the vehicle. The maximum amount of hydrogen used in a single test was approximately 14,340 l (239 lpm for 1 hour). Hydrogen was monitored during seven leak scenarios. Two primary leak scenarios represent a damaged automobile where hydrogen leaks directly into the compartments:

- 1 leak fed directly into the trunk compartment (Figure I-7).

Figure I-7. Hydrogen leak originating in the trunk.

- 1 leak fed directly into the passenger compartment (Figure I-8).

Figure I-8. Hydrogen leak originating from the rear passenger compartment.

Injecting hydrogen directly into these compartments was done to create a *worst-case* scenario by providing the quickest, most direct means for hydrogen to accumulate to potentially combustible mixtures within these compartments.

Five secondary leak scenarios represented leaks originating from the fuel tank and system line underneath the automobile. Four locations were under the vehicle near its lengthwise midpoint along the centerline at an envisioned hydrogen tank position:

- 1 leak flowed straight up (Figure I-9).

Figure I-9. Hydrogen leak straight up from tank position underneath automobile.

- 1 leak flowed straight down (Figure I-10).

Figure I-10. Hydrogen leak straight down from tank position underneath automobile.

- 1 leak flowed at 45^{o} oriented forward (Figure I-11).

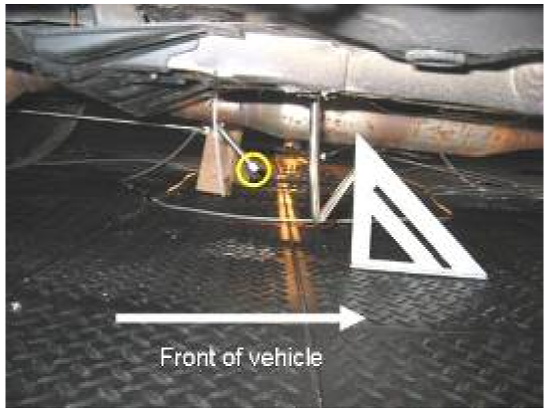

Figure I-11. Hydrogen leak 45° forward from tank position underneath automobile.

- 1 leak flowed at 45^{o} oriented rearwards (Figure I-12).

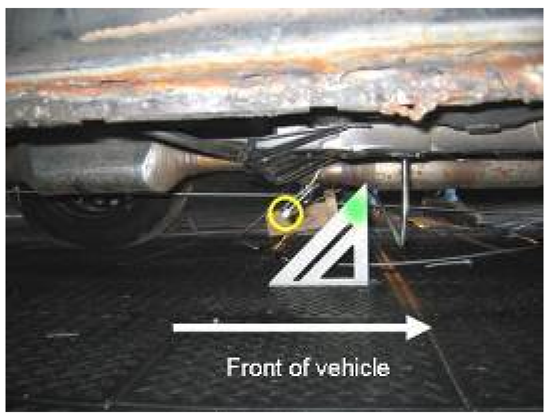

Figure I-12. Hydrogen leak 45° rearward from tank position underneath automobile.

The final position was near the automobile's firewall with an orientation set to maximize hydrogen flow into the engine compartment. This scenario was added to the test matrix because none of the other leakage locations resulted in significant hydrogen concentrations in the engine compartment.

- 1 leak flowed up forward of the firewall (Figure I-13).

Figure I-13. Hydrogen leak slightly forward at firewall position underneath automobile.

Cameras. Still photographs were employed to capture setup work involving the test vehicle preparation, sensor installation and alignment, venting system construction, data acquisition setup, and gas supply line integration. Photographs also were taken to document each test.

A standard video camera was used throughout the test period to capture any unexpected events, although none were encountered. This camera was placed in a sealed metal box inside the test chamber (Figure I-14). The sealed box contained a Lexan port in front of the camera lens to provide proper viewing of the test and also being able to protect the camera lens from damage in case accidental ignition of hydrogen occurred. The real-time feed from this camera was captured, monitored, and temporarily recorded using a television and a DVD recorder system located inside the control room.

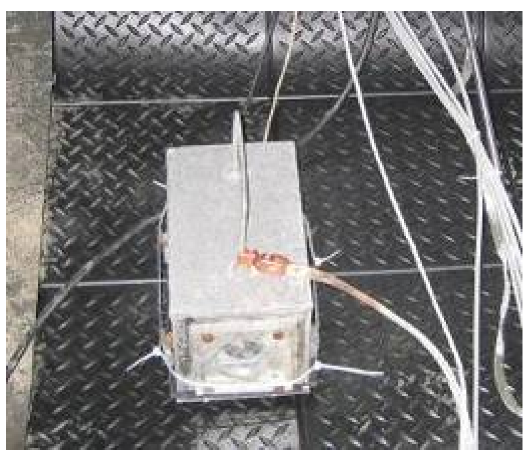

Figure I-14. Video camera armored box inside the blast chamber.

Results and Discussion

Test Matrix. Hydrogen concentration data were measured at each sensor location for a total of 12 sensor data sets per test. Hydrogen concentrations were monitored for 60 min unless a steady-state value was reached before this time limit. The test matrix for Task 2a is shown in Table I-1. Tests 1 and 2 used a flow diffuser attached to the hydrogen line. The purpose of this diffuser was to provide less turbulent introduction of the hydrogen to limit mixing of the gas with the surrounding air. The majority of tests were conducted without the diffuser, with the end of the tubing open, creating turbulence that would be similar to a sheared fuel line.

Table I-1. Test Matrix for Task 2a.

<table>
<tr><th colspan="2" rowspan="2">Leakage Location</th><th colspan="4">Flowrate
(lpm)</th><th rowspan="2">Duration
(min)</th></tr>
<tr><th>0</th><th>58</th><th>118</th><th>239</th></tr>
<tr><td colspan="2" rowspan="5">Trunk</td><td>--</td><td>--</td><td>Test 1*</td><td>--</td><td rowspan="9">60</td></tr>
<tr><td>Test 1 decay</td><td>--</td><td>--</td><td>--</td></tr>
<tr><td>--</td><td>--</td><td>Test 4</td><td>--</td></tr>
<tr><td>--</td><td>Test 11</td><td>--</td><td>--</td></tr>
<tr><td>--</td><td>--</td><td>--</td><td>Test 12</td></tr>
<tr><td colspan="2" rowspan="3">Passenger compartment</td><td>--</td><td>--</td><td>Test 5</td><td>--</td></tr>
<tr><td>Test 5 decay</td><td>--</td><td>--</td><td>--</td></tr>
<tr><td>--</td><td>--</td><td>Test 13</td><td>--</td></tr>
<tr><td rowspan="8">Under vehicle</td><td rowspan="4">Up</td><td>--</td><td>--</td><td>Test 2*</td><td>--</td></tr>
<tr><td>--</td><td>Test 8</td><td>--</td><td>--</td><td>30</td></tr>
<tr><td>--</td><td>--</td><td>Test 10</td><td>--</td><td rowspan="3">60</td></tr>
<tr><td>--</td><td>--</td><td>--</td><td>Test 9</td></tr>
<tr><td>down</td><td>--</td><td>--</td><td>Test 6</td><td>--</td></tr>
<tr><td>45^{o} forward</td><td>--</td><td>--</td><td>Test 3</td><td>--</td><td rowspan="2">30</td></tr>
<tr><td>45^{o} rearward</td><td>--</td><td>--</td><td>Test 7</td><td>--</td></tr>
<tr><td>engine</td><td>==</td><td>--</td><td>--</td><td>Test 14</td><td>60</td></tr>
</table>

* Test conducted with diffuser on end of tubing as opposed to tube being open-ended.

Data Recording and Analysis. As previously mentioned, hydrogen concentration data was recorded for three different leak rates at 12 positions in a 2008 Mitsubishi Lancer to determine the potential for creating combustible mixtures of hydrogen in air. Temporal and spatial hydrogen concentrations were graphed for both leak rate and decay tests. Concentrations versus time plots were created for each sensor in each test to present rise times and the steady-state levels. A series of visual, color-coded displays of hydrogen concentrations at 10 percent intervals, ranging from 0 to 100 percent, were generated for each test to elucidate when and where combustible mixtures of hydrogen and air occurred during testing and how long the concentrations were in the combustible regime (approximately 4% to 75% hydrogen in air).

The hydrogen concentration data are discussed for each sensor compartment (trunk, rear passenger, front passenger, and engine) for select leakage locations. The resulting data show that the leakage location dictated the extent hydrogen accumulated in the individual vehicle compartments. To this end, leakage locations directed into the individual compartments yielded the highest concentrations of hydrogen in the vehicle compartments and are discussed explicitly; the leaks originating from underneath the vehicle produced negligible vehicle compartment hydrogen concentrations and are discussed in more general terms.

Data comparing the effects of the leakage flowrate and the presence of the diffuser on the end of the hydrogen line also are presented and analyzed. Data demonstrating how quickly hydrogen leaks out of the vehicle after the leak is stopped also are presented in an effort to evaluate the approximate time when a vehicle can be considered safe to enter. Finally, data is presented that show when stoichiometric levels of hydrogen in air are reached in trunk, rear passenger, or front passenger compartments to assess how much time elapses before a *worst-case* scenario is reached.

On the following graphs, a yellow band is displayed from the 4 percent to the 75 percent level for the hydrogen concentrations. This band represents when the mixture is within the flammable range. A darker yellow band also is included on each graph, from 28 percent to 32 percent, to represent when the hydrogen mixtures are near or at the stoichiometric level.

Trunk Compartment Leak (Test 4) – 118 lpm Leakage Flowrate. Hydrogen concentrations for a leak directed into the trunk at a flowrate of 118 lpm and no diffuser are presented in Figure I-15. Shown are the concentrations passing through the 30 percent regime at all sensor levels in the trunk, rear-passenger, and front-passenger compartments, except at the front-passenger compartment 10 percent height sensor which reached steady-state just below this regime. The sensors placed in the engine did not see any appreciable amount of hydrogen accumulation. Furthermore, the hydrogen concentrations in all compartments, except for the engine, reach the lower flammability limit in a very short amount of time from when the leak starts and remains in the flammability range for the entire duration of the test.

This data shows that the trunk and passenger compartments are constructed such that the hydrogen/air mixture can flow from one compartment to the other. Only a slight difference in concentration rise times is evident from the trunk compartment to the passenger compartments. The engine sensors show that neither of these compartments allows significant flow of hydrogen/air mixture into the engine.

In examining the data more closely, the worst-case condition under this leakage flowrate and location appears to occur in the rear passenger compartment, at the 10 percent height sensor location. With respect to a passenger seated in this compartment, this sensor would be located at the waist or thigh level. At this location, the hydrogen concentration dwells the longest in the near- or at-stoichiometric range and reaches a steady-state concentration just above the 32 percent concentration level. Almost equally dangerous is the steady-state condition at the 10 percent front-passenger sensor. Although the hydrogen concentration never reaches the stoichiometric value, the steady-state concentration value at this sensor is just below 28 percent.

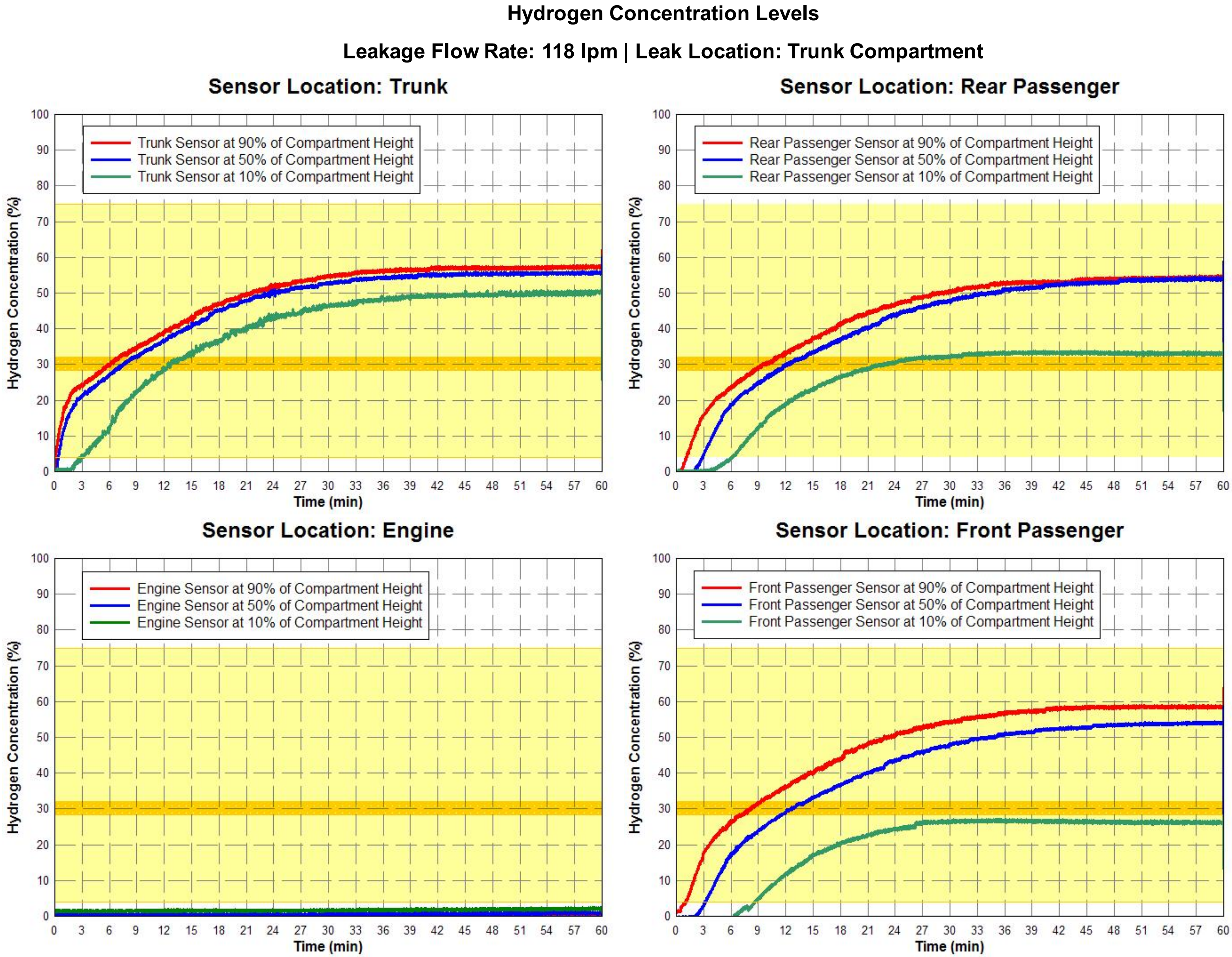

Figure I-15. Hydrogen concentration data for (clockwise from top left) trunk, rear-passenger, front-passenger, and engine compartments; 118 lpm flowrate directed into the trunk.

Table I-2 summarizes the amount of time in which a near-stoichiometric mixture (28%) is reached at each sensor location; how long the level remains near the stoichiometric value (28%–32% hydrogen concentration in air); and the steady-state concentration at each sensor. The data shows that the 28 percent concentration can be reached as early as 2 min from the start of the leak. In general, the 90 percent and 50 percent height sensors reach a final concentration between 50 percent and 60 percent, while the 10 percent height sensors tend to settle at values closer to the stoichiometric range.

Table I-2. Stoichiometric and steady-state hydrogen concentration data for the 118 lpm leakage flowrate originating from the vehicle trunk.

Sensor Location	Time (min) for Concentration to Reach 28% Percent	Length of Time (min) Spent in Stoichiometric Range (28%–32%)	Steady-state Hydrogen Concentration (%)
90% Trunk	4.7	2.2	57
50% Trunk	6.4	2.0	55
10% Trunk	11.6	2.5	50
90% Rear Passenger	8.2	2.5	54
50% Rear Passenger	10.8	2.9	54
10% Rear Passenger	19.4	6.9	33
90% Front Passenger	6.7	2.5	58
50% Front Passenger	11.2	2.9	54
10% Front Passenger	Does not reach 28%	---...	26

Passenger Compartment Leak (Test 5) – 118 lpm Leakage Flowrate. The next test involved locating the hydrogen leak in the back seat of the passenger compartment at a leakage flowrate of 118 lpm with no diffuser. Results for hydrogen concentration at each sensor located in the trunk, rear-passenger, front-passenger, and engine compartment are shown in Figure I-16. This figure shows that every sensor, except those located in the engine compartment, detected hydrogen concentrations within the flammability range for nearly the entire test duration. Each sensor in the trunk, rear-, and front-passenger compartments detect hydrogen levels passing within the stoichiometric regime at some point in time during testing. All of these sensors also reach a steady-state value within the range of 45 percent to 50 percent, similar to the results that were presented for the trunk. The trunk and passenger compartments behave essentially as a single compartment; flow is able to move between the two compartments.

For this data set, no single sensor location represents the worst-case scenario; instead, all sensors in the trunk and passenger compartments exhibit a similar trend in which the levels pass through the near- and at-stoichiometric levels and reach a steady-state level (45% to 50%) that can result in a considerably energetic event. Furthermore, the test results show no noticeable gradient in hydrogen concentrations within a set of sensors in one compartment and suggest that the steady-state value in each compartment is uniform throughout the compartment. This observation differs from the results from the test in which the leak was directed into the trunk. In that test, a more noticeable gradient existed between the 10 percent and 50 percent sensors located in the rear and front passenger compartments.

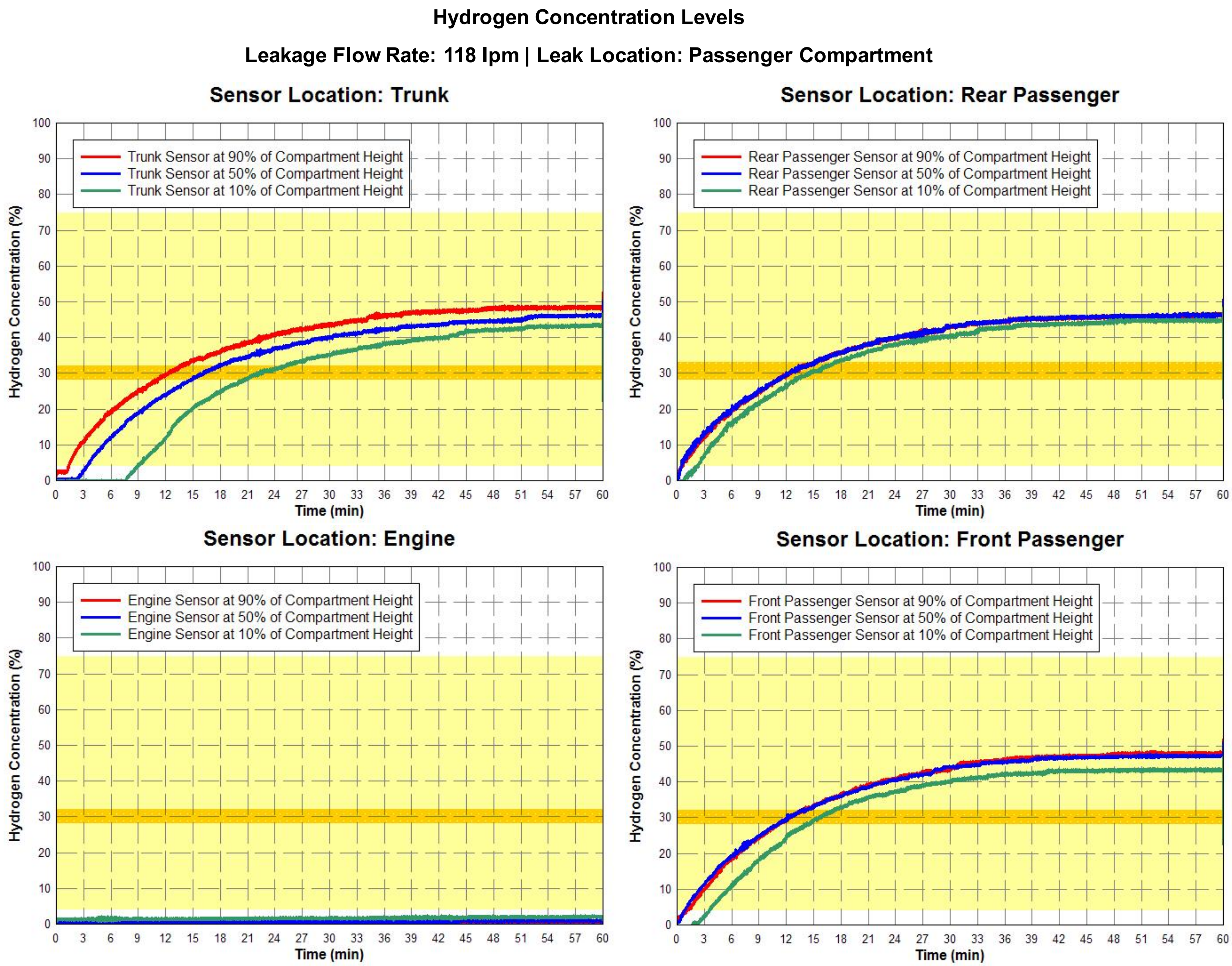

Figure I-16. Hydrogen concentration data for (clockwise from top left) trunk, rear-passenger, front-passenger, and engine compartments; 118 lpm flowrate directed into the passenger compartment.

Tabularized data are shown in Table I-3 and are arranged according to the time a near-stoichiometric mixture (28%) is reached at each sensor location; how long the level remains near the stoichiometric value (28% to 32%) hydrogen concentration in air; and the steady-state concentration at each sensor.

Table I-3. Stoichiometric and steady-state hydrogen concentration data for the 18 lpm leakage flowrate originating from the passenger compartment.

Sensor Location	Time (min) for Concentration to Reach 28% Percent	Length of Time (min) Spent in Stoichiometric Range (28%–32%)	Steady-state Hydrogen Concentration (%)
90% Trunk	10.7	2.7	48
50% Trunk	14.5	3.0	46
10% Trunk	20.1	4.7	43
90% Rear Passenger	10.8	3.9	46
50% Rear Passenger	10.9	4.0	46
10% Rear Passenger	12.9	4.3	45
90% Front Passenger	11.0	2.6	48
50% Front Passenger	10.9	2.6	47
10% Front Passenger	13.9	3.1	43

Under Vehicle Leaks. Several tests were performed with the leak placed underneath the vehicle, oriented in the following directions: straight up, straight down, forward and down at a 45^{o} angle and rearward and down at a 45^{o} angle. One of the straight-up tests included the use of a diffuser on the end of the gas line. The leakage flowrate also was varied for these tests: 59, 118, and 239 lpm rates. None of these leakage locations or flowrates produced any significant hydrogen concentration accumulation in the vehicle compartments. A typical test result from a leak placed underneath the vehicle is shown in Figure I-17.

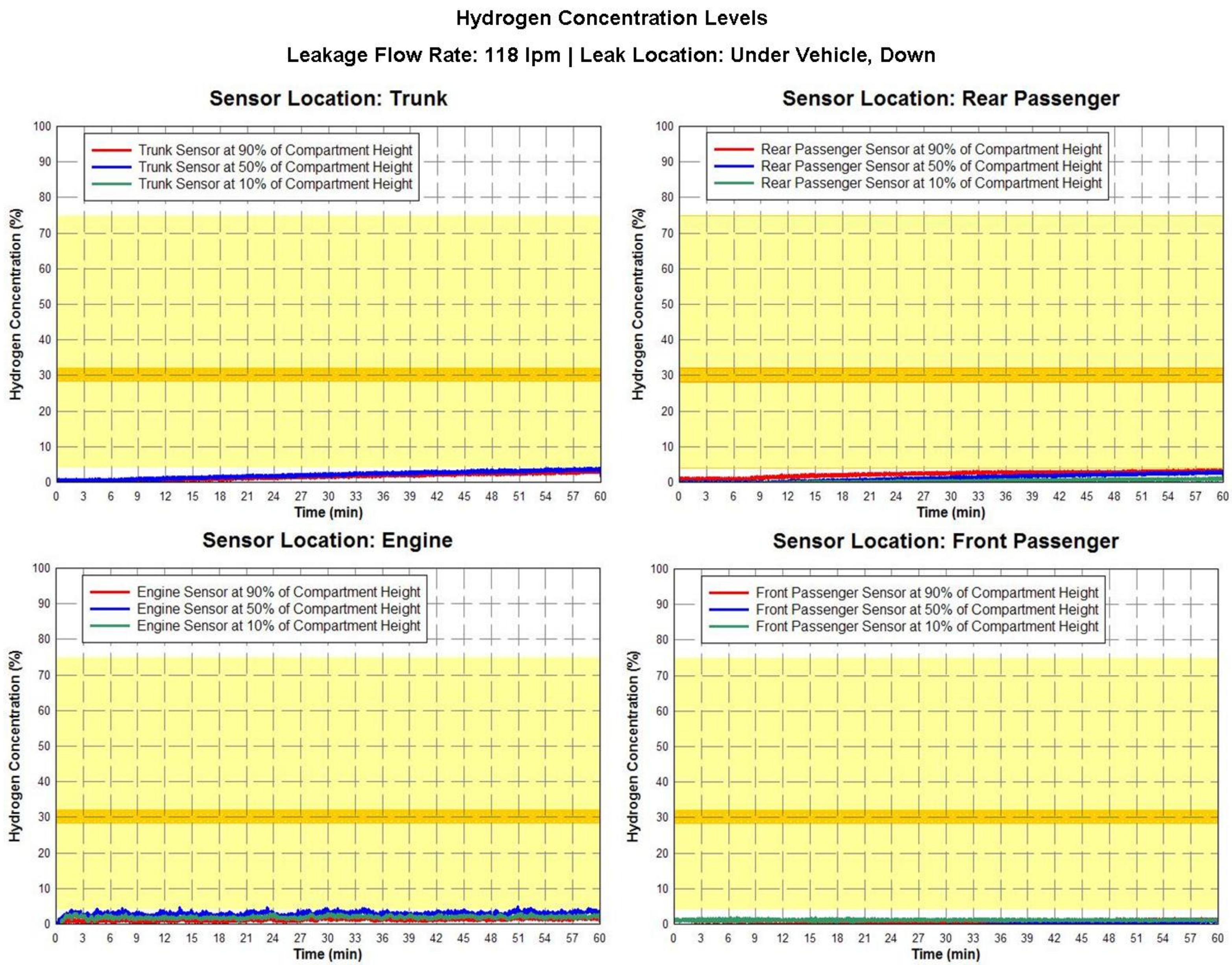

Figure I-17. Hydrogen concentrations at the vehicle sensors for the 118 lpm flow located underneath the vehicle and oriented straight down.

As Figure I-17 shows, none of the sensors detect hydrogen concentrations above the lower limit of the flammability range (4%). This result was typical for all of the leaks located under the vehicle at any of the three leakage flowrates. This lack of accumulation of hydrogen in the vehicle compartments appears to be the result of well-sealed doors and trunk lid. A wide metal plate, observed across the base of the engine compartment and shown in Figure I-18, appears to have prevented the flow of hydrogen to the engine.

Figure I-18. Metal plate located underneath the engine compartment.

Direct Injection Effect of Flowrate. The effect of the leakage flowrate on the time the hydrogen/air mixture exists in the near- and at-stoichiometric range was compared in tests involving three different leakage flowrates (58, 118, and 239 lpm) originating from the trunk compartment. All 12 vehicle sensors were monitored at each leakage flowrate to observe any differences in the time when the hydrogen concentrations reached the near-stoichiometric range, how long the levels dwelled in this range, and the steady-state concentration level.

Results from the trunk compartment are shown in Figure I-19. As shown in this figure, increasing the leakage flowrate decreased the time required for the concentration to reach the stoichiometric level and increased the steady-state value for the trunk sensors. A similar relationship was seen in the passenger compartment sensors. Furthermore, comparing the steady-state values between the 50 percent and 10 percent height sensors as the leakage flowrate increased showed that the hydrogen concentration gradient decreased with increasing leakage flowrate.

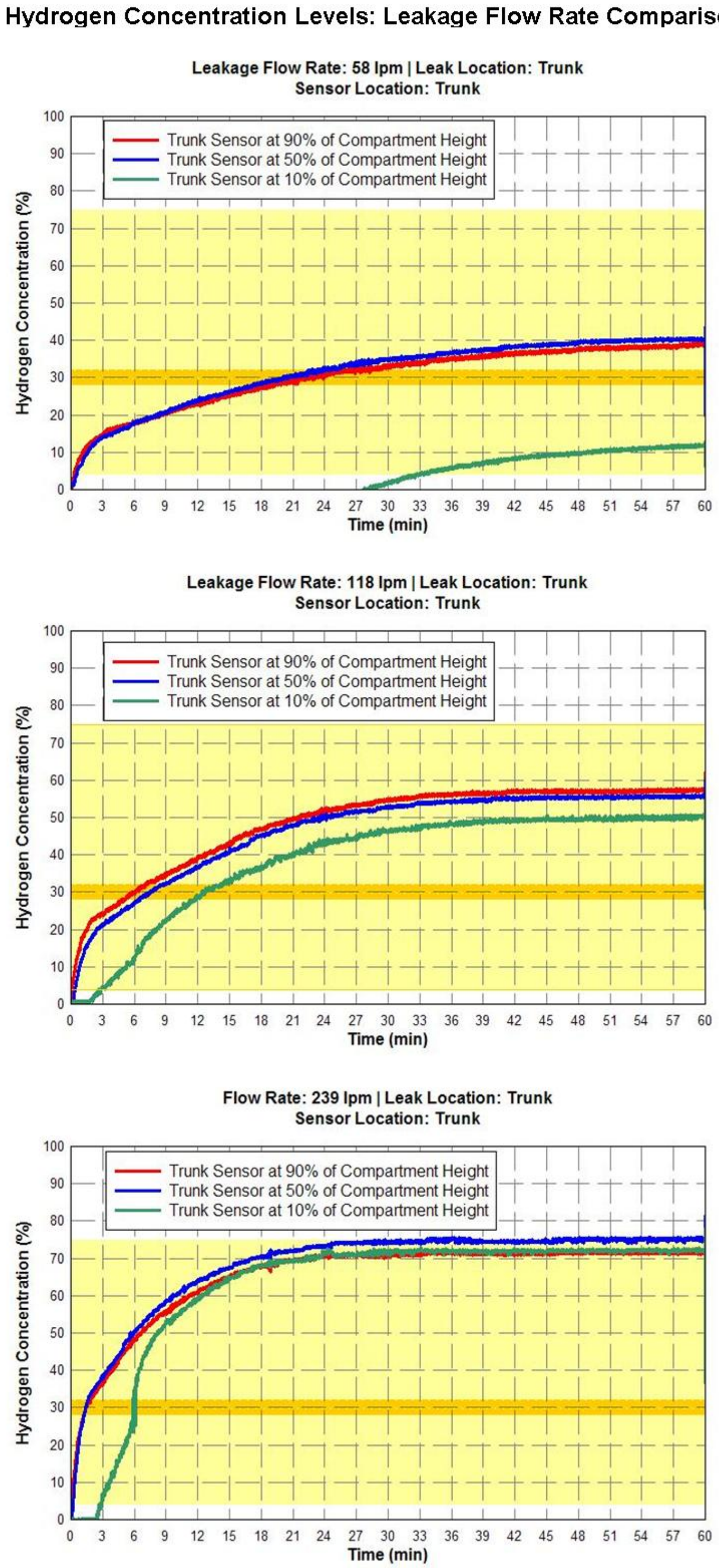

Figure I-19. Effect of leakage flowrate on hydrogen concentrations in the trunk compartment.

Table I-4 summarizes for each trunk sensor at each leakage flowrate the time a near-stoichiometric mixture (28%) was reached at each sensor location; how long the level remains near the stoichiometric value (28% to 32% hydrogen concentration in air); and the steady-state concentration at each sensor. Based on these data, it is difficult to identify the leakage flowrate that represents the worst-case scenario. The test involving the highest leakage flowrate (239 lpm) spends the shortest amount of time near the stoichiometric range; however, this range is reached early in the test. Alternatively, the test with the lowest flowrate (58 lpm) reaches the stoichiometric range much later in the test, but spends much more time in this dangerous regime.

Table I-4. Stoichiometric and steady-state hydrogen concentration data as a function of the flowrate originating from the vehicle trunk.

Leakage Flowrate (lpm)	Sensor Location	Time (min) for Concentration to Reach 28% Percent	Length of Time (min) Spent in Stoichiometric Range (28%–32%)	Steady-State Hydrogen Concentration (%)
58	90% Trunk	18.7	6.3	38
	50% Trunk	17.2	5.5	40
	10% Trunk	Does not reach 28%	…	12
118	90% Trunk	4.8	2.2	57
	50% Trunk	6.4	2.0	55
	10% Trunk	11.6	2.5	50
239	90% Trunk	1.2	0.7	72
	50% Trunk	1.2	0.4	75
	10% Trunk	5.9	0.2	73

Additionally, although the tests with the highest and medium leakage flowrates are in the stoichiometric range for a shorter amount of time, the entire volume is essentially uniform. At the low flowrate, only the sensors placed at 90 percent and 50 percent of the trunk height reach the stoichiometric range; thus, the entire volume is not homogeneous.

Finally, in instances where the leakage flowrate is highest, the hydrogen concentration in air approaches the upper flammability limit for the mixture. While theses concentrations can be more difficult to ignite and less energetic than the stoichiometric condition, asphyxiation now becomes a major concern to a trapped or unconscious occupant.

Engine Compartment Leak. As previously noted, placing the hydrogen leak directly into the trunk compartment, passenger compartment, and directly underneath the vehicle in a variety of orientations did not result in any appreciable amount of hydrogen accumulation in the engine compartment. Based on these results, an additional test was performed. The leak was placed directly under the engine of the vehicle, pointed up towards the exhaust opening in the cover plate and with no diffuser. The 239 lpm flowrate was used for this test in an attempt to identify and bracket the worst-case condition, assuming one existed.

Hydrogen concentrations in each compartment for this test are shown in Figure I-20. As seen in this figure, limited to no accumulation of hydrogen was observed in any of the four compartments. Only very small percentages of hydrogen were sensed in the trunk and rear-passenger compartments; however, it is not clear if these small percentages are due to sensor noise or are actual hydrogen readings. In either case, the levels are at or below the lower flammability limit of hydrogen in air and do not occur until approximately 30 min into the test. A more noticeable accumulation of hydrogen was observed for the sensor placed at 10 percent of the engine compartment height. This sensor showed a peak concentration of approximately 10 percent, which slowly decreased and fell below the 4 percent flammability limit after approximately 20 min.

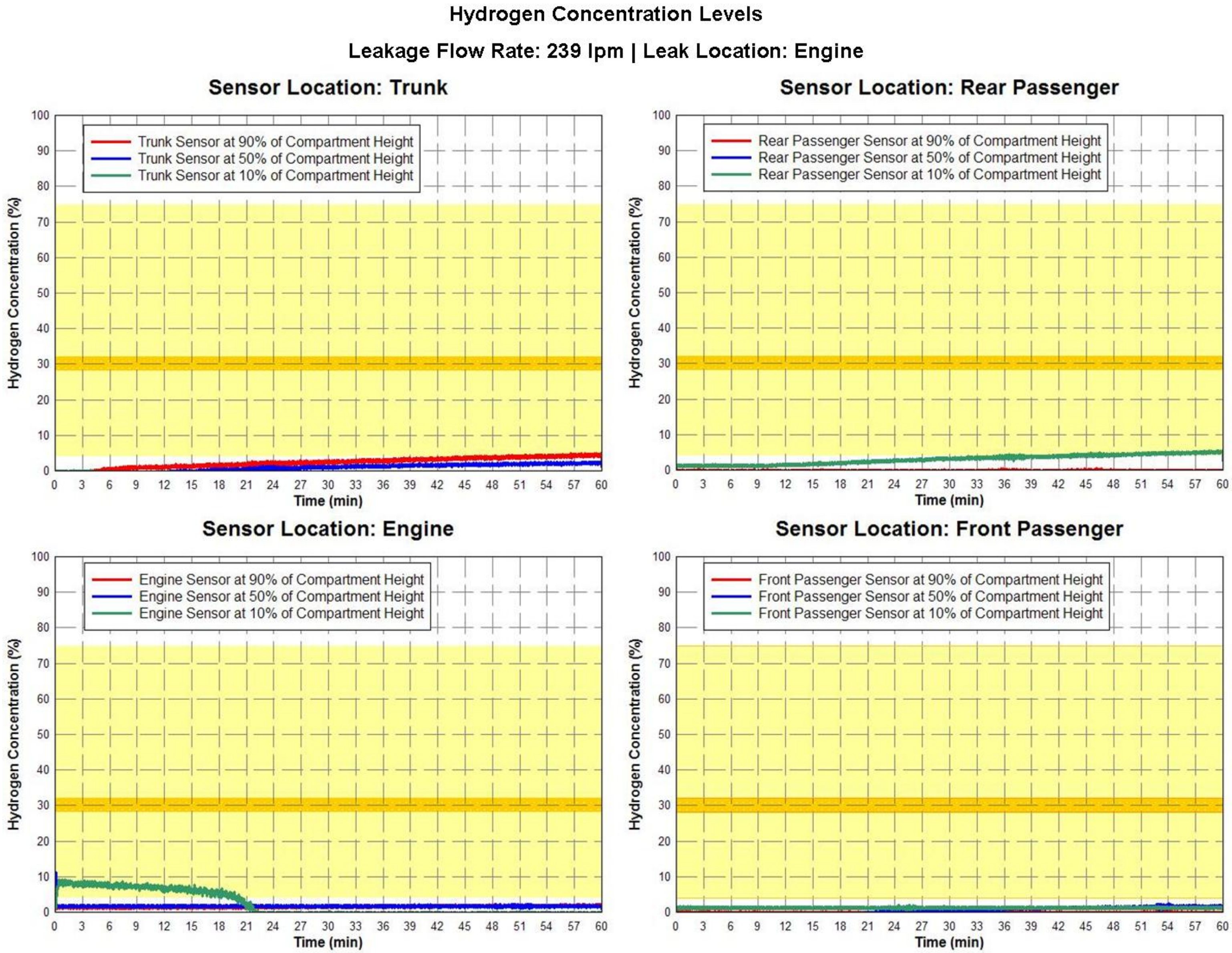

Figure I-20. Hydrogen concentration data for (clockwise from top left) trunk, rear-passenger, front-passenger, and engine compartments; 239 lpm flowrate located directly underneath the engine compartment.

Thus, the highest test leakage flowrate (239 lpm), which could yield the worst-case scenario for this leak location, resulted in only a minor accumulation of hydrogen in the lowest section of the engine compartment. Similar to the results found for the other leaks placed underneath the vehicle, the data presented in Figure I-20 suggest that the design of the vehicle aids in preventing hydrogen flow into the individual vehicle compartments.

Effect of Diffuser. Most of the tests performed under this effort did not use the diffuser attached to the end of the hydrogen supply line. It was thought that the use of the diffuser to reduce flow turbulence could limit the ability of the hydrogen to mix with the air, thus distributing the hydrogen less uniformly throughout a given compartment. Therefore, a comparative test was performed to determine if the diffuser had a noticeable effect on the resulting data.

The variables in these tests were identical, except for the presence or absence of the diffuser. The results for the hydrogen concentrations in the trunk compartment at a 118 lpm flowrate are shown in Figure I-21. From this figure, it is clear that there is little difference in the rise times, steady-state hydrogen concentrations, time when the near-stoichiometric regime is reached, and time spent in the stoichiometric range. Similar comparative results also were observed for hydrogen concentrations in the rear and front passenger compartments.

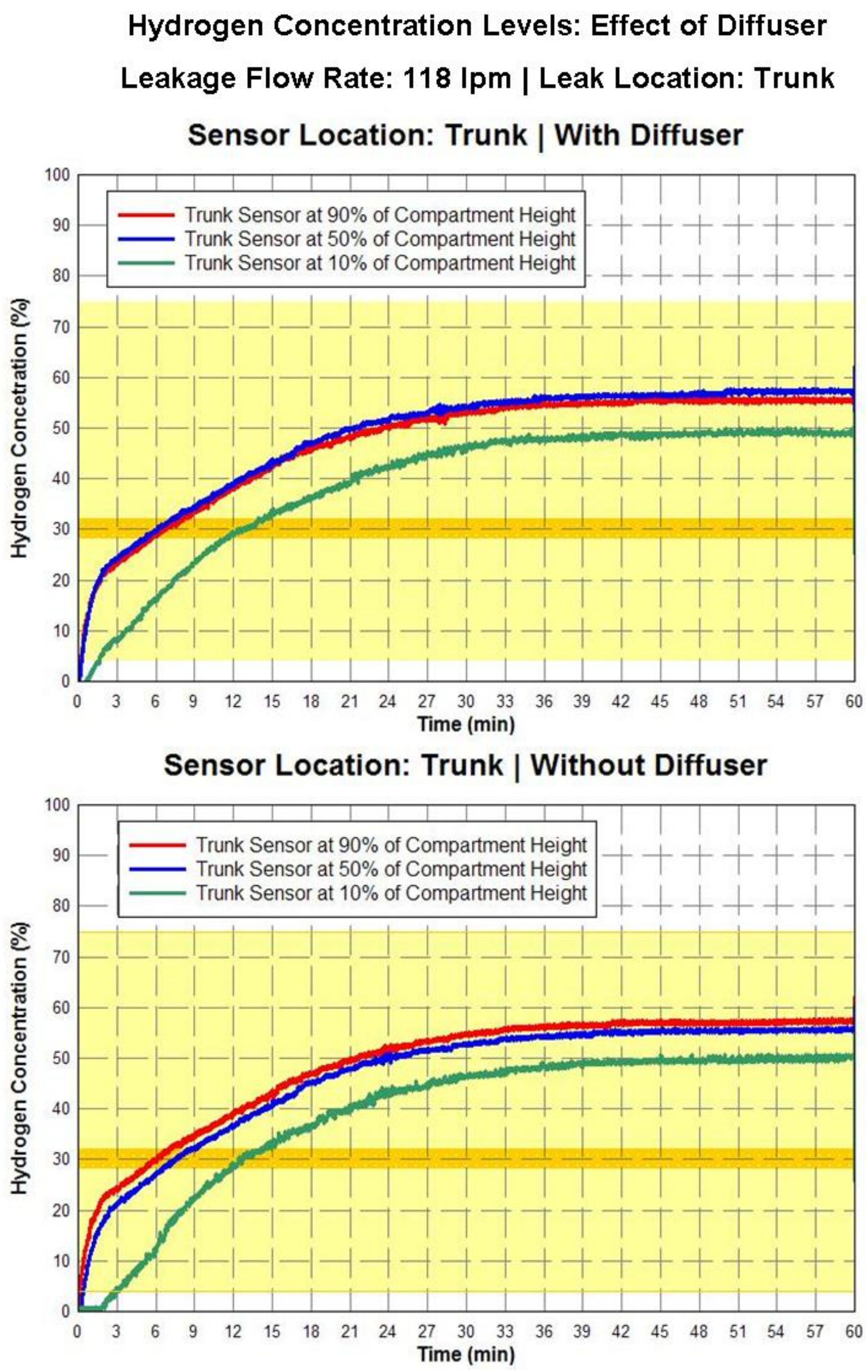

Figure I-21. Comparison of hydrogen concentrations in tests with (top) and without (bottom) diffuser

Table I-5 shows the comparable data for the time when the stoichiometric regime was reached; how long the concentration remained in this regime; and the concentration steady-state value. From this data and the graphical data shown in Figure I-21, there appears to be no significant difference due to reduced turbulence using the diffuser.

Table I-5. Comparison of the effect of the diffuser on the stoichiometric and steady-state hydrogen concentration data.

Test Type	Sensor Location	Time (min) for Concentration to Reach 28% Percent	Length of Time (min) Spent in Stoichiometric Range (28%–32%)	Steady-state Hydrogen Concentration (%)
With diffuser	90% Trunk	5.2	2.6	56
	50% Trunk	4.8	2.4	57
	10% Trunk	11.0	2.9	49
Without diffuser	90% Trunk	4.8	2.2	57
	50% Trunk	6.4	2.0	55
	10% Trunk	11.6	2.5	50

Post-Leak Decay. The decay rate of hydrogen concentration in the vehicle following the termination of a test was recorded for several tests. These data were used to assess how long a combustible hydrogen/air mixture existed in a vehicle after the source of the leak was removed. Such data can provide insight on the time required to render a vehicle safe to enter following the cessation of a leak or complete depletion of the hydrogen storage tank.

Figure I-22 presents the decay rate for all four vehicle compartments for an additional 60 min after a hydrogen injection test had ended. The data for the trunk, rear-, and front-passenger compartments show hydrogen concentration depletion occurring fastest in the region containing the sensor placed at the 10 percent height. In turn, the 50 percent height decays more quickly than the 90 percent. This characteristic is most likely a result of the lighter density hydrogen molecules moving towards the top of the vehicle compartments as the heavier air molecules replace the hydrogen that is escaping through various paths.

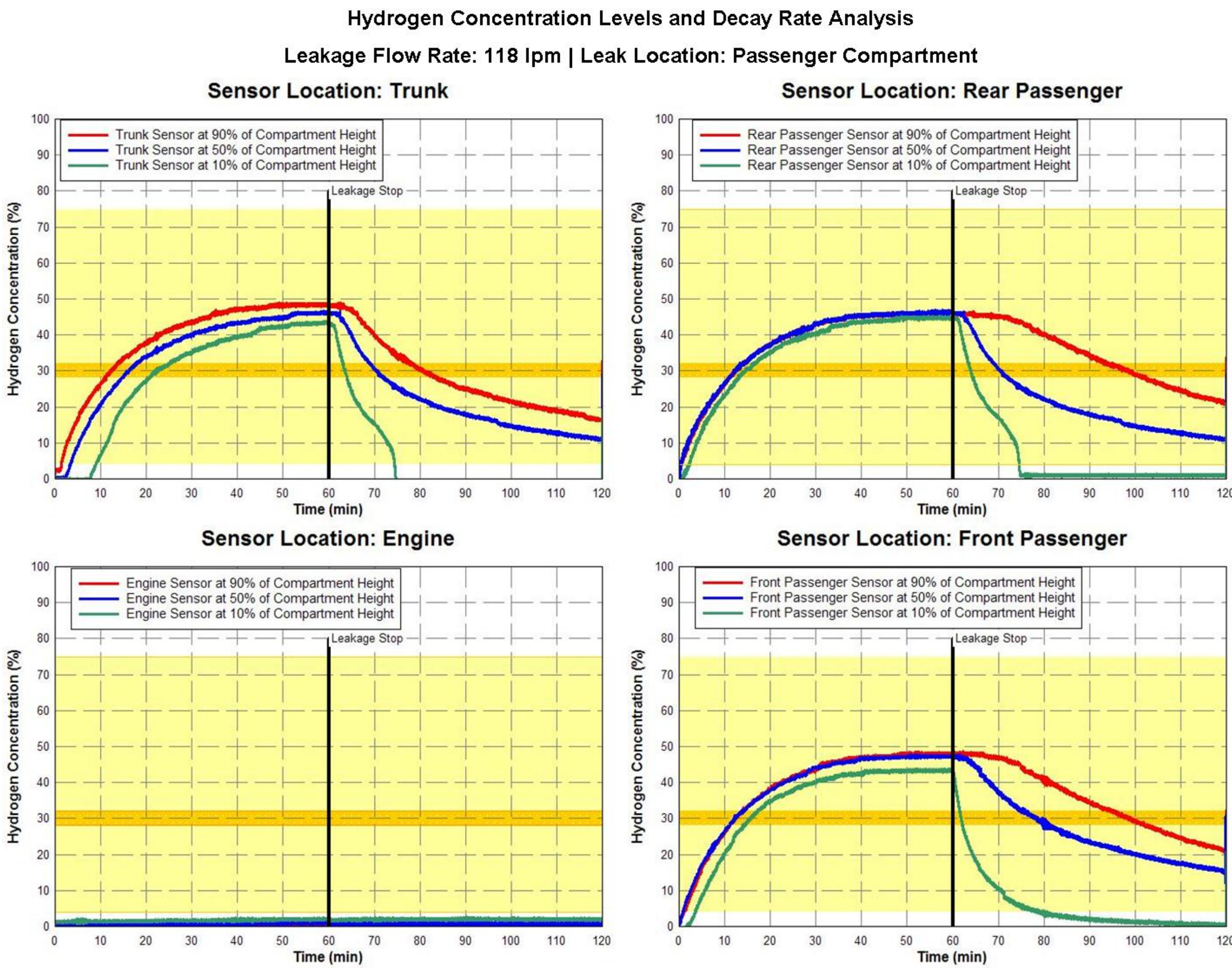

Figure I-22. Hydrogen concentration data and decay rate for (clockwise from top left) trunk, rear-passenger, front-passenger, and engine compartments.

During the decay rate process, the hydrogen concentrations in the trunk, rear- and front-passenger compartments again pass through the stoichiometric range. Table I-6 shows the data on when the decay process reaches the upper limit of the stoichiometric range (32%); how long the concentration remains in this range; and the concentration at the end of the 60 min decay time. From the data presented, the hydrogen concentration in the vehicle is still within the flammability range in the trunk, rear-, and front-passenger compartments after the leak has stopped.

Table I-6. Post-test hydrogen decay analysis stoichiometric and hydrogen concentration data.

Sensor Location	Time (min) for Concentration to Reach 32% Percent	Length of Time (min) Spent in Stoichiometric Range (28%–32%)	Hydrogen Concentration (%) at End of Test
90% Trunk	77.6	5.7	17
50% Trunk	68.9	3.2	11
10% Trunk	63.1	0.9	0
90% Rear Passenger	93.0	8.4	21
50% Rear Passenger	68.9	3.2	11
10% Rear Passenger	63.4	0.9	1
90% Front Passenger	94.6	7.4	21
50% Front Passenger	75.0	5.0	15
10% Front Passenger	61.5	0.6	1

Hydrogen Concentration Dispersion Path. Analyzing when a given percentage of hydrogen has accumulated at each sensor can provide clues on how a forced flow of hydrogen disperses into a volume. Such an analysis was performed for two tests: 118 lpm leakage flowrate originating from the trunk and 118 lpm leakage flowrate originating from the passenger compartment. For each test, the time required for each sensor in the trunk and passenger compartment to reach a 30 percent concentration was captured.

The time recorded for each sensor to reach 30 percent was graphed as a function of the location of each sensor, as shown in Figure I-23. Displayed in this figure is the concentration reaching 30 percent first at the sensor at 90 percent of the trunk compartment height. The next sensor to reach 30 percent is the trunk sensor at 50 percent of the trunk height, followed by the front passenger compartment sensor located at 90 percent of the compartment height. This data gives some clues on how the hydrogen flows once dispersed into the trunk: accumulating at the top of the trunk displacing the ambient air downwards and at the same time migrating into the rear- and front-passenger compartments, most likely along the roof. The 90 percent passenger compartment height sensors are first to detect the 30 percent hydrogen concentrations. The sensor located at 90 percent in the front passenger compartment registers the 30 percent hydrogen level before the rear sensor, perhaps because of the contour of the vehicle roof.

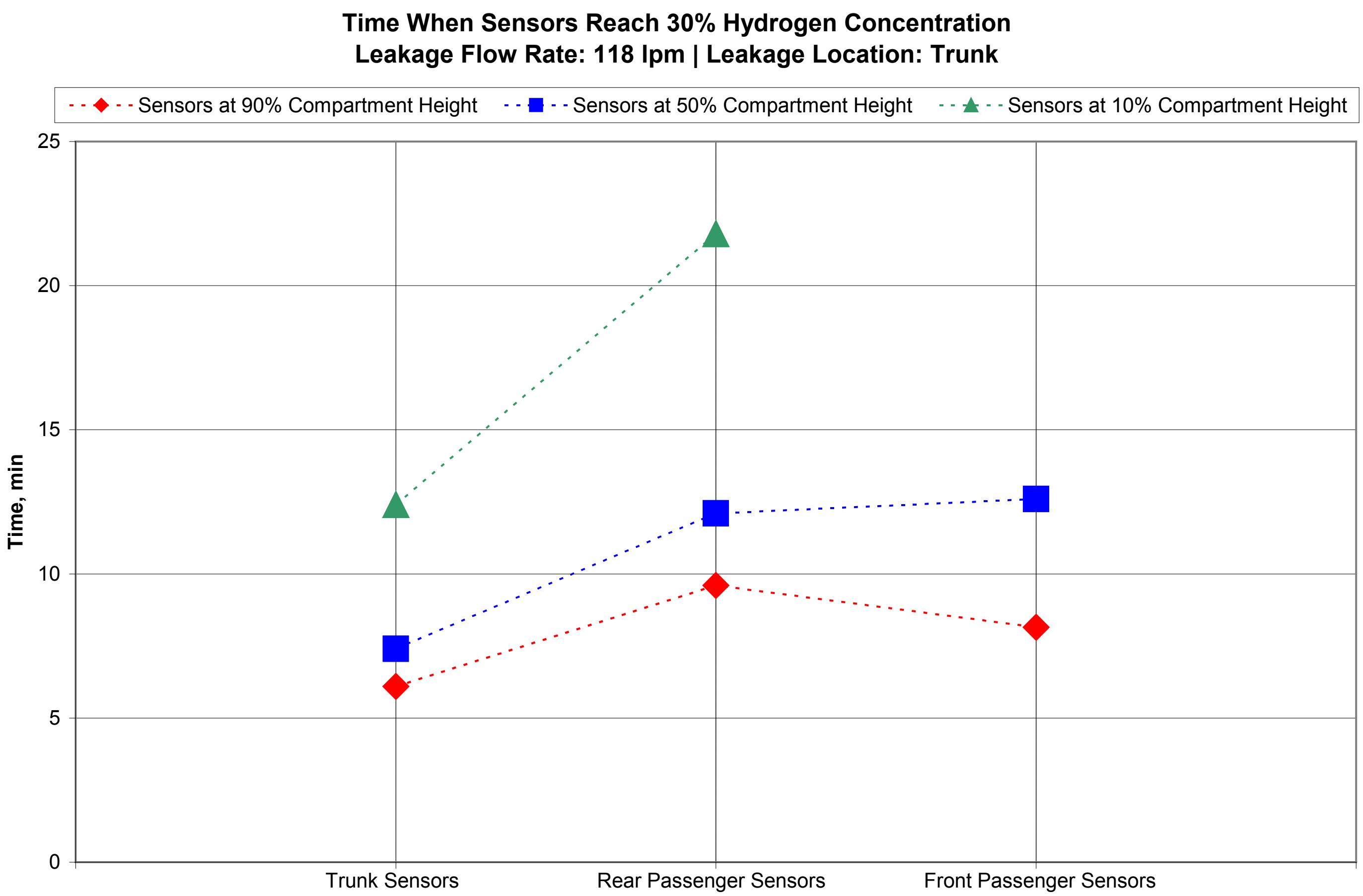

Figure I-23. Time when the hydrogen concentration reaches 30 percent at the trunk, rear-passenger, and front-passenger compartment sensors; 118 lpm leakage flowrate located in the trunk.

For comparison, results for the dispersion of a hydrogen leak placed in the passenger compartment are shown in Figure I-24. This data shows the 90 percent compartment height sensors in all three of the compartments reading 30 percent levels of hydrogen at approximately the same time. Furthermore, the sensors placed at 50 percent in the passenger compartment also reach the 30 percent concentration at the same time.

The hydrogen concentrations at the 10 percent passenger compartment height reach 30 percent before the higher sensor located at 50 percent of the trunk compartment. Thus, this data shows that the larger passenger compartment volume and passenger/trunk interface create some delay in migration between compartments.

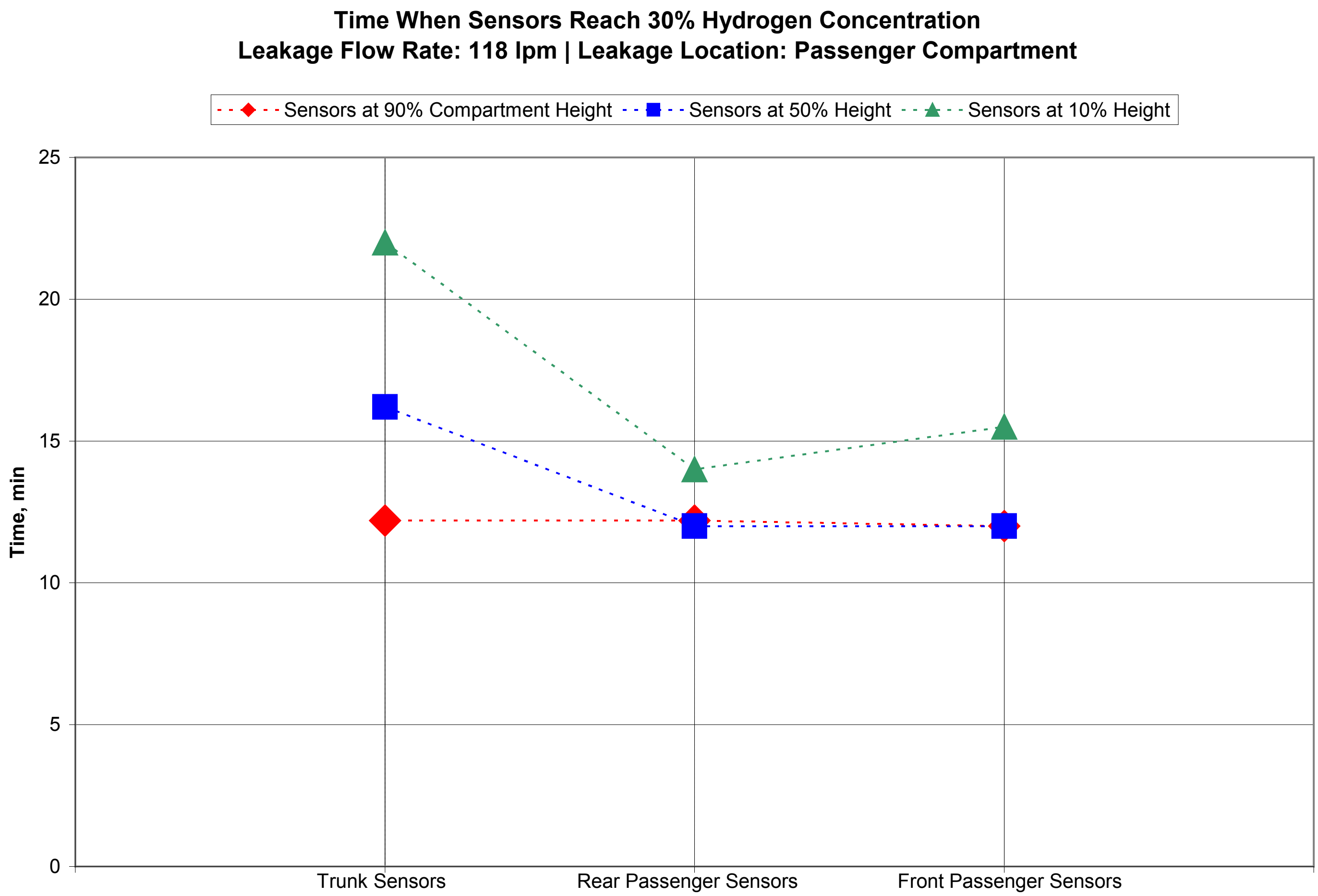

Figure I-24. Time when the hydrogen concentration reaches 30 percent at the trunk, rear-passenger, and front-passenger compartment sensors; 118 lpm leakage flowrate located in the passenger compartment.

Some generalities can be made in comparing the two cases. The data suggests that a leak located in the trunk will disperse through the vehicle more quickly than a leak located in the passenger compartment. However, regardless of leak location, the sensors located at the 90 percent and 50 percent levels in the passenger compartment reach 30 percent hydrogen concentrations within 15 min of leak initiation. Thus, a leak located in either the trunk or passenger compartment can be considered an equal threat to occupants in the vehicle.

SUMMARY

A series of tests were conducted in which hydrogen concentrations were recorded in different vehicle compartments to determine the effect of leak rate on the creation of worst-case conditions, defined as stoichiometric hydrogen levels (30%) in air. The flow of hydrogen originated from specific locations directly into or underneath the vehicle. Hydrogen leakage flowrates varied between 59 to 239 lpm, corresponding to half and double the energy equivalence to leakage limits specified in FMVSS 301 for liquid fuels and FMVSS 303 for CNG. The test duration did not exceed one hour or until hydrogen concentrations essentially achieved steady-state conditions.

Hydrogen concentration data was recorded from the time the leak was initiated to when a steady-state concentration of hydrogen was achieved. Additionally, several tests were conducted to measure the decay rate of hydrogen concentration inside the vehicle after the leak had ceased.

Results were summarized in a series of graphs which showed when hydrogen concentrations in the trunk, rear passenger, front passenger, and engine compartments were within the flammability range (4% to 75%), with an emphasis on when the concentrations were in the stoichiometric range (28% to 32%). These data will be used to assess the potential hazard posed to passengers in Tasks 2b and 2c of this program.

The data showed that leaks located underneath the vehicle did not increase significantly the concentration of hydrogen in any vehicle compartment. The entire sensor array, located in the trunk, rear- and front-passenger compartments and engine compartment, consistently showed that no appreciable amount of hydrogen accumulated.

However, the data was not the same for leaks directly into the trunk or passenger compartments. In these scenarios, hydrogen concentrations achieved the stoichiometric regime for all the leakage rates tested. Under the identified standard leakage rate limit (118 lpm), a leak into the trunk compartment created hydrogen concentrations in the 50 percent to 60 percent range at the higher sensor positions. Sensors located at occupant waist-level measured around 30 percent. The same leak rate into the passenger compartment yielded steady-state hydrogen concentrations in the 40 percent to 50 percent range.

Decreasing the flowrate to 58 lpm did not render the leak safer; on the contrary, at this rate the trunk compartment leak resulted in steady-state concentrations closer to 30 percent at all sensor locations, establishing longer dwell times in the 30 percent regime. Increasing the flowrate to 239 lpm did not assuage the danger of leaks into the trunk. Although at this flowrate, the hydrogen concentrations spent less time in the 30 percent regime, the final steady-state values were closer to 75 percent. At this level, asphyxiation becomes a serious concern. Similar results were observed for lower and higher rate leaks into the passenger compartment.

OBSERVATIONS

Hydrogen concentration test data has been reported in the technical literature to compare to the hydrogen concentration data captured in Tasks 2a, 2b, and 2c[4,5]. In the earlier of these two reports[4], a 131 normal lpm hydrogen leak was placed underneath the vehicle, and hydrogen concentrations were monitored at several discreet locations in the engine compartment and along the front of the car. Among the results discussed was the observation that hydrogen levels reached a steady-state concentration value of approximately 20 percent to 23 percent within approximately 200 sec from the test start at sensors located at the center of the front hood and at the top of the radiator. No appreciable data was obtained for a third sensor located at the bottom of the radiator.

In the more recent of the two referenced reports[5], hydrogen leaks were placed underneath the vehicle front, middle, and rear portions, and the flowrate was varied from rates less than 131 lpm to 1000 lpm. Hydrogen concentrations again were monitored in discreet locations in and around the engine compartment. These levels were plotted as a function of the leakage flowrate and as a function of the shape of the vehicle underfloor, among other variables. Results at lower leakage flowrates (less than 200 lpm) that originated from the center of the vehicle yielded concentrations in the engine less than or equal to the lower flammability limit of hydrogen in air (4%).

In comparing the results from these previous reports to those reported for Task 2a, the results from Task 2a for the sensor located in the engine under the influence of leaks originating from underneath the vehicle appear to agree with the near-zero concentrations at a flowrate of about 118 lpm reported in the more recent paper. However, the exact concentrations detected are not explicitly clear in the report. This report also noted the influence of the vehicle underfloor on the ability of hydrogen to accumulate in the engine. A similar relationship was noted for the results in Task 2a with respect to the hydrogen levels detected by the engine sensors.

In Tasks 2b and 2c, heat flux and pressure data for hydrogen leaks that are directed into the vehicle trunk and passenger compartments and then ignited will be acquired and compared to the values reported in the referenced reports for leaks into the engine compartment. Task 2b and 2c data and subsequent comparison will be used to show the leak that produces the most severe threat to vehicle occupants in terms of pressure and temperature.

VOLUME II: TASK 2B

The objective of Task Order 3, *Post-Crash Hydrogen Leakage Limits and Fire Safety Research*, is to conduct research on the fire safety of proposed hydrogen leakage limits, including calculations and experimental verification. This assessment provides the technical data that correlate hydrogen fuel system leak rates to the accumulation of ignitable mixtures of hydrogen in enclosed trunk, passenger, and engine compartments.

The three tasks being conducted as part of Task Order 3 are:

- Task 2a. Conduct Leak Rate vs. Hydrogen Concentration Tests on Intact Automobile;
- Task 2b. Conduct Ignition and Combustion Tests on Simulated Automobile Compartments; and
- Task 2c. Conduct Full-Scale Leak, Ignition, and Fire Tests on Intact and Crashed Automobiles.

This report explains the work performed and results obtained under Task 2b. Its scope was the measurement of heat flux and overpressure created upon ignition and combustion of flammable levels of hydrogen accumulating in the trunk and passenger compartments following plausible leak rates from a post-crash hydrogen fuel system. The objective was to quantify hydrogen combustion effects and relate them to predictions on the extent of personal injury. These tests were conducted in an automobile compartment simulator (ACS) that reconstructed the volumes of the trunk, rear- and front-passenger compartments of the 2008 Mitsubishi Lancer used as a test vehicle in Task 2a. The ACS allowed multiple ignition tests to be conducted on the same test system in a relatively short period of time via the use replaceable compartment panels.

In Task 2b leak accumulation calibration tests, time-dependent hydrogen concentration profiles were measured using the same hydrogen sensors employed in Task 2a. Modifications were performed to allow ACS compartments to accumulate hydrogen in as similar a manner as possible compared to the Task 2a test vehicle. This effort was partially successful because accumulation differences between the two could not be reconciled completely. Although the dimensions and volumes of the Task 2b ACS were very similar to the 2a test vehicle, the flow characteristics of the hydrogen into and out of the test vehicle and accumulations were not, especially at early times in the calibration test when concentrations were low. However, overall hydrogen accumulation levels in the Task 2b ACS quantitatively matched those of the Task 2a test vehicle; the time-resolution of the concentration was only qualitatively similar. This lack of one-to-one correspondence between the test vehicle and ACS did not prevent Task 2b from achieving its objective. Tests were configured to acquire the targeted accumulations for ignition testing, namely, 5 percent, 15 percent, 30 percent, or 60 percent hydrogen in air.

In Task 2b ignition tests, diagnostics used to assess fireballs and blasts at 5 percent, 15 percent, 30 percent, and 60 percent hydrogen were high-speed digital imaging, heat flux sensors, and pressure transducers. The ACS included, in its driver's seat, an instrumented manikin, a Hybrid III (RA Denton), representing the 50th percentile male pedestrian (height: 5 ft 6 in.; weight: 170 lb).

This manikin had heat flux and pressure sensors in its head, torso, arms, hands, and legs to record thermal and blast effects from hydrogen combustion. This data was used to formulate injury predictions using a burn-injury algorithm (BURNSIM) and data on injuries versus blast effects.

The most significant observation derived from Task 2b test data is that at all levels of accumulated hydrogen inside the vehicle, ~5 percent, ~15 percent, ~30 percent, or ~60 percent, the most probable predicted consequence of a driver's exposure to the combustion of hydrogen is second-degree burns to exposed skin (face and hands).

Ignition tests following leaks at 5 percent accumulated hydrogen in the ACS yielded the lowest temperatures and burn threats (some first-degree burns). This result was anticipated because this concentration is near the lower flammability limit of hydrogen (4%), which is known to yield cooler, slower burning fireballs than at stoichiometric (~30%) levels(3).

Ignition tests at 15 percent, 30 percent, and 60 percent accumulated hydrogen resulted in higher exposure temperatures, with 30 percent and 60 percent hydrogen yielding longer-duration fireballs and higher temperatures than at 15 percent (all second-degree burns). Predictions for burn threshold depths indicate that 30 percent and 60 percent hydrogen combustion created the most severe threats. Ignition of 30 percent hydrogen was the expected worst-case (near stoichiometric) concentration, which yields the hottest fireball. The maximum burn threshold depth value for 30 percent hydrogen was more than 1.5 times higher than other measured values.

No observable overpressure was detected at ~5 percent or ~15 percent hydrogen concentrations, but a slight overpressure was observed via high-speed imagery in the form of panel motion. No personal injury would be expected.

Ignition of ~60 percent hydrogen generated about 1.0 psi of overpressure. The physiological consequence of exposure to ~1.0 psi is the rupture of eardrums in an estimated 20 percent of the exposed population levels(7, 8).

Overpressure posed a very serious threat during the combustion of ~30% hydrogen, i.e., possible death. Blast overpressures in excess of 80 psi peak overpressure was measured at the right ear.

An important overall observation to be made from Task 2a and Task 2b tests is that the flow characteristics of hydrogen are complex, expectedly so as a result of its low density (high buoyancy) and high diffusivity. Large differences in hydrogen accumulations in the ACS could be observed after small test changes were made to the tightness of its structure, such as taping a few additional seams. In short, this experience indicates that different makes and models of automobiles are likely to exhibit significant differences in terms of hydrogen fill profiles and accumulation levels. Information from manufacturers can assist in determining the extent to which the data acquired in this program are vehicle-specific.

TASK SCOPE AND OBJECTIVE

This report describes the work performed and results obtained under Task Order 3 Task 2b: *Conduct Ignition and Combustion Tests on Simulated Automobile Compartments*. The scope of Task 2b was the measurement of heat flux and overpressure created subsequent to ignition and combustion of flammable levels of hydrogen accumulating in the trunk and passenger compartments following plausible leak rates from a post-crash hydrogen fuel system. The objective is to quantify hydrogen combustion effects, including their potential for personal injury (physical trauma and burns). These tests were conducted in an ACS that reconstructed the volumes of the trunk, rear, and front passenger compartments of the 2008 Mitsubishi Lancer test vehicle used in Task 2a.

The objective of Task 2b was accomplished in two series of tests. The purpose of the first test series (accumulation) was to calibrate the ACS with respect to the hydrogen concentrations created in the trunk and passenger compartments and to compare the results with the Task 2a test vehicle. Assessment of hydrogen accumulation in the engine compartment of the ACS was not included because the Task 2a test vehicle did not accumulate appreciable hydrogen concentrations in this compartment when exposed to a variety of leak orientations and flowrates. Furthermore, leaks located underneath the vehicle in Task 2a did not result in any accumulation in the trunk or passenger compartments. Based on Task 2a test results, only two compartments were selected for the origin of the leak: one leak directly into the trunk compartment and one leak directly into the passenger compartment.

The purpose of the second series of tests (ignition) was to ignite specific hydrogen concentrations and measure the resulting heat flux and overpressure. The criteria for accumulation levels were 5 percent, 15 percent, 30 percent, and 60 percent hydrogen concentrations in the ACS, distributed in the trunk and passenger compartments. These accumulation values represent the minimum flammability (5%), fuel-lean (15%), stoichiometric (30%), and fuel-rich (60%) levels for hydrogen combustion in air at standard temperature and pressure. Ignition of the stoichiometric mixture provided physical data for the highest potential for injury or fatality to vehicle occupants. The minimum, fuel-lean, and fuel-rich level reactions are also of interest to demonstrate the threat reduction for mixtures other than stoichiometric.

The output data correlated hydrogen accumulation to the level of injury imparted to vehicle occupants as well as damage sustained by the ACS and surroundings. Injury assessments were made with respect to burn assessment (first-, second-, or third-degree) and overpressure exposure.

TEST FACILITY, INSTRUMENTATION, AND HARDWARE

Test Facility. Tests were conducted at the Battelle HERLA inside JS-10, a 40-ft diameter, steel-reinforced concrete, domed chamber capable of containing up to 50 lbs of TNT explosive or energy equivalent of other flammable materials, including hydrogen and CNG. Conducting tests inside this large blast containment chamber precluded the influence of variable meteorological conditions, which could affect the dispersion and ignition properties of the hydrogen. Factors such as ventilation, temperature, and relative humidity were recorded during the testing (quiescent and within a controllable range). JS-10, shown in Figure II-1, is large enough to accommodate a vehicle and allows leak and ignition-fire tests to be conducted with flammable hydrogen-air mixtures.

Figure II-1. ACS and manikin in JS-10 blast chamber for hydrogen ignition testing.

ACS. The purpose of the ACS was to allow multiple ignition and combustion tests using volumes similar to the Task 2a test vehicle. An actual automobile could not be used for multiple testing due to the resultant damage. The ACS offered the advantage of being able to replace damaged components readily, thus allowing multiple ignition tests to be performed in a relatively short period of time using minimal resources. The ACS, Figure II-2, was built to represent the Task 2a test vehicle trunk and passenger compartments in terms of internal volume and overall dimensions.

The ACS framework, Figure II-3, consisted of 2 in. steel tubing welded together to approximate the overall geometry and dimensions of the Lancer. A section of the ACS framework representing the engine compartment was included in the design; however, no use of this compartment was planned based on test results from Task 2a (no significant hydrogen accumulation in the engine compartment).

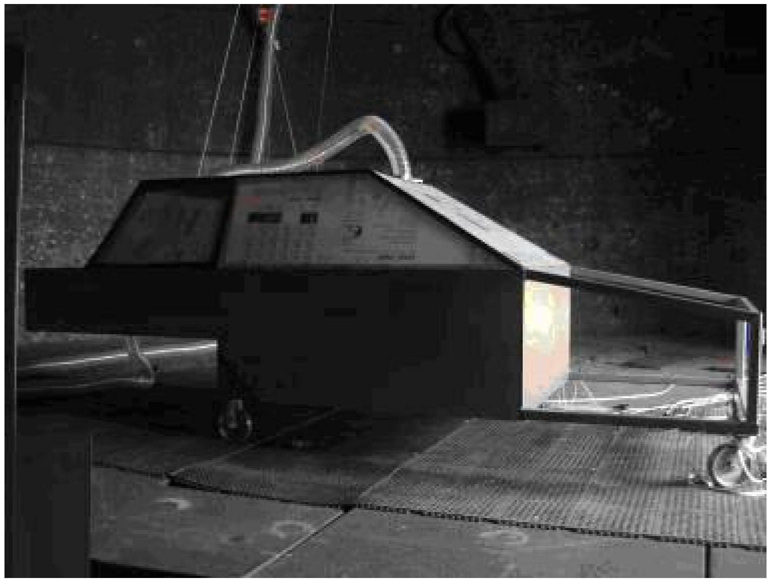

Figure II-2. Fully assembled ACS.

Figure II-3. Welded framework of ACS.

Table II-1 displays a comparison of the ACS compartment volumes and the Task 2a test vehicle. The manufacturer's staff verified the free volumes used for the ACS design. Front seat and dashboard components were represented by oak timbers in the ACS to preserve both the internal volume and overall dimensions of the test vehicle's passenger compartment, see Figure II-4. The total volume occupied by the timber front seat and dashboard was $\approx$ 22 ft^3. The Task 2a test vehicle's lower trunk free volume (storage space for the spare tire) was not available and was not included as part of ACS design. The ACS trunk volume in Table II-1 is ~32 percent larger than the test vehicle compartment; but with the addition of the lower level spare tire compartment in the actual vehicle, the two in reality are actually closer in volume.

Table II-1. Comparison of ACS compartment volumes with those of Task 2a test vehicle.

	Volume (ft^3)	Difference (%)
ACS Passenger Compartment	92.9	-2.0
Task 2a Test Vehicle Passenger Compartment	94.8	
ACS Trunk Compartment	15.4	~32.7
Task 2a Test Vehicle Trunk Compartment	~11.68*	
ACS Total Free Volume	108.8	2.3
Task 2a Test Vehicle Total Free Volume	106.4	

*The stated volume does not include the free volume around the spare tire in the trunk lower level.

Figure II-4. View of simulator front seat (A) and dashboard (B) components in ACS.

Sheet steel panels, 20-gauge, were attached to the ACS frame with magnets to represent doors, the trunk, undercarriage, and engine panels of the Task 2a test vehicle. Eleven individual steel panels were placed at the following locations, see Figure II-5.

- fire wall (A)
- driver and passenger doors (B)
- roof (C)
- driver and passenger rear sides (D)
- passenger floor (E)
- trunk bottom (F)
- passenger back (G)
- trunk lid (H)
- trunk back (I).

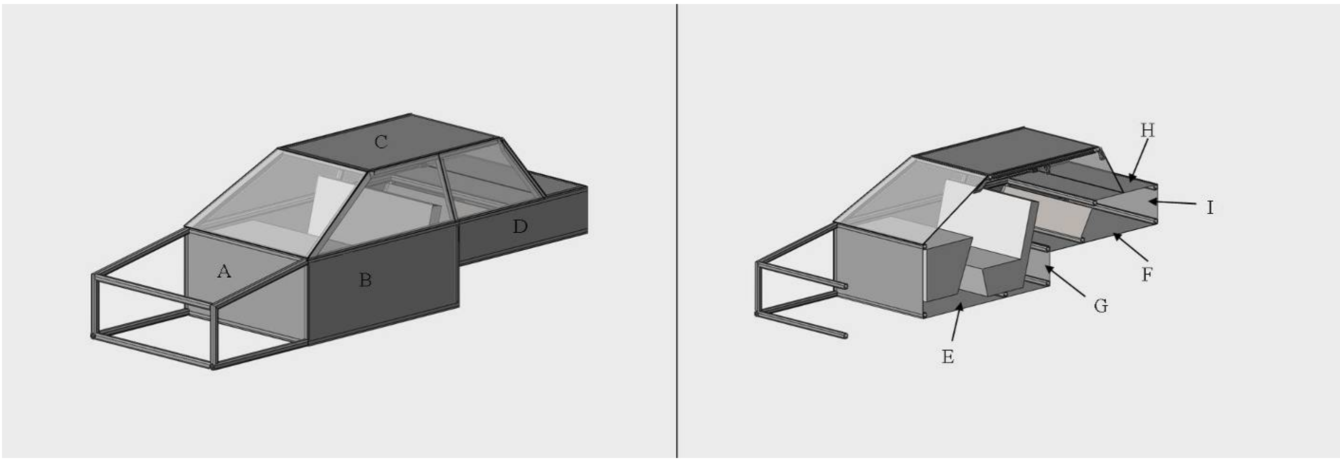

Figure II-5. Full (left) and cross-sectional (right) views of clear and opaque ACS panels.

Lexan panels, 0.25 in. thick, were used to represent windows. Six panels were used in the following positions.

- windshield
- right and left front passenger windows
- right and left rear passenger windows
- rear window.

Lexan panels were employed in sheet-steel positions in some of the ignition tests to give the high-speed imager a better view of the ignition and combustion propagation. These panels were employed in other tests simply because of they would not bend and flex after and ignition event.

Both the steel and Lexan panels were mounted to the ACS frame using magnetic strips. In later tests, duct tape was used along all the seams or edges of panels to provide improved sealing. Small bar magnets also were mounted on five 2-by-4 pieces of lumber, which were placed on the bottom of the passenger and trunk compartments to aid in securing the bottom panels.

In Task 2a, the design of the interior of the test vehicle permitted rapid flow of hydrogen between the trunk and passenger compartments. To replicate this interaction in the ACS, a separation panel, Figure II-6, was placed in the position occupied by the back of the rear seat in the test vehicle. A cardboard version of this panel was used for ACS hydrogen concentration calibration tests, which allowed on-the-fly changes to the panel. The number and locations of holes on the separation panel were adjusted after each test until an adequate accumulation of hydrogen in the trunk and passenger compartments occurred for leaks fed directly into either the trunk or passenger compartment.

A plywood version of the panel was used for the ignition tests after a satisfactory design was identified. The final separation panel contained a set of six 1.0 in. diameter holes along the top and bottom of the panel. The panel also had a 1.0 in. gap along the top edge to allow sufficient flow between the two compartments.

Figure II-6. Cardboard (left) and plywood (right) separation panels in ACS.

Hydrogen Sensors. Two types of hydrogen sensors were used during testing. Neodym Panterra hydrogen sensors with remote heads were used to measure hydrogen concentrations from 0 to 100 percent. These sensors have a measured rise time of approximately 1.5 sec and were employed to measure hydrogen concentrations inside the ACS and on the blast chamber ceiling.

Neodym HydroKnowz sensors equipped with alarms were placed on the ceiling in the blast chamber and in the control room to monitor the presence of hydrogen during testing to safeguard against the accumulation of potentially dangerous (flammable) hydrogen in either location while personnel were present. These sensors have higher resolutions, but can measure only 0 to 4 percent hydrogen concentrations. The alarms were set to activate when hydrogen concentrations reached 1 percent (10,000 ppm) in air. Figure II-7 shows the two sensor types in their respective housings.

Figure II-7. Neodym Panterra (left) and HydroKnowz (right) sensors.

Hydrogen Sensor Locations. In hydrogen accumulation calibration tests, the ACS was instrumented with Neodym Panterra sensors in the trunk and passenger compartment. Each compartment contained a suite of hydrogen sensors, positioned as follows:

- 3 in the trunk compartment;
- 3 in the rear of the passenger compartment; and
- 3 in the front of the passenger compartment.

Each compartment contained sensors positioned at 10 percent, 50 percent, and 90 percent of the vertical compartment dimension. The sensor suites were aligned with the centerline of the ACS. The sensor positions were in the same positions employed in the Task 2a test vehicle. The face of each sensor was oriented downward to aid in detection of rising hydrogen. The sensor positions also were referenced to the leading edge of the front of the ACS framework, subsequently referred to as the sensor reference point.

Trunk compartment sensors were located approximately 138 in. back from the sensor reference point, Figure II-8. Sensors were mounted along a vertical pole that extended from the trunk bottom inside surface to the top inside surface, covering a vertical dimension of approximately 15.5 in. This sensor array was positioned above the spare tire location.

Figure II-8. Position of trunk compartment sensor suite at 10 percent, 50 percent, and 90 percent height.

The rear passenger compartment sensors were mounted in a similar fashion, Figure II-9, and were located approximately 107 in. from the vehicle sensor reference point. The compartment height, approximately 35 in., was defined as the rear passenger seat (trunk floor) to the roof panel.

Figure II-9. Position of rear passenger compartment sensor suite at 10 percent, 50 percent, and 90 percent height.

The front passenger compartment sensors were placed approximately 76.25 in. back from the reference point, Figure II-10. The sensors were mounted on a pole placed on the front seat and extended to the roof panel, approximately 38.25 in.

Figure II-10. Position of front passenger compartment sensor suite at 10 percent, 50 percent, and 90 percent height.

During ignition tests, up to two hydrogen sensors were present in the ACS as a check to verify that hydrogen concentrations were tracking with the concentration calibration curve. Limited hydrogen sensors were employed because of the potential for damage from exposure to high heat and high pressure during combustion. When used they were mounted at the 50 percent front passenger and trunk positions.

Hydrogen Leak Locations: The flow of hydrogen originated from specific locations within the ACS. These leak locations replicated the locations used in the Task 2a testing: directly into the trunk and directly into the rear passenger compartment. In Task 2a, additional leak locations were underneath the vehicle; however, this position did not create an appreciable accumulation of hydrogen in vehicle compartments.

The leak originating from the trunk, Figure II-11, was positioned near the bottom of the ACS trunk compartment, 8 in. forward of sensor mounting post, with the nozzle aligned so that the hydrogen flow was directed towards the front of the ACS.

Figure II-11. Hydrogen leak originating in trunk, flow towards the front of the ACS.

The leak originating from the passenger compartment, Figure II-12, was positioned near the floor of the ACS, 7 in. forward of the rear passenger sensor mounting post, with the nozzle aligned so that the hydrogen flow was directed towards the rear of the ACS.

Figure II-12. Hydrogen leak originating in rear passenger compartment, flowing to rear of ACS.

Manikin. During the ACS ignition tests, an instrumented and articulated manikin, Figure II-13, was used to measure relevant burn (heat flux) and overpressure injury characteristics from the combustion of hydrogen mixtures. This anthropometric test device is a Hybrid III (RA Denton) representing the 50th percentile male pedestrian (height of 5 ft, 6 in.; weight of 170 lbs). This manikin had heat flux sensors and/or pressure transducers mounted in the head, torso, arms, hands, and legs. This fully operational manikin was seated in the ACS driver's seat during ignition testing.

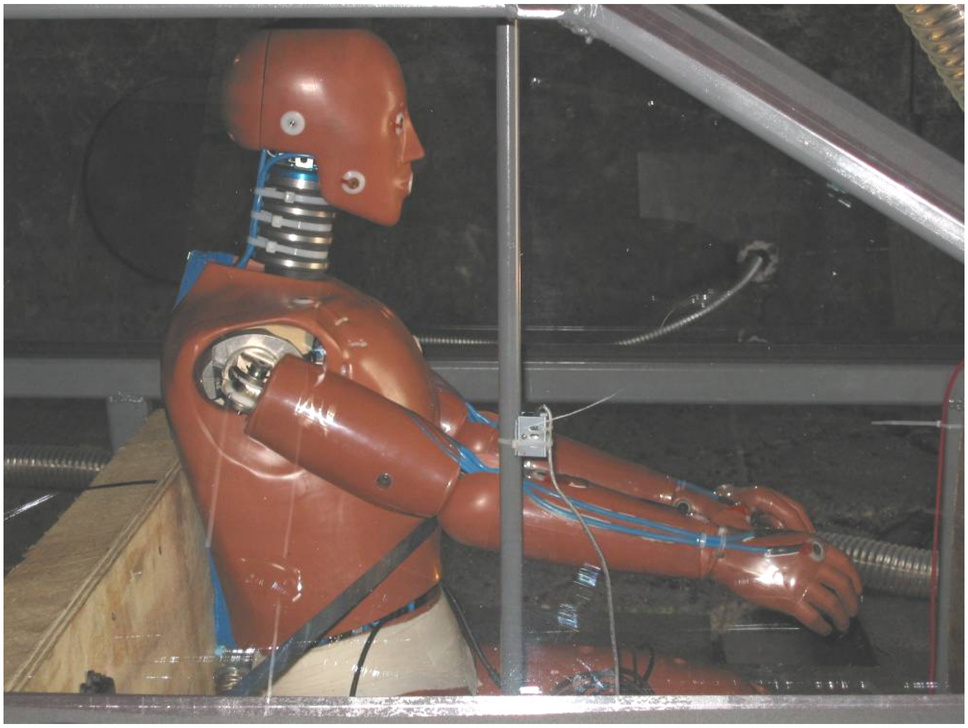

Figure II-13. 50th percentile Hybrid III articulated, instrumented manikin in the ACS.

Heat Flux Sensors. Vatell HFM7-E/L heat-flux sensors with modified housings were used for acquiring heat flux data during ignition testing. The sensors have a reported response time of 17 μsec and were calibrated to approximately 100+ $\mu V/W/cm^2$.

Heat Flux Sensor Locations. The heat flux sensors were placed at several discrete positions within the manikin to capture thermal data which could be processed using BURNSIM, a burn injury assessment computer program. BURNSIM can determine the temperature, degree of burn injury (first-, second-, or third-degree) and depth of burn on the skin (burn threshold depth) at different areas on the manikin. Heat flux sensors were mounted at the following locations on the manikin, as shown in Figure II-14.

- right eye (A)
- right cheek (B)
- left cheek (C)
- right shoulder (D)
- right underarm (E)
- left underarm (F)
- right inner elbow (G)
- right inner wrist (H)
- left outer wrist (I)
- right palm (J)
- left backside hand (K)
- right hand between fingers (L)
- left hand between fingers (M)
- groin (N)
- right back knee (O).

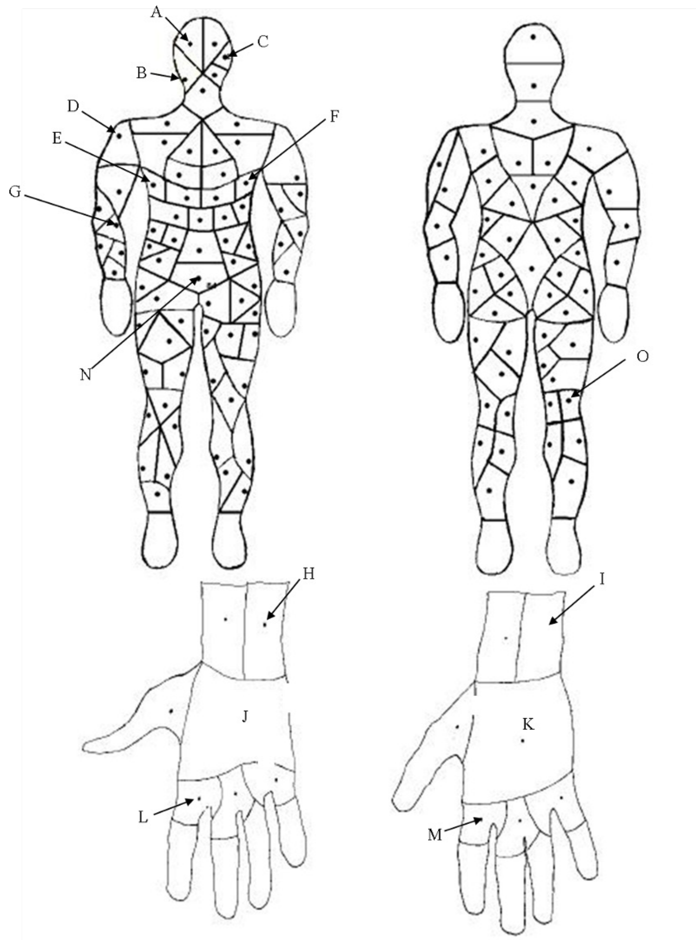

Figure II-14. Heat flux sensor locations on manikin.

One additional heat flux sensor was positioned on a test stand approximately 57 in. from the centerline of the ACS (≈ 37 in. from the roof edge) and just forward of the B pillar. The sensor was aligned with the vertically stacked timbers representing the front passenger seat back, 65 in. above the test chamber floor. This sensor was used to measure the thermal exposure to be experienced by personnel, such as a first responder, approaching the outside of the automobile. Some ignition tests did not use all sensors due to damage to the sensors and electronics. The sensors that were not used for each test will be noted in the discussion of the test results.

Overpressure Transducers. PCB ICP pressure sensors, model 102A16, were used to capture blast overpressure data during ignition testing. The reported response time (reflected shock) of the pressure sensors is ≤ 1.0 μsec, and the sensors were calibrated to ≈ 50 mV/psi.

Overpressure Transducers Locations. The four overpressure transducers were situated either in the manikin or on the test stand outside of the ACS. The three transducers in the manikin were located at the following positions:

- right ear,
- mouth, and
- left chest.

The transducer placed on the test stand was approximately 57 in. from the centerline of the ACS, aligned with the front passenger seat back, 61.8 in. above the test chamber floor (a few inches below the heat flux gauge).

Ignition Source. A standard small gasoline engine spark plug was employed as the spark source. The spark plug was connected to a 100 J Cordin 640 Pulser. The pulser's energy delivery circuitry consisted of a charged capacitor and spark gap trigger. The charging voltage was 5000 V and the discharge time was a few μsec.

The spark plug was positioned on the dashboard for all ignition tests, except the 5 percent concentration tests. In these tests, the spark plug was moved near the leak point to ensure adequate hydrogen was available to start the ignition process. The spark plug was positioned approximately 9 in. above the leak and 4 in. away from the leak in the direction of flow.

Cameras. Still photographs were employed to capture setup work involving the ACS preparation, sensor installation and alignment, static dissipative matting and grounding system installation, venting system installation, data acquisition setup, and gas supply line integration. Photographs also were taken to document each test. Details of the aforementioned test systems are shown in Appendices A–D.

A standard speed video camera was used throughout the task to capture any unexpected events during accumulation calibration tests and to record real-time data for the ignition tests. This camera was placed in one of the chamber view ports. A translucent Lexan panel was placed over the chamber viewing port on the chamber side to protect the camera from possible damage. The real-time feed from this camera was captured, monitored, and temporarily recorded using a television and DVD recorder located inside the control room.

A Vision Research Phantom v7.3 high-speed imager also was employed during all ignition tests to capture the ignition and subsequent combustion of hydrogen. The imager was mounted in the same port as the standard video camera and was setup to record at a rate of 200 frames per second (fps) with a 600 × 800 pixel resolution. The exposure time was 4.7 msec.

BURNSIM. The heat flux measurements were processed using BURNSIM to predict potential burn injury. BURNSIM[(6)] uses heat flux data to compute the tissue temperature as a function of exposure time and depth. Using this temperature information, BURNSIM estimates the tissue damage at a particular depth by integrating an Arrhenius rate equation (the damage integral). The value of the damage integral then determines the burn depth and, by extension, the degree of injury.

The threshold depth is the maximum depth the burn achieves during an exposure. The extent of injury, or burn degree, is determined by the burn threshold depth. If this depth is less than the depth of the epidermal/dermal interface (approximately 100 microns), the injury is considered a first-degree burn. The result is reddening of the skin. Second-degree burns are those injuries in which the threshold depth lies between the epidermal/dermal and dermal/subcutaneous (approximately 1,500 microns) interfaces. The result is blistering. Third-degree injuries are those burns in which the skin tissue is completely damaged, i.e., the burn threshold depth reaches or exceeds the dermal/subcutaneous interface. The result is destroyed and charred tissue.

RESULTS AND DISCUSSION

Test Matrix. Task 2b was performed by conducting two types of tests: accumulation calibration tests and ignition tests as shown in Table II-2. Hydrogen accumulation calibration initially focused on obtaining a representative leakage rate between the trunk and passenger compartments of the ACS. Additional openings were added to the separation panel until the exchange flow between the two was characteristic of the Task 2a test vehicle.

Ignition testing commenced after calibration curves had been measured and were reproducible. At least one hydrogen sensor was present in each ignition test as a monitor to verify that the accumulation was following the expected trend.

Table II-2. Test matrix for Task 2b accumulation and ignition tests.

Accumulation Tests		
Leakage Location	**Test #**	**Leak Duration (min:sec)**
Trunk	16	10:00
	17	10:00
	18	37:35
	19	20:00
	20	15:00
	21	30:00
	30	60:00
	31	30:00
Passenger compartment	22	30:00
	23	30:00
	27	60:00

Ignition Tests			
Leakage Location	**Test #**	**Hydrogen Concentration (%)**	**Leak Duration (min:sec)**
Trunk	32	5	1:30
	33	15	4:30
	34	60	24:30
Passenger compartment	24	15	5:00
	25	15	4:30
	26	30	20:00
	28	60	24:30
	29	5	1:30

Hydrogen Accumulation Calibration. Hydrogen accumulation calibration tests were performed with the ACS at the reference leak rate of 118 lpm in two leak positions: the trunk and passenger compartments. Panel seams on the ACS were taped iteratively to adjust hydrogen accumulation levels. In the end, the best performance was obtained when the ACS was sealed as completely as possible. The ACS was used in this configuration for the majority of the ignition tests.

In general, the ACS was configured to replicate qualitatively the time-dependent hydrogen concentration data measured in Task 2a. Although the dimensions and volumes of the ACS were similar to the Task 2a test vehicle, the flow characteristics of hydrogen and its accumulation were not, particularly early in the leak cycle when concentrations were low. An important observation in this test series and Task 2a was that the flow characteristics of hydrogen were complex in nature, apparently as the result of its low density.

The large changes in hydrogen accumulation witnessed when small test changes were made, such as taping a few additional seams, indicate that different makes and models of automobiles likely exhibit significant differences in hydrogen accumulation characteristics. Further efforts to modify the ACS were abandoned; it became apparent that the ACS could never mimic exactly the accumulation characteristics of the Task 2a test vehicle with regard to time. Target concentrations, however, were readily achieved and provided the necessary conditions required for ignition testing.

Final accumulation calibration curves for a 118 lpm leak rate located in the trunks of the Task 2a test vehicle and ACS are shown in Figure II-15. As indicated in the ACS plots, the geometry had a tendency to trap a pocket of air in the roof area of the passenger compartment, probably because of the flatness of the roof panel and compartment symmetry. The 50 percent sensor height positions initially showed the highest concentrations of hydrogen in each calibration test. Eventually, the hydrogen bubble breached the air pocket and displaced it, leading to a rapid increase in concentration at the 90 percent height. The trunk was somewhat better in terms of response, probably because of the turbulence created by the leak.

The yellow band in the plots denotes the 4 percent to 75 percent range of hydrogen concentration, i.e., the mixture is within the flammable range in air. The darker yellow band denotes the 28 percent to 32 percent range; the mix has reached the stoichiometric concentration (~30%).

Hydrogen Concentrations

Leakage Flow Rate: 118 lpm | Leak Location: Trunk Compartment

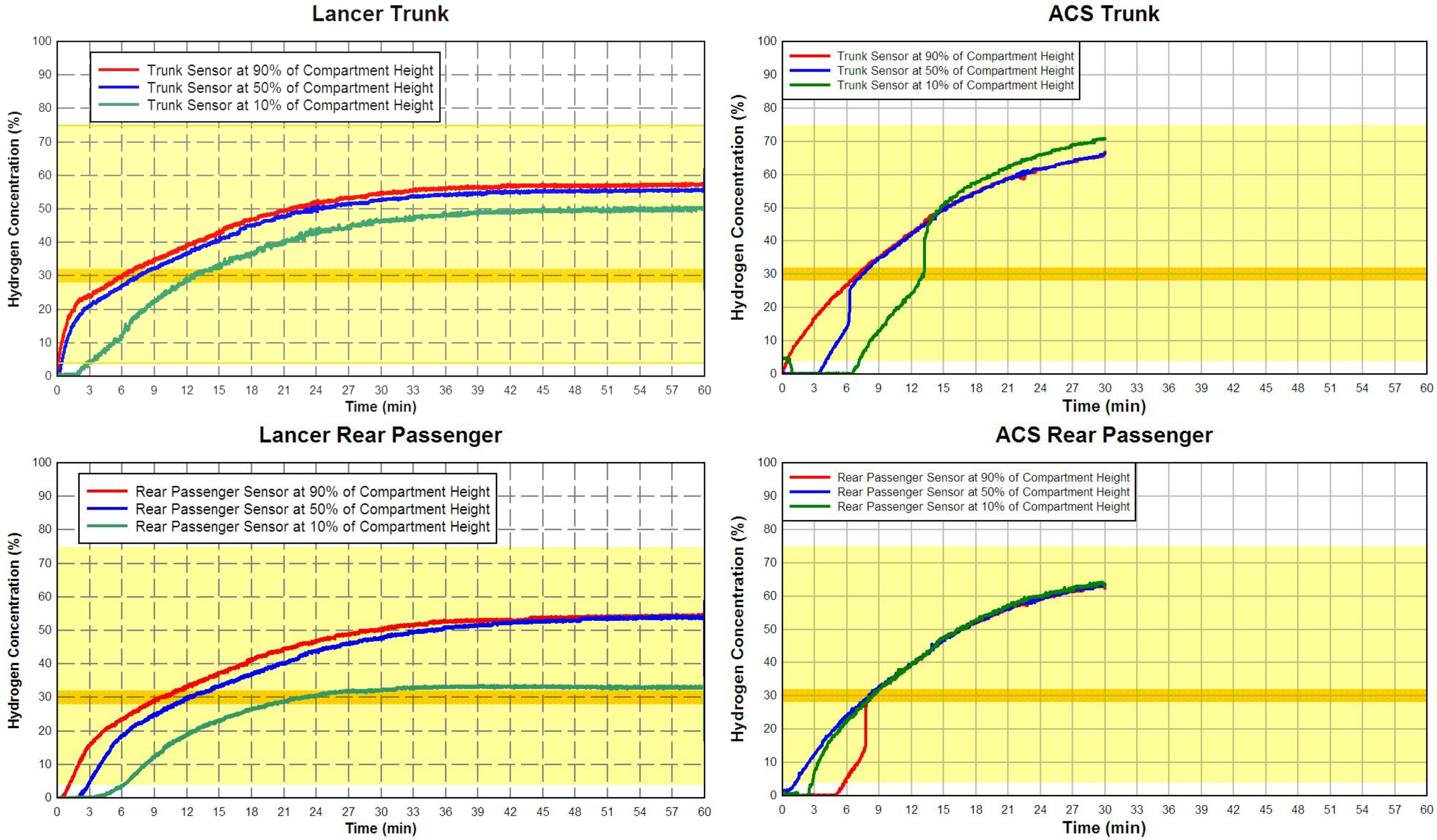

Figure II-15. Comparison of calibration profiles for 118 lpm leak rate in trunk for Task 2a intact vehicle (left) and Task 2b ACS (right).

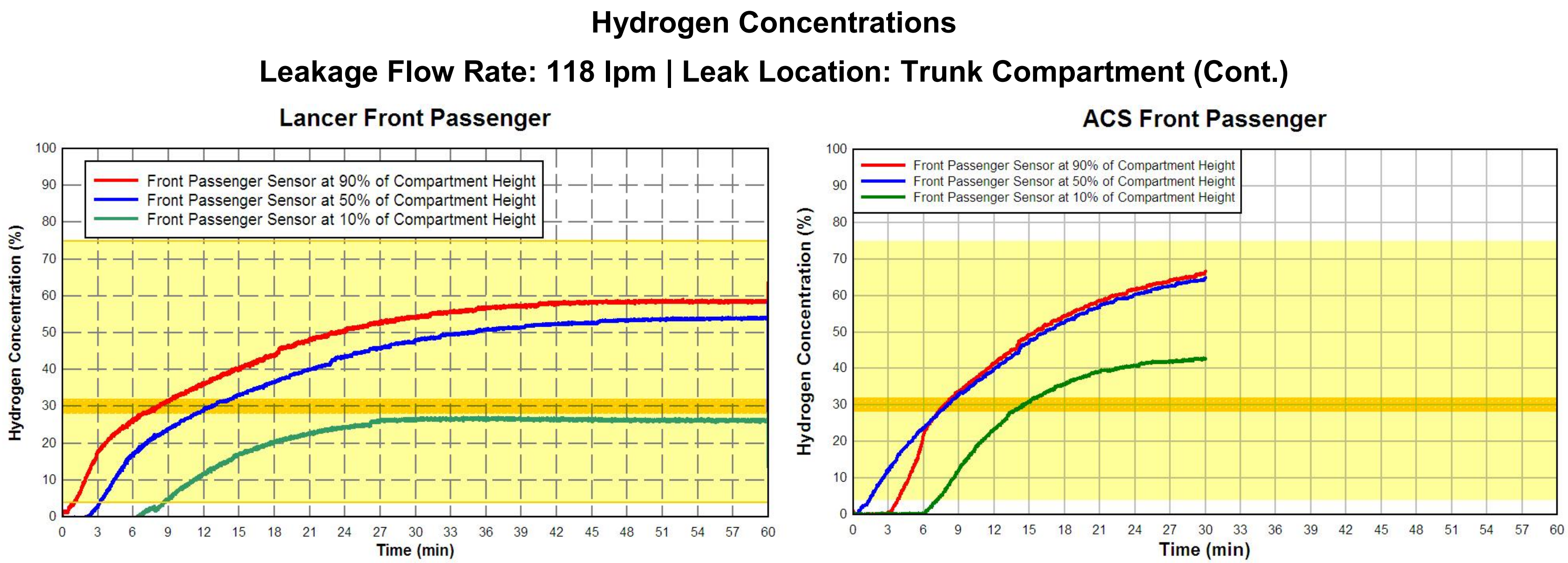

Figure II-15. Comparison of calibration profiles for 118 lpm leak rate in trunk for Task 2a intact vehicle (left) and Task 2b ACS (right). (Cont.)

Final accumulation calibration curves for the 118 lpm leak located in the passenger compartment of the Task 2a test vehicle and the ACS are shown in Figure II-16. Accumulation characteristics were similar to the plots presented above because both the test vehicle and ACS allowed free exchange of flow between the trunk, back and front passenger compartments.

Hydrogen Ignition Tests. Ignition tests on mixtures of 5 percent, 15 percent, 30 percent, and 60 percent hydrogen in air were conducted using the ACS. Heat flux and pressure sensors were placed inside and outside the ACS to acquire fireball thermal and blast overpressure data. Ignition tests were performed with leaks located in trunk or rear passenger compartment. Only one ignition test was performed at the stoichiometric level of hydrogen (30%) due to the damage inflicted to the sensors on the instrumented manikin from blast overpressure incited motion.

All but one or two of the nine hydrogen sensors used in ACS calibration tests were removed during ignition testing to minimize the number of sensors exposed to the explosive environment.

One sensor was retained in the ACS at the 50 percent level in the front of the passenger compartment; a second one was positioned at the 50 percent level in the trunk on some tests. These sensors served as a check during the hydrogen fill portion of the ignition tests to confirm that the level of accumulation in the ACS matched the concentration calibration data.

Prior to the start of testing, the ACS calibration curves were analyzed to determine when to spark the flammable mixtures. The time of ignition selected was when the sensor at the 50 percent front passenger position reached the target concentration. The unique times for the 5 percent, 15 percent, 30 percent, and 60 percent levels hydrogen are listed in Table II-2. This methodology allowed a single hydrogen sensor at a fixed position distant from the leak sites to confirm that the target hydrogen level had been achieved.

The spark plug used for ignition was positioned near the middle of the dashboard for all tests, except the ones at the 5 percent concentration level. In these tests, the spark plug was moved near the leak point to ensure adequate hydrogen for ignition. The spark plug was positioned approximately 9 in. above and 4 in. away from the leak in the direction of flow.

Ignition time was defined as the time the spark was applied. For hydrogen and other flammable gases, combustion occurs after the application of sufficient spark discharge energy at either subsonic (deflagration) or supersonic (detonation) rates. This interval between spark ignition and combustion is called the ignition-delay or induction time, which is dependent on concentration. Combustion and flame follow this induction time, starting at deflagration and proceeding to detonation at certain conditions. For hydrogen, the detonation limits are 18 percent to 59 percent.

In the following sections, each ignition test is discussed in detail in terms of test setup, hydrogen concentration at the time of sparking, heat flux and overpressure data acquired, degree of burn injury predicted by BURNSIM, physiological blast injury as predicted by peak pressure, and fireball characteristics as observed using high-speed imagery.

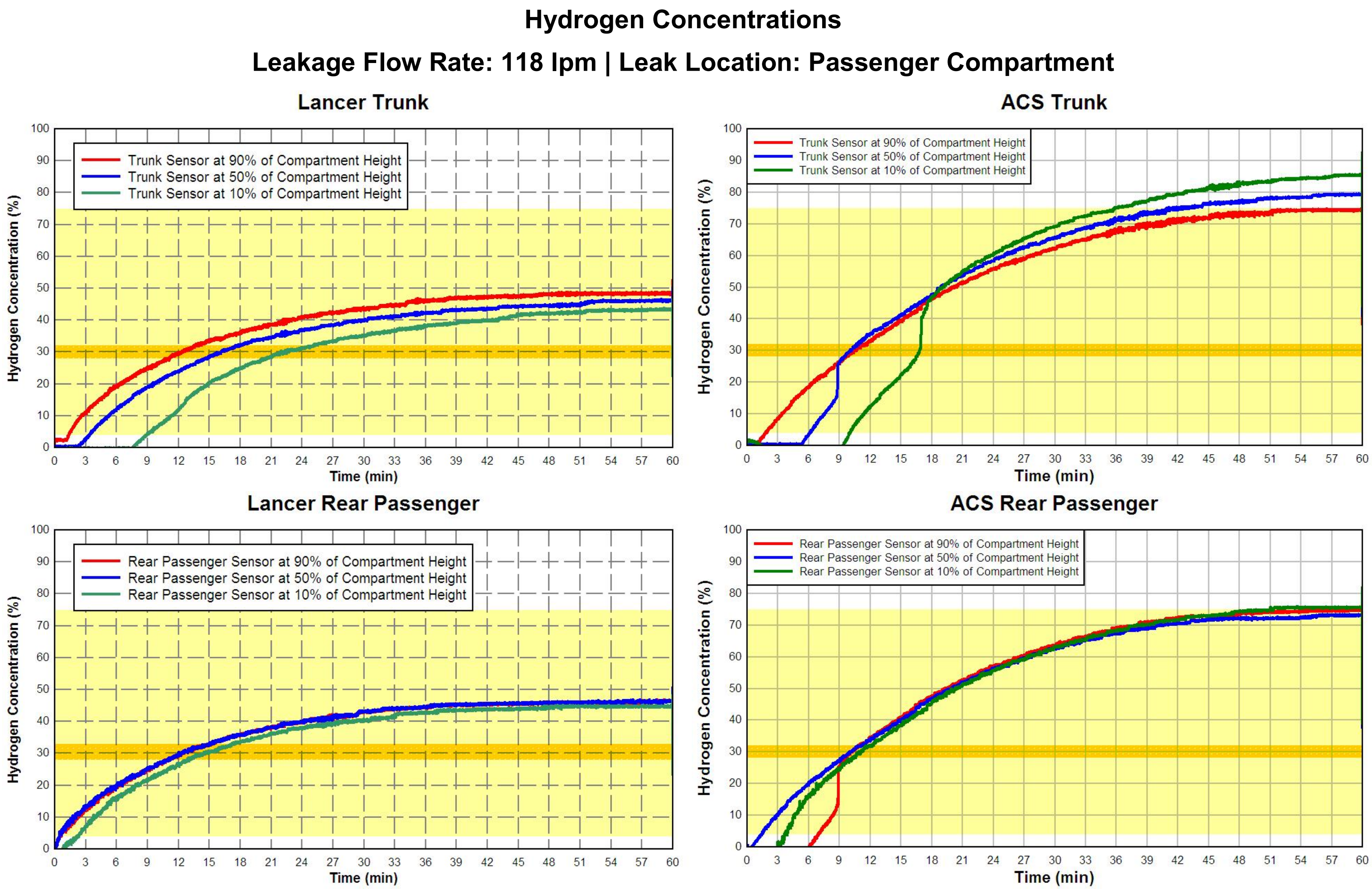

Figure II-16. Comparison of calibration profiles for 118 lpm leak rate in passenger compartment for Task 2a intact vehicle (left) and Task 2b ACS (right).

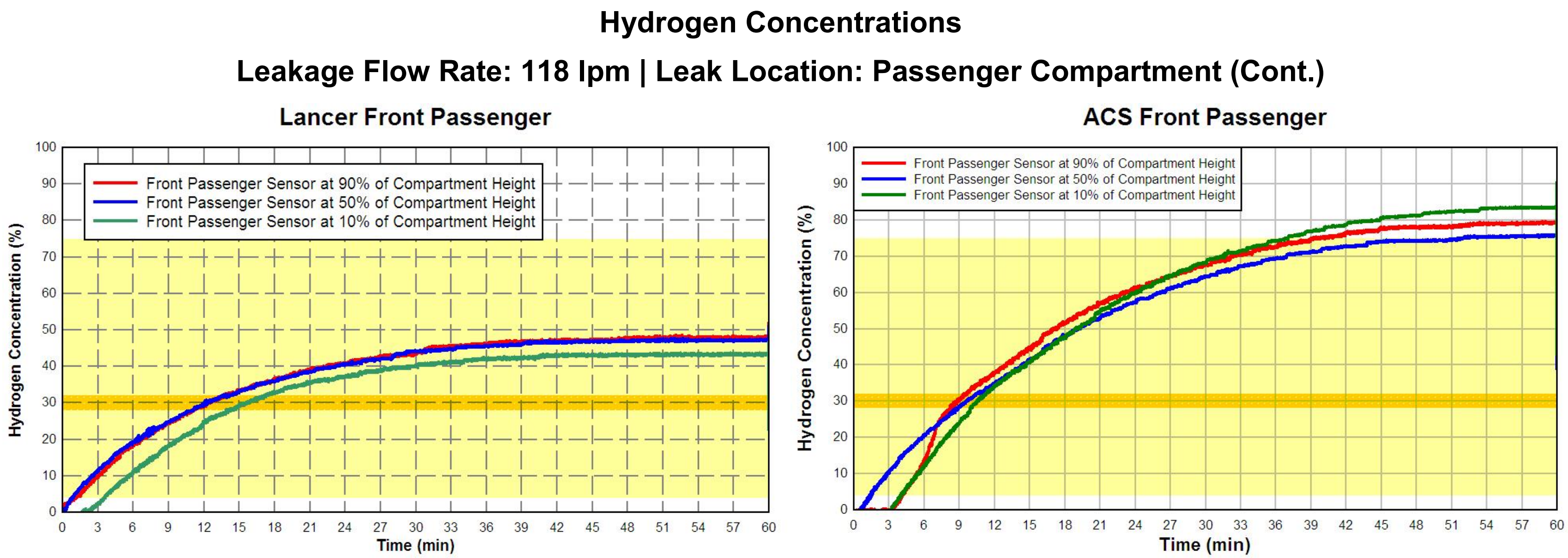

Figure II-16. Comparison of calibration profiles for 118 lpm leak rate in passenger compartment for Task 2a intact vehicle (left) and Task 2b ACS (right). (Cont.)

Test 32: 5 Percent Ignition, Trunk Leak. All exterior seams were taped, including the bottom panels. Lexan panels were used in most locations to provide a better view of the ignition and combustion propagation. Also, as testing progressed (this test was near the end of the series), Lexan was favored over sheet steel due to its robustness. The ignition source was located in the trunk. Heat flux sensors located in the right underarm, right back knee, left outer wrist, and left cheek of the manikin were not used in this test. Hydrogen sensors were located at the 50 percent heights of the front passenger and trunk compartments. The test setup is shown in Figure II-17.

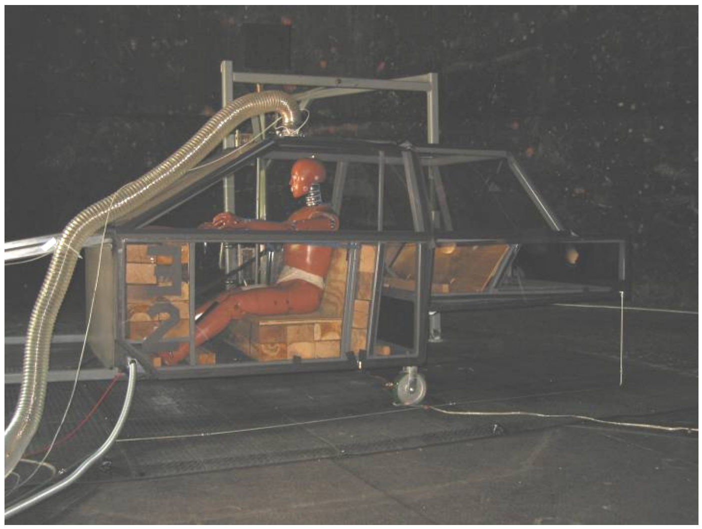

Figure II-17. Test 32 ACS setup.

The ignition time was 1.0 min, 30 sec at which time the 50 percent front passenger compartment sensor was expected to reach 5 percent. A bar graph comparing the concentrations of the Task 2a test vehicle, ACS, and Test 32 is shown in Figure II-18. The graph shows corresponding concentrations during Lancer and ACS Calibration trials when the 50 percent front passenger sensor registered 5 percent. ACS ignition concentrations were as-measured at the time of ignition. The hydrogen concentration at the front passenger monitor position was somewhat lower than during calibration tests and was somewhat higher in the trunk. This variance was common at the 5 percent concentration because of the small amount of hydrogen leaked into the large volume. Concentrations at levels of higher accumulations were more consistent.

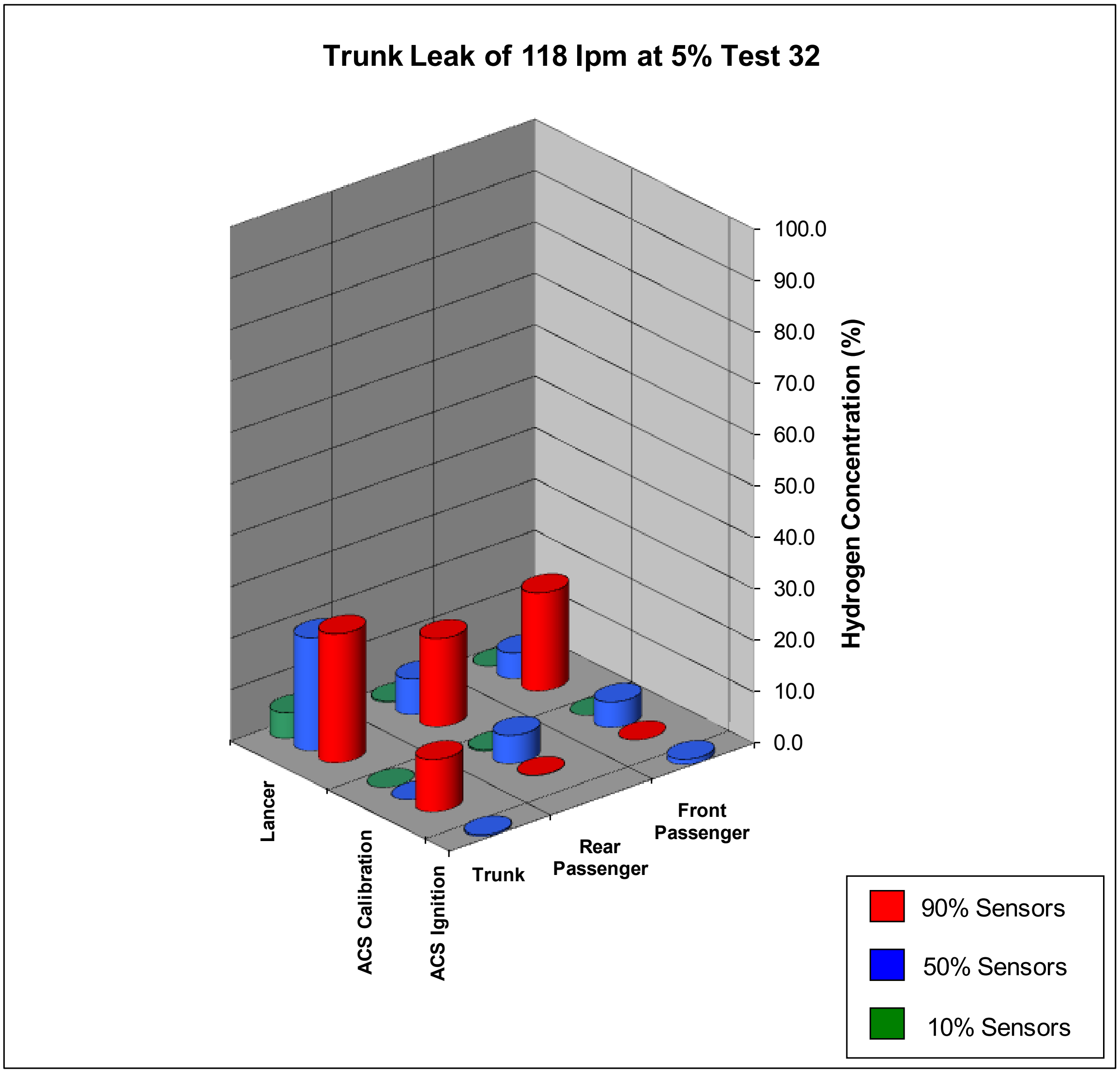

Figure II-18. Concentrations in the Task 2a test vehicle and Task 2b ACS during calibration and at ignition (118 lpm and 5%).

Sensors located in the right cheek and right eye detected heat fluxes that could cause first- and second-degree burns, respectively. A complete heat flux data set is available in Appendix G. The sensor on the test stand outside the ACS did not register any measurable heat flux.

Burn injury predictions from BURNSIM are shown in Figure II-19; temperature and burn threshold depths corresponding to these burns are shown in Table II-3.

No detectable overpressure was observed; no injury potential from blast would be expected.

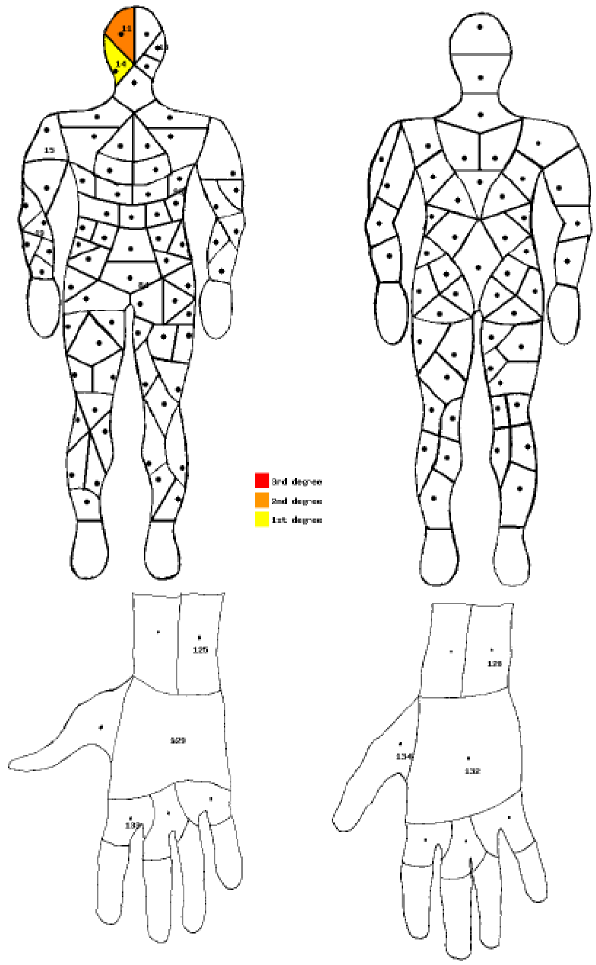

Figure II-19. BURNSIM results on manikin for Test 32 (5% hydrogen).

Table II-3. BURNSIM data for Test 32 (5% hydrogen).

Sensor Location	Degree of Burn	Maximum Temperature (^oC)	Burn Threshold Depth (μm)
Right Eye	2nd	75	183
Right Cheek	1st	62	175

Stills from the high-speed imagery are shown in Figure II-20. The first visible combustion occurred at approximately 260 msec, was small in size, and remained in the trunk area. The combustion was visible only for about 28 msec after being detected. The imagery also shows a few panels coming off the ACS as a result of a small overpressure inside.

Figure II-20. High-speed still image at 254 msec (left) and 264 msec (right).

Test 33: 15 Percent Ignition, Trunk Leak. All seams were taped; hydrogen sensors were mounted at the 50 percent front passenger compartment and trunk locations; and Lexan was used for most panel locations. The ignition source was located on the dashboard. The heat flux sensors located in the right back knee, right underarm, left cheek, right inner wrist, and left outer wrist were not used in this test. A photograph of Test 33 is shown in Figure II-21.

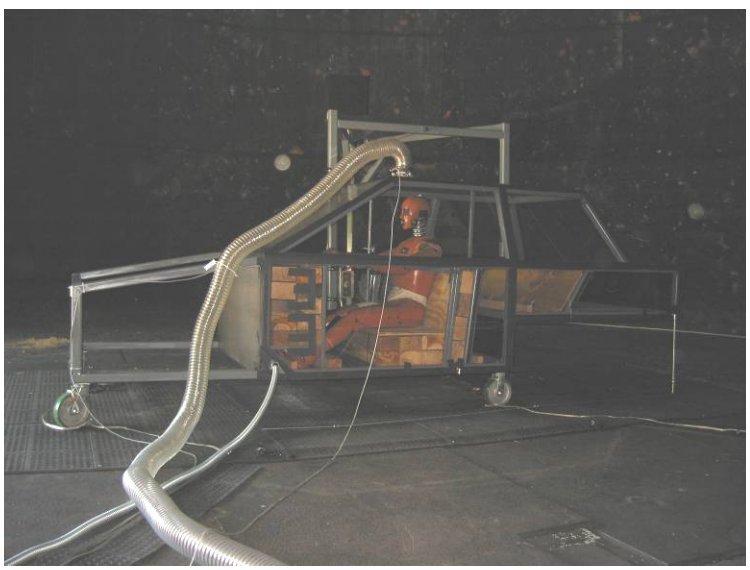

Figure II-21. Test 33 ACS setup.

The ignition time was 4 min, 30 sec. A bar graph comparing the concentrations of the Task 2a test vehicle, ACS, and Test 33 is shown in Figure II-22. Only the 50 percent front passenger hydrogen sensor recorded data during this ignition test; the 50 percent trunk sensor did not respond.

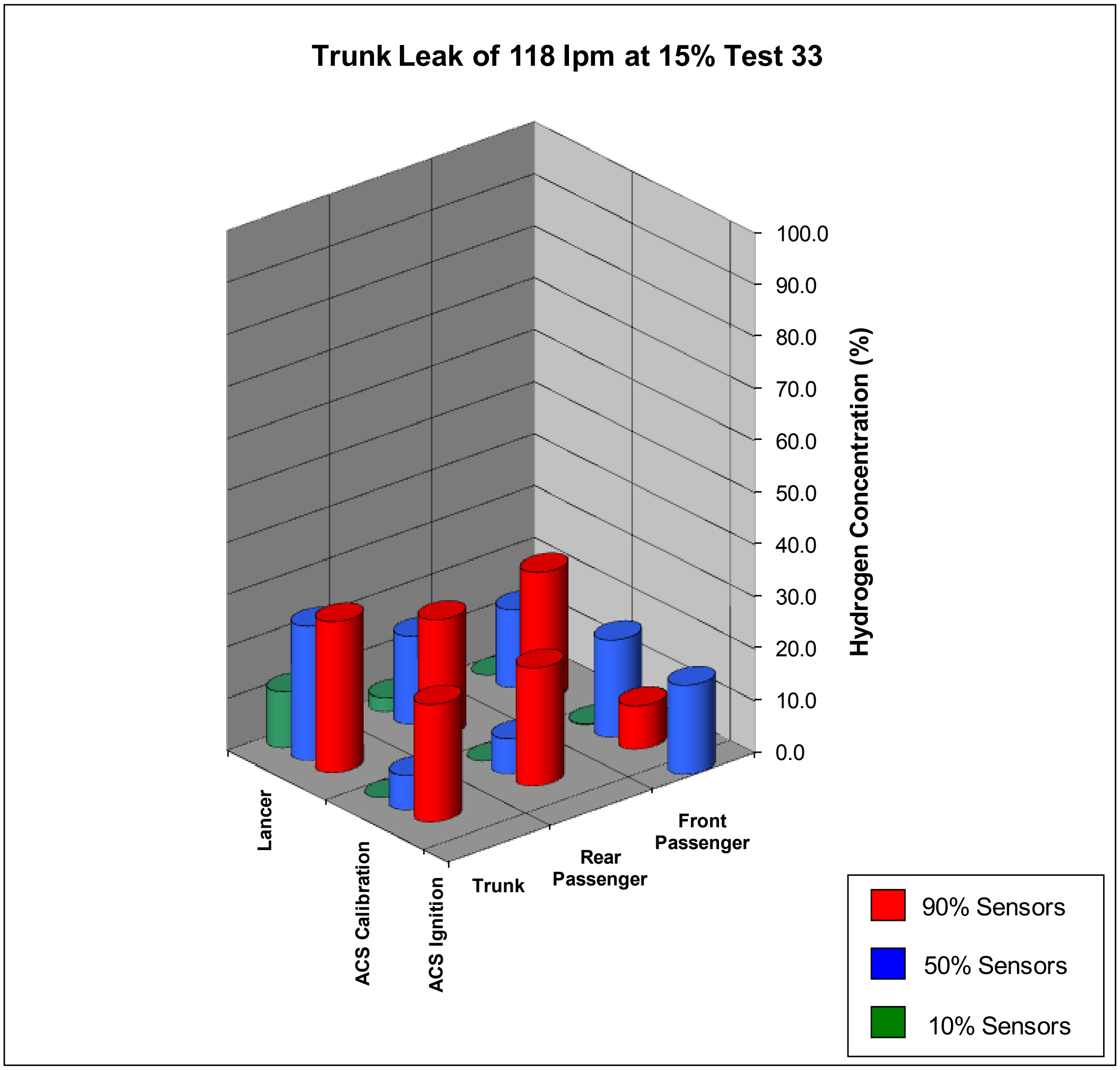

Figure II-22. Concentrations in the Task 2a test vehicle and Task 2b ACS during calibration and at ignition (118 lpm and 15%).

Sensors in the right eye, right cheek, right shoulder, right inner elbow, groin, left underarm, right hand palm, right hand between fingers, and left hand between fingers detected heat fluxes that could cause second-degree burns. Heat flux data at these locations are presented in the complete data set in Appendix G.

Burn injury predictions from BURNSIM are shown in Figure II-23. BURNSIM also was used to predict the maximum temperature and the depth of skin burned as a result of these heat fluxes. These results are shown in Table II-4.

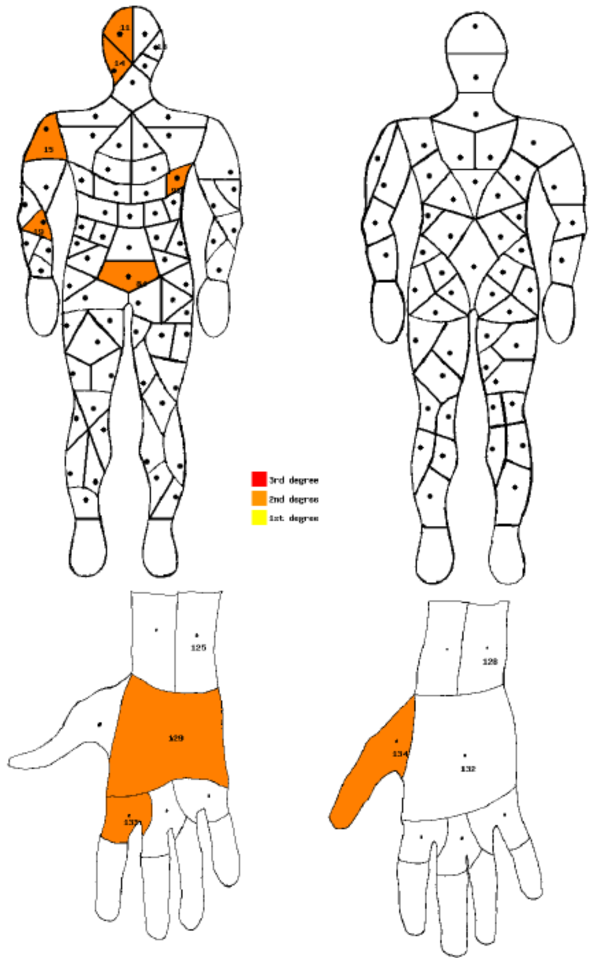

Figure II-23. BURNSIM results on manikin for Test 33 (15% hydrogen).

Table II-4. BURNSIM data for Test 33 (15% hydrogen).

Sensor Location	Degree of Burn	Maximum Temperature (^oC)	Burn Threshold Depth (µm)
Right Eye	2nd	178	319
Right Cheek	2nd	174	392
Right Shoulder	2nd	225	354
Right Inner Elbow	2nd	165	320
Groin	2nd	178	385
Left Underarm	2nd	154	220
Right Hand Palm	2nd	131	188
Right Hand Between Fingers	2nd	163	361
Left Hand Between Fingers	2nd	173	341
Test Stand	None	55	0

No detectable overpressure was observed; therefore, there was no injury potential from blast.

Stills from the high-speed imagery are shown in Figure II-24. Because of the nonvisible luminosity of the flame, it was difficult to determine the initial combustion of the hydrogen/air mixture. The ignition source was located on the dashboard. Bulging of ACS panels was observed as early as 30 msec. The combustion event was not nearly as bright as the 30 percent or 60 percent hydrogen tests. The slight overpressure from the combustion caused panels to separate either partially or completely from the ACS framework.

Figure II-24. High-speed stills showing combustion in Test 33.

Test 34: 60 Percent Ignition, Trunk Leak. All seams were taped; hydrogen sensors were mounted at the 50 percent front passenger compartment and trunk locations; and Lexan was used for most panel locations. The ignition source was located on the dashboard. Heat flux sensors located in the right back knee, right underarm, left cheek, right inner wrist, and left outer wrist were not used. A photograph of Test 34 is shown in Figure II-25.

Figure II-25. Test 34 ACS setup.

The ignition time was 24 min, 30 sec. A bar graph comparing the concentrations of the Task 2a test vehicle, ACS, and Test 34 is shown in Figure II-26.

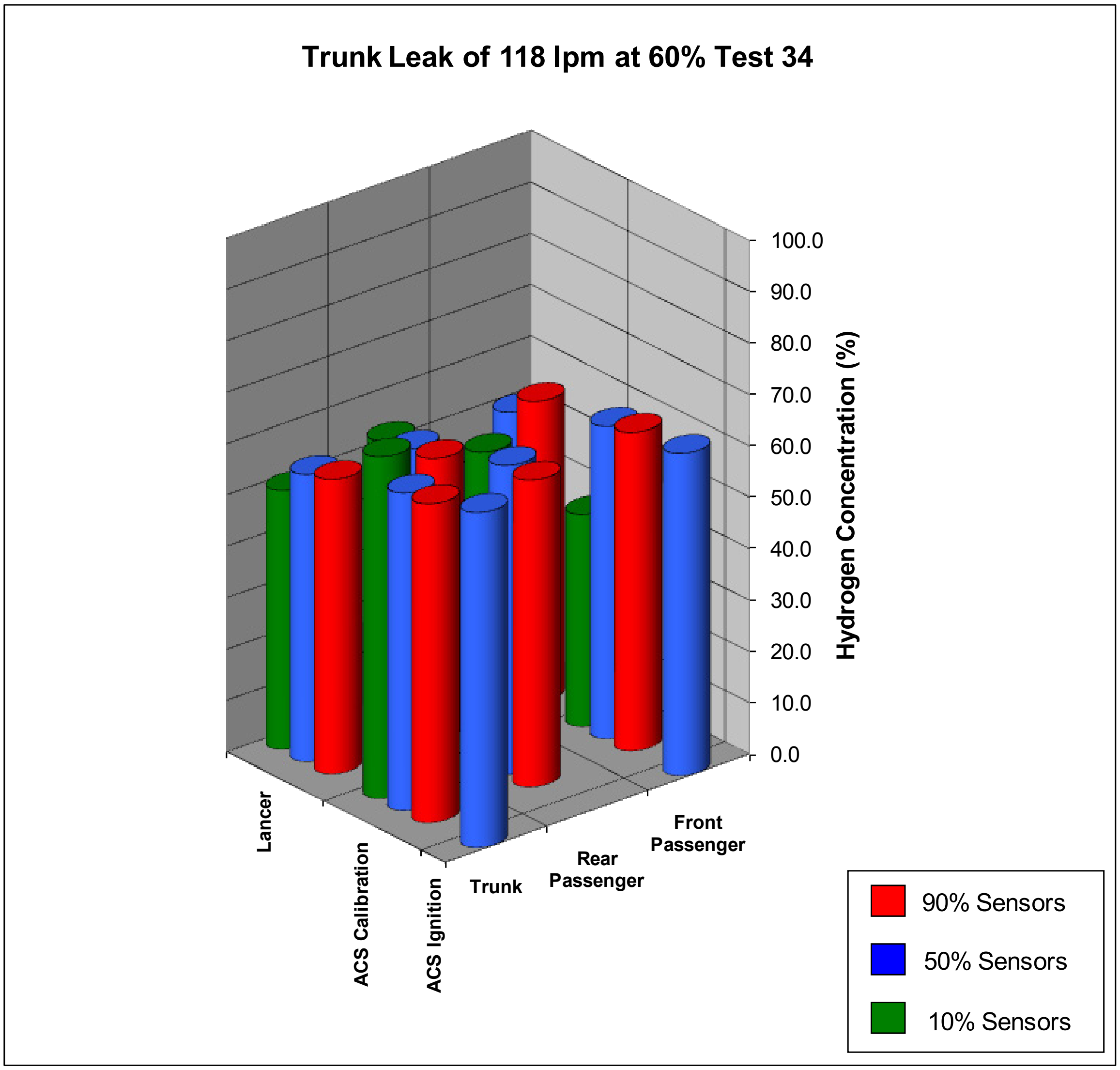

Figure II-26. Concentrations in the Task 2a test vehicle and Task 2b ACS during calibration and at ignition (118 lpm and 60%).

Heat flux sensors were located in the right eye, right cheek, right shoulder, right inner elbow, groin, left underarm, right-hand palm, right hand between fingers, and left hand between fingers. Each sensor detected heat fluxes that could cause second-degree burns. The complete thermal data set is presented in Appendix G.

Burn injury predictions from BURNSIM are shown in Figure II-27 for the sensors on the manikin and test stand; all correspond to a second-degree burn. BURNSIM also was used to predict the maximum temperature and the depth of skin burned. Results are listed in Table II-5.

The highest temperature occurred at the left hand between the fingers; the most severe burn threshold depth was located at the left underarm.

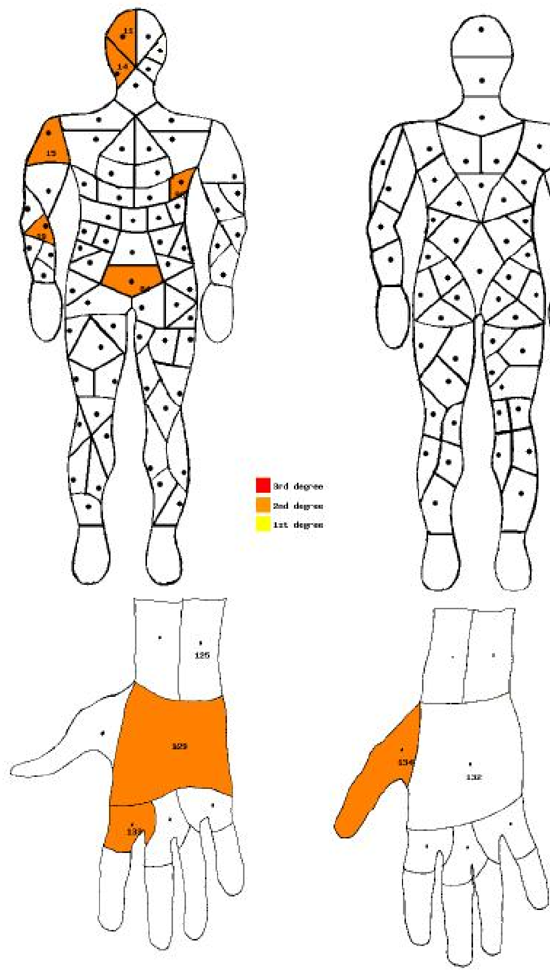

Figure II-27. BURNSIM results on manikin for Test 34 (60% hydrogen).

Table II-5. BURNSIM data for Test 34 (60% hydrogen).

Sensor Location	Degree of Burn	Maximum Temperature (^{o}C)	Burn Threshold Depth (µm)
Right Eye	2nd	226	631
Right Cheek	2nd	237	723
Right Shoulder	2nd	233	658
Right Inner Elbow	2nd	251	638
Left Underarm	2nd	170	770
Groin	2nd	231	698
Right Hand Palm	2nd	178	548
Right Hand Between Fingers	2nd	259	648
Left Hand Between Fingers	2nd	299	550
Test Stand	2nd	183	464

A small overpressure was detected during combustion. Figure II-28 shows that pressure slowly built to around 1.0 psi inside the ACS and registered only slightly more at the test stand after the panels yielded. This low pressure is near the detection limit of the pressure transducers. The negative trend observed for the manikin sensors is the result of lowering ambient pressure (loss of slight positive pressure during leak), exceeding the discharge time constant of the piezoelectric circuitry (a slow, long pressure for this type of transducers), and thermal effects from the long duration fireball. The physiological consequence of exposure to ≈ 1.0 psi is the rupture of eardrums in 20 percent of the exposed population[10].

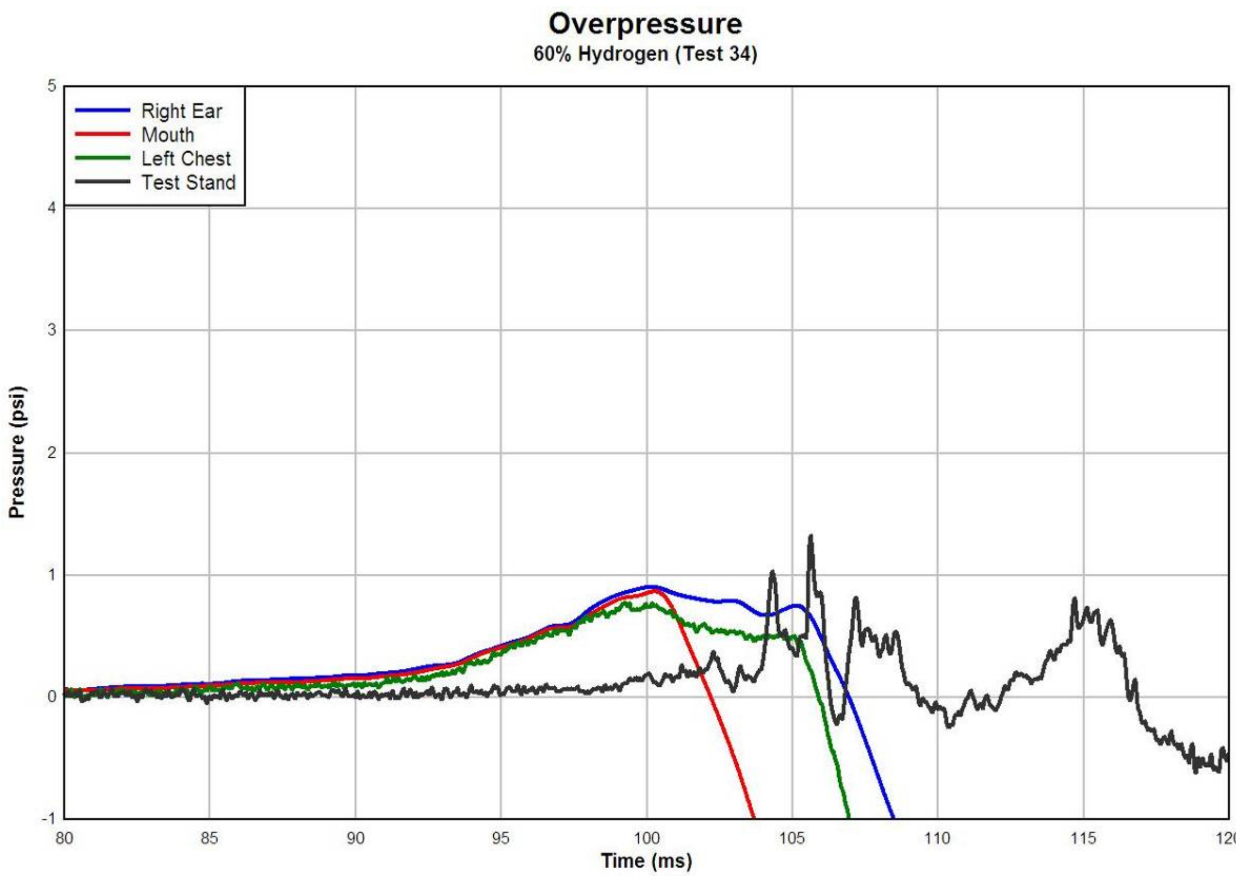

Figure II-28. Test 34 overpressure composite.

Stills from the high-speed imagery of Test 34 are shown in Figure II-29. These stills showed the onset of hydrogen combustion occurring approximately 90 msec after ignition (spark). Figure II-29 also shows the characteristics of combustion propagation. Compared to the 5 percent and 15 percent ignition Tests 32 and 33, respectively, the fireball at 60 percent is much larger and luminous.

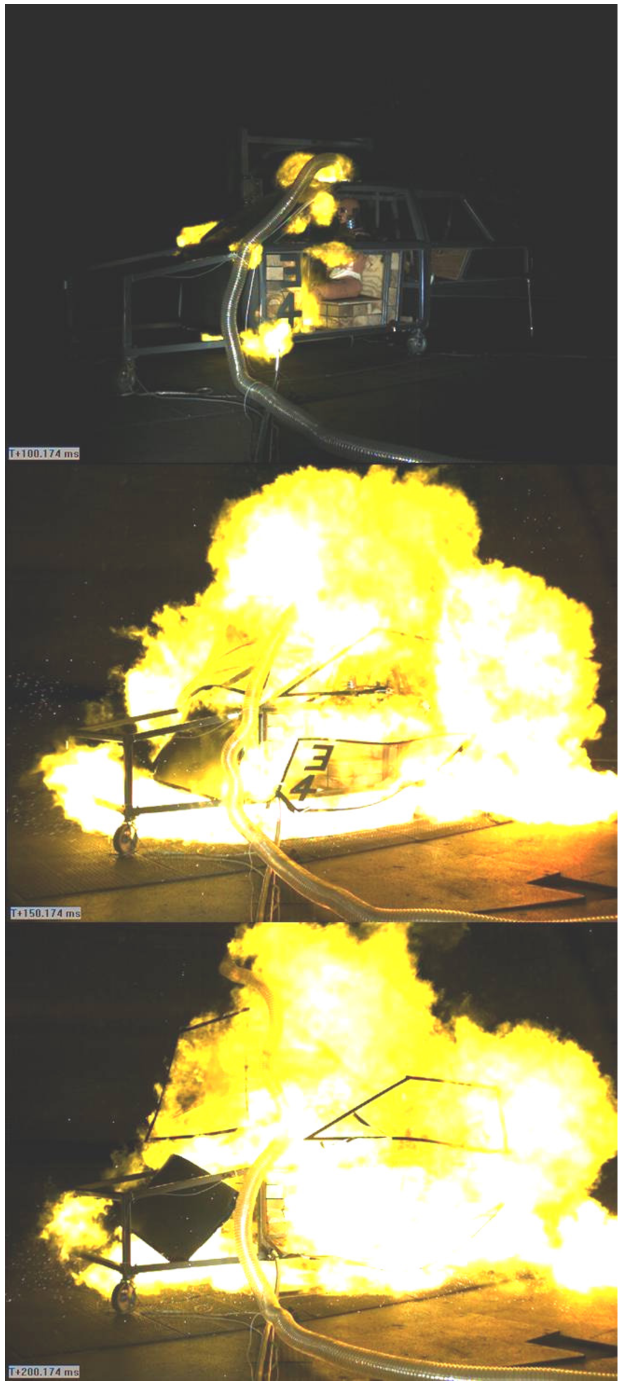

Figure II-29. High-speed stills showing combustion and panel separation in Test 34.

Test 29: 5 Percent Ignition, Passenger Leak. Steel panels were employed in all locations, except the windows and driver front side panel where Lexan was used. All exterior ACS panel seams were taped with duct tape, and hydrogen sensors were positioned at the 50 percent trunk and front passenger compartments. The ignition source was located on the dashboard. The right underarm, right back knee, left outer wrist, and left cheek sensors were not active in this test. The setup for Test 29 is shown in Figure II-30.

Figure II-30. Test 29 ACS setup.

The ignition time was 1.0 min, 30 sec. A bar graph comparing the concentrations of the Task 2a test vehicle, ACS, and the Test 29 is shown in Figure II-31. Evident in this figure is the difficulty in achieving a 5 percent accumulation in the ACS as compared to the Task 2a test car.

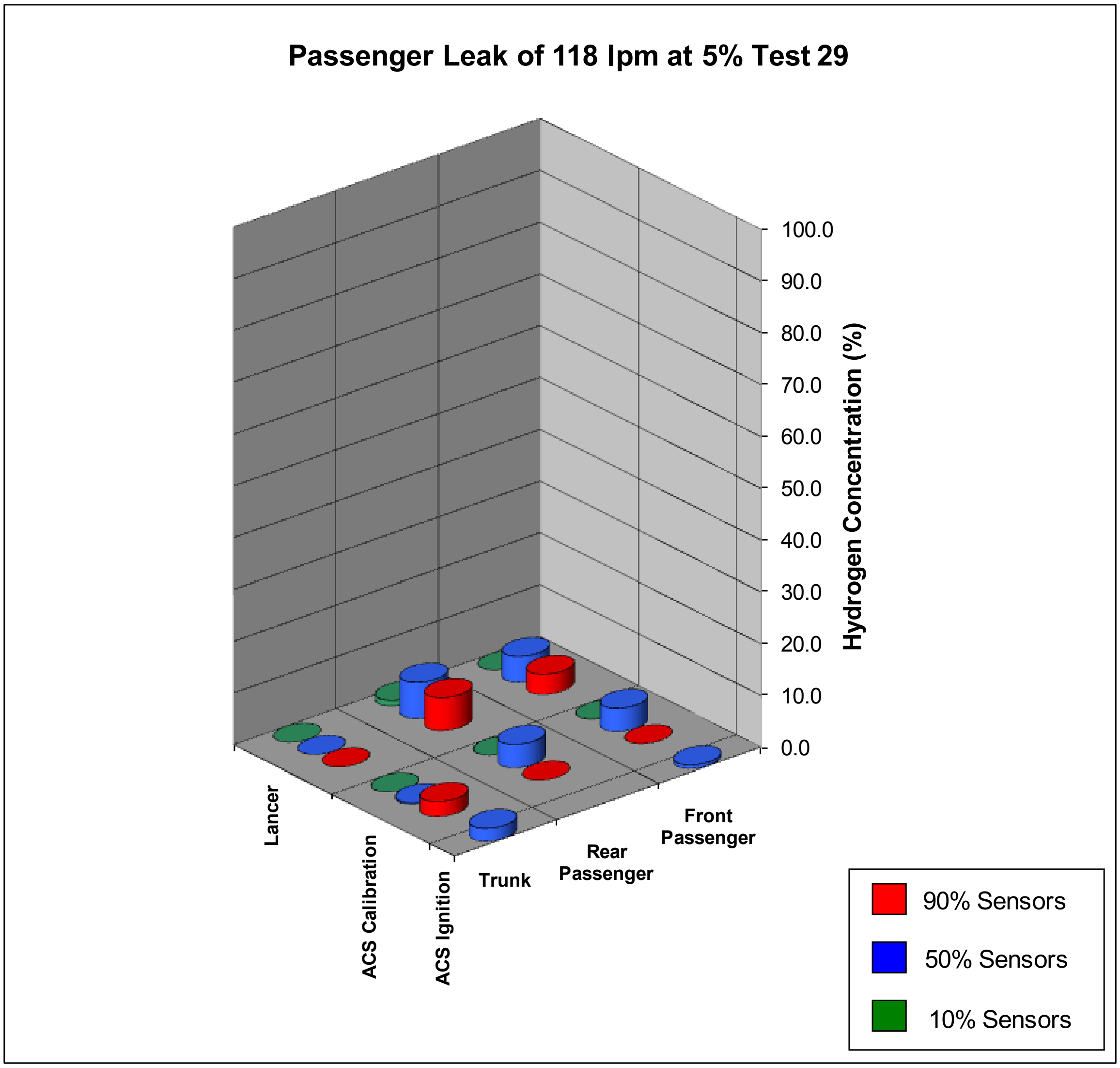

Figure II-31. Concentrations in the Task 2a test vehicle and Task 2b ACS during calibration and at ignition (118 lpm and 5%).

Heat flux sensors in the right eye, right cheek, right shoulder, right inner elbow, left underarm, right inner wrist, right hand between fingers, left hand between fingers, and left hand backside positions registered thermal levels that could result in first- or second-degree burns. The heat flux sensor on the test stand outside the ACS did not detect any significant radiant energy.

Burn injury predictions from BURNSIM are shown in Figure II-32 for the sensors that detected heat fluxes. BURNSIM data for the maximum temperatures and burn threshold depths as a result of these heat fluxes are shown in Table II-6. The highest temperature reading occurred at the right shoulder, and the highest burn threshold depth reading was at the right cheek.

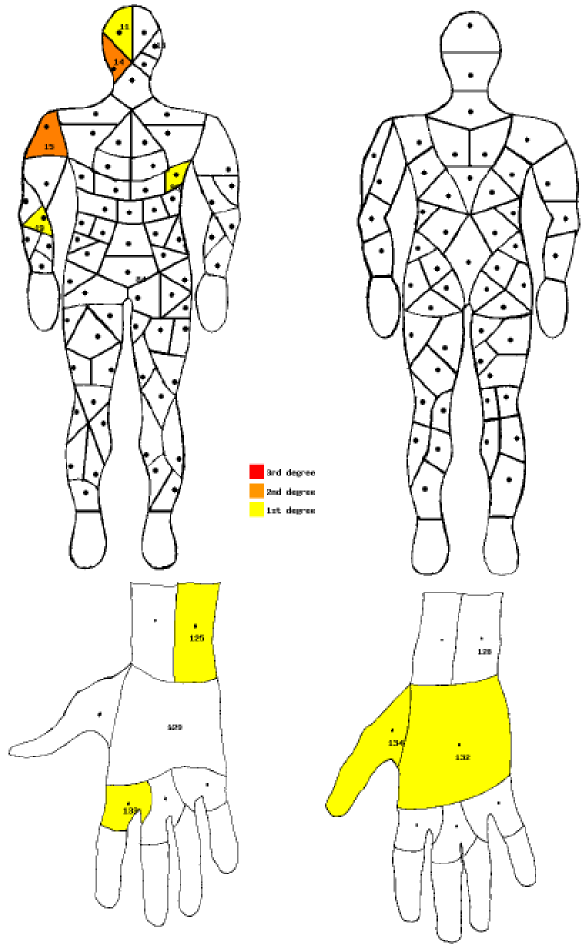

Figure II-32. BURNSIM results on manikin for Test 29 (5% hydrogen).

Table II-6. BURNSIM data for Test 29 (5% hydrogen).

Sensor Location	Degree of Burn	Maximum Temperature (^oC)	Burn Threshold Depth (μm)
Right Eye	1st	63	82
Right Cheek	2nd	76	190
Right Shoulder	2nd	77	183
Right Inner Elbow	1st	60	39
Left Underarm	1st	66	60
Right Inner Wrist	1st	64	106
Right Hand between Fingers	1st	64	113
Left Hand between Fingers	1st	65	46
Left Hand Backside	1st	62	28

No detectable overpressure was observed; no injury potential from blast was expected. No luminous combustion was observed using the high-speed imagery. The panels remained attached to the ACS, but did display slight bulging.

Test 25: 15 Percent Ignition, Passenger Leak. Steel was used for all panels, except window locations where Lexan was employed. All seams were sealed with duct tape, except the bottom passenger and trunk panels. The ignition source was located on the dashboard. All heat flux sensors and pressure transducers were active for this test. One hydrogen sensor, located at the 50 percent front passenger position, was used. The setup for this test is shown in Figure II-33.

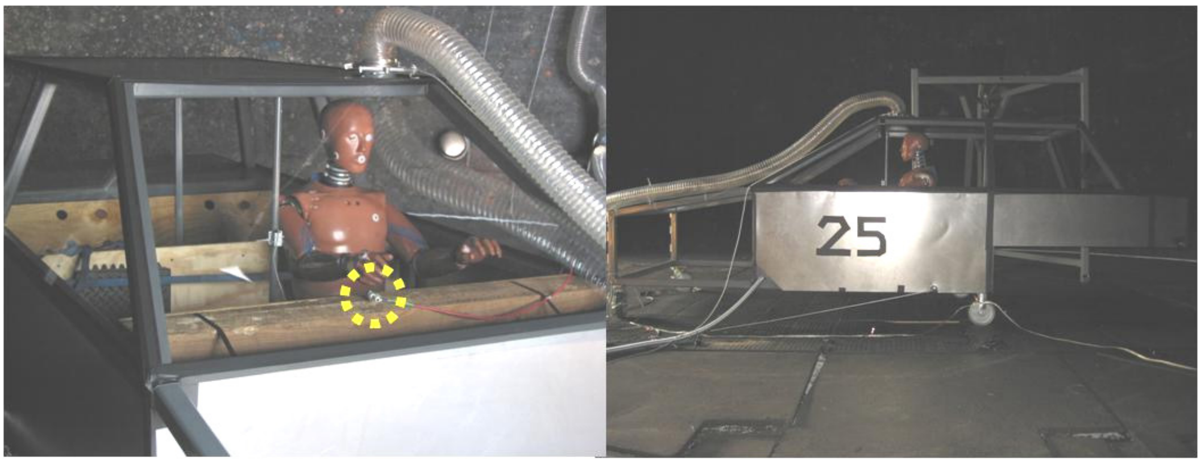

Figure II-33. Test 25 setup showing location of ignition source (left, circled) and overall ACS setup (right).

The ignition time was 4 min, 30 sec. A bar graph comparing the concentrations of the Task 2a test vehicle, ACS, and Test 25 is shown in Figure II-34.

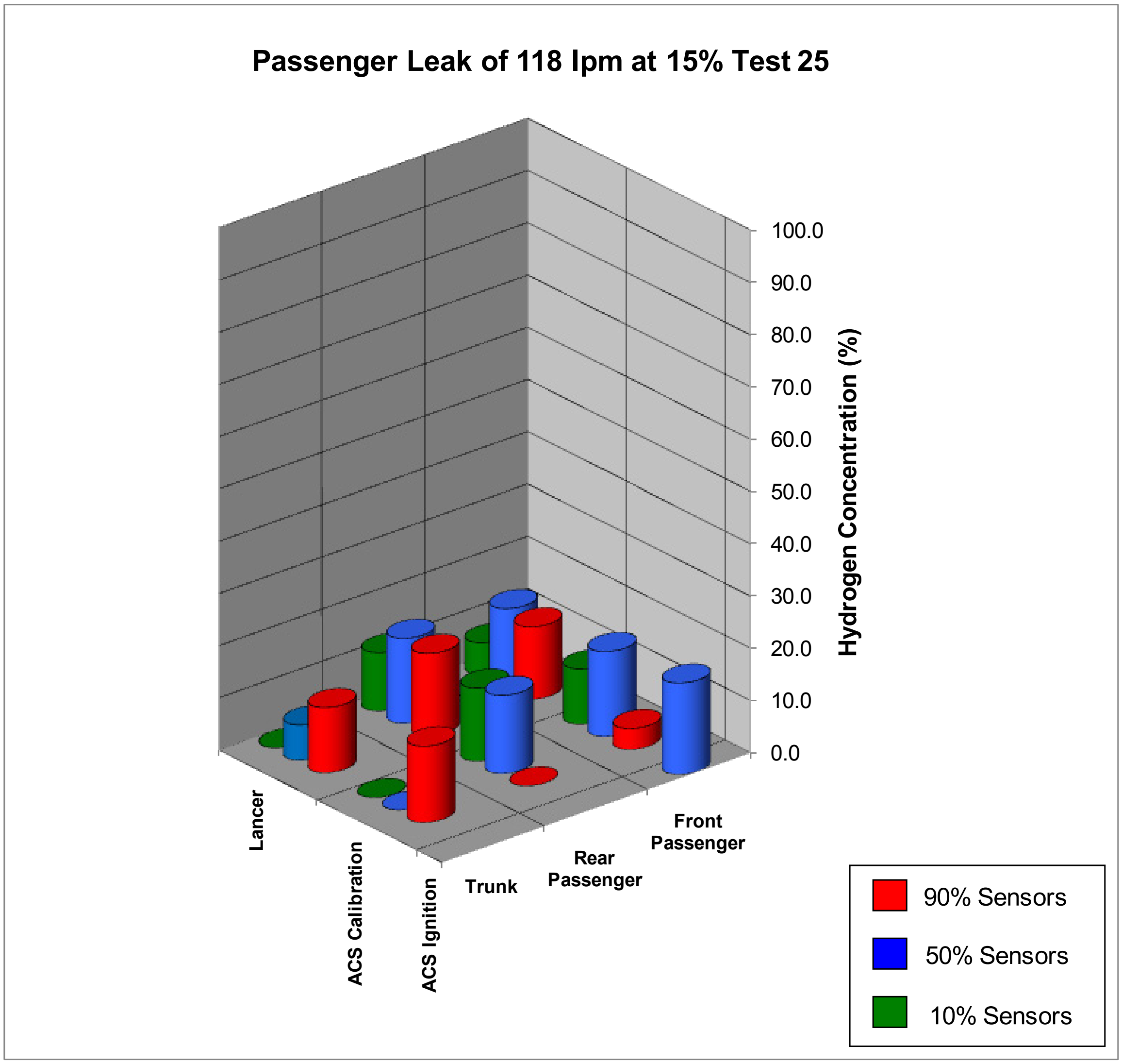

Figure II-34. Concentrations in the Task 2a intact car and Task 2b ACS during calibration and at ignition (118 lpm and 15%).

Sensors in the right eye, right cheek, right shoulder, right inner elbow, right underarm, right back knee, right inner wrist, right hand between fingers, right hand palm, left cheek, left underarm, left hand between fingers, and left hand backside detected heat fluxes that could result in first- or second-degree burns.

Burn injury predictions from BURNSIM are shown in Figure II-35; the maximum temperature and depth of skin burned are listed in Table II-7. The highest temperature occurs at the right back knee, and the most severe burn depth occurs at the left hand between fingers. The heat-flux recorded at the test stand also suggests a person there could experience a serious burn injury.

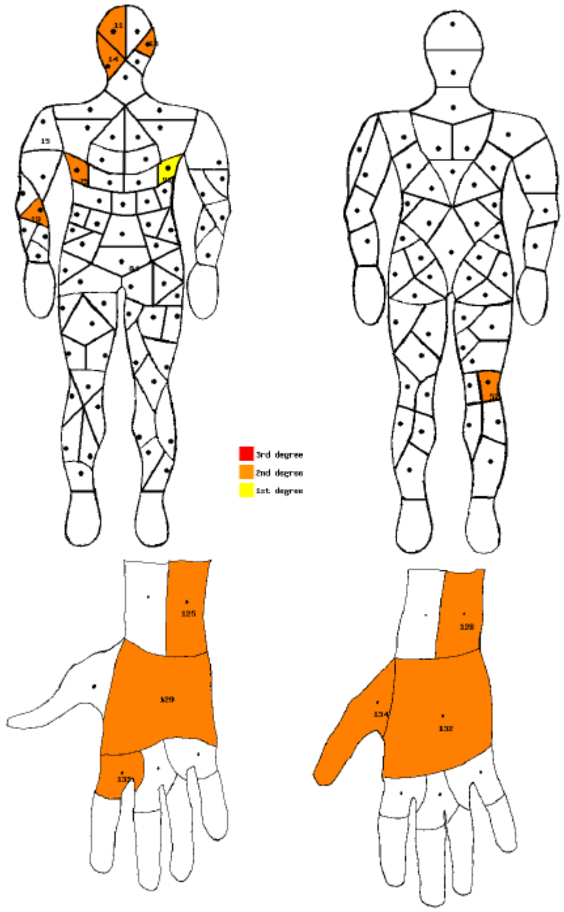

Figure II-35. BURNSIM results on manikin for Test 25 (15% hydrogen).

Table II-7. BURNSIM data for Test 25 (15% hydrogen).

Sensor Location	Degree of Burn	Maximum Temperature (^{o}C)	Burn Threshold Depth (µm)
Right Eye	2nd	108	177
Left Cheek	2nd	138	200
Right Cheek	2nd	180	197
Right Inner Elbow	2nd	163	296
Right Underarm	2nd	174	245
Left Underarm	1st	97	51
Right Back Knee	2nd	229	271
Right Inner Wrist	2nd	166	326
Right Hand Palm	2nd	136	180
Right Hand between Fingers	2nd	138	248
Left Outer Wrist	2nd	147	279
Left Hand Backside	2nd	163	237
Left Hand between Fingers	2nd	145	353
Test Stand	2nd	157	219

No detectable overpressure was observed; no injury potential from blast was expected.

Stills from the high-speed imagery are shown in Figure II-36. Combustion was significant and forced some of the steel panels from the ACS framework. Only a *glow* from the fireball was observed. It was difficult to determine when the hydrogen mixture began to combust with respect to the time of ignition; however, the front driver side panel began to move at approximately 43 msec.

Figure II-36. High-speed stills showing combustion and movement of ACS panels in Test 25.

Test 26: 30 Percent Ignition, Passenger Leak. Steel was used for all 11 body panels and Lexan, for all 6 window panels. All panel seams were sealed, except for the passenger and trunk bottom panels. All heat flux sensors and pressure transducers were active. A sensor located at 50 percent height in the front passenger compartment was used to monitor the hydrogen. A photograph of Test 26 is shown in Figure II-37.

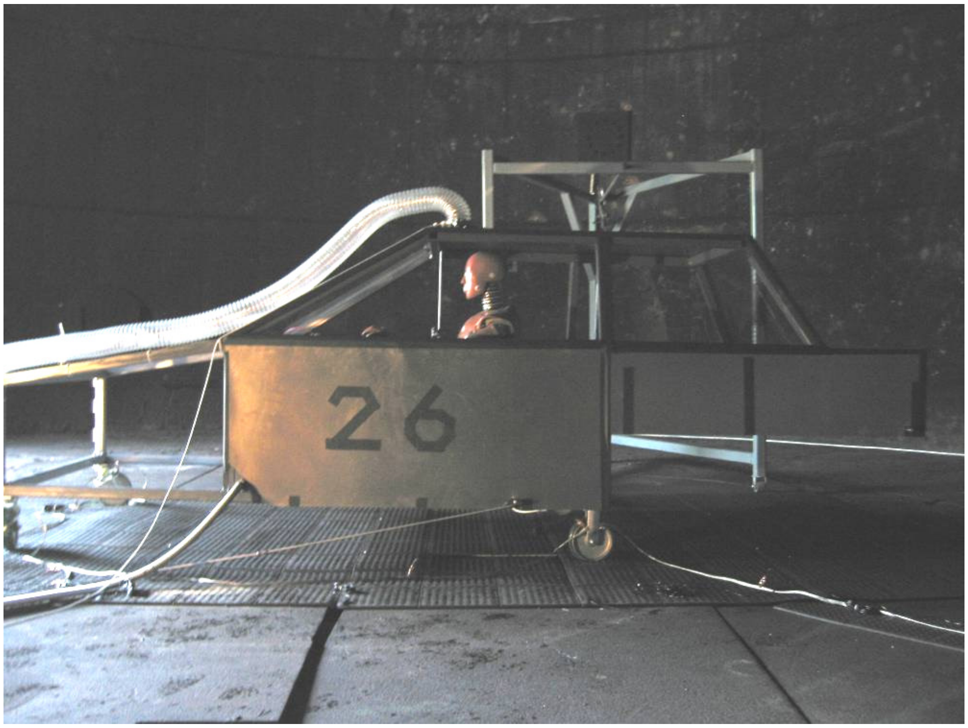

Figure II-37. Test 26 ACS setup.

The ignition time was 20 min. A bar graph comparing the concentrations of the Task 2a test vehicle, ACS, and Test 26 is shown in Figure II-38.

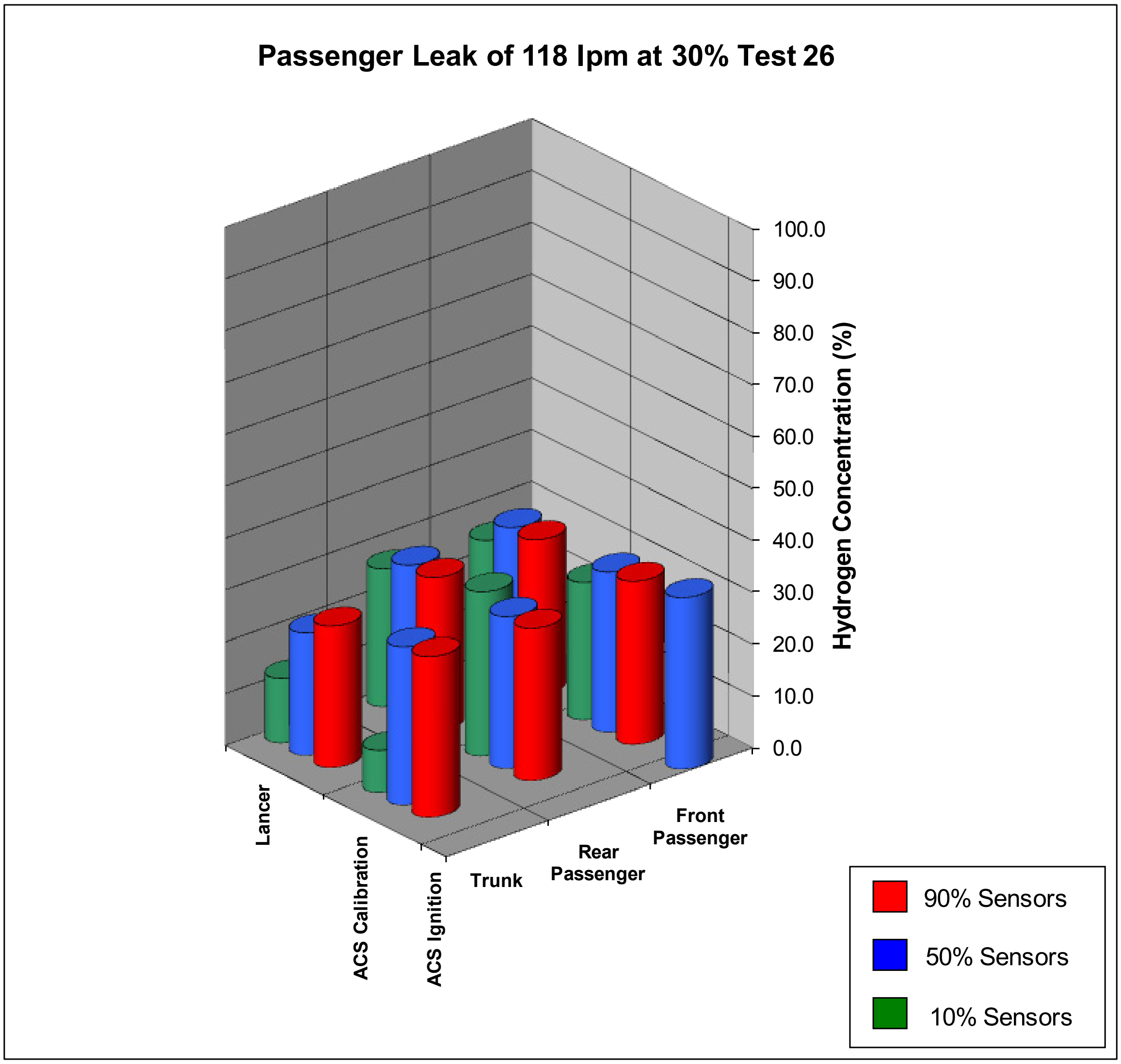

Figure II-38. Concentrations in the Task 2a intact car and Task 2b ACS during calibration and at ignition (118 lpm and 30%).

Sensors in the right eye, left cheek, right cheek, right shoulder, right inner elbow, right underarm, right back knee, right inner wrist, right hand palm, right hand between fingers, left outer wrist, left hand backside, and left hand between fingers detected heat fluxes that could result in first- or second-degree burns. Detailed data are presented in Appendix G,

Burn injury predictions from BURNSIM are shown in Figure II-39; maximum temperature and the depth of skin burned are shown in Table II-8. The highest temperature occurs at the left outer wrist with the most severe depth occurring at the right hand palm. The heat flux recorded at the test stand also could pose serious burn injury potential to personal (first responders) at this location.

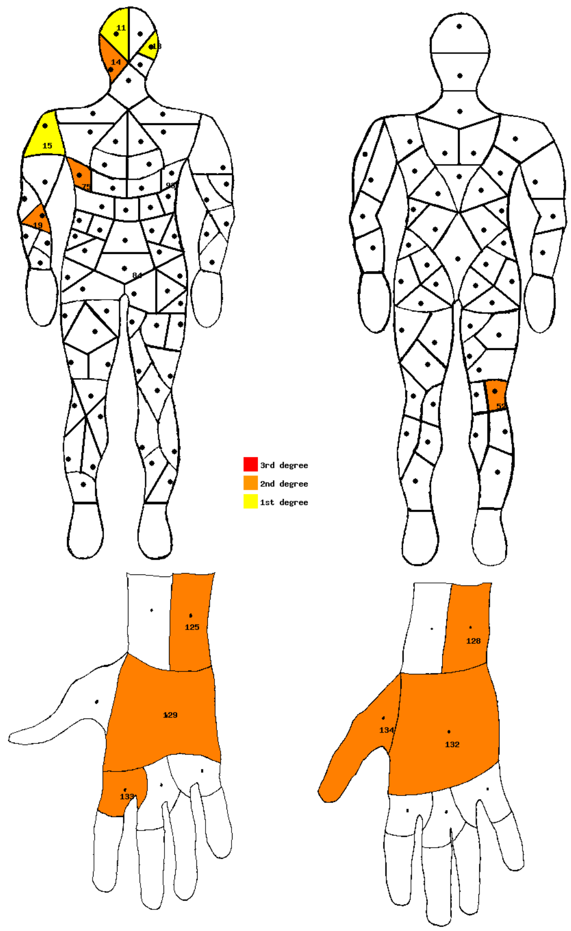

Figure II-39. BURNSIM results on manikin for Test 26 (30% hydrogen).

Table II-8. BURNSIM data for Test 26 (30% hydrogen).

Sensor Location	Degree of Burn	Maximum Temperature (^oC)	Burn Threshold Depth (µm)
Right Eye	1st	146	111
Left Cheek	1st	100	35
Right Cheek	2nd	113	364
Right Shoulder	1st	76	113
Right Inner Elbow	2nd	215	1,240
Right Underarm	2nd	180	431
Right Back Knee	2nd	122	195
Right Inner Wrist	2nd	251	857
Right Hand Palm	2nd	187	1,317
Right Hand between Fingers	2nd	238	252
Left Outer Wrist	2nd	267	696
Left Hand Backside	2nd	174	1,281
Left Hand between Fingers	2nd	187	132
Test Stand	1st	133	175

Significant overpressure was generated inside the passenger compartment during combustion, apparently a transition from deflagration to detonation. Low pressures are evident at about 15 msec and rapidly transition to about 80 psi at about 22 msec. Assuming that time zero is defined as the time at which the spark is applied (zero induction time) and that the shock front was measured at the window (37 in. away on the test stand), the approximate velocity of the combustion is ≈ 2,400 ft/sec, about twice (Mach 2) the speed of sound. The three separate shocks observed at the test stand location can be rapid, separate detonations of the front, rear, and then trunk compartment volumes. Figure II-40 is an overpressure composite.

The consequence of this overpressure exposure is probable lethality to passengers. Various technical references report empirical correlations developed to predict the thresholds for and extent of injury to ears and lungs from the exposure to blast overpressure[7, 8, 10].

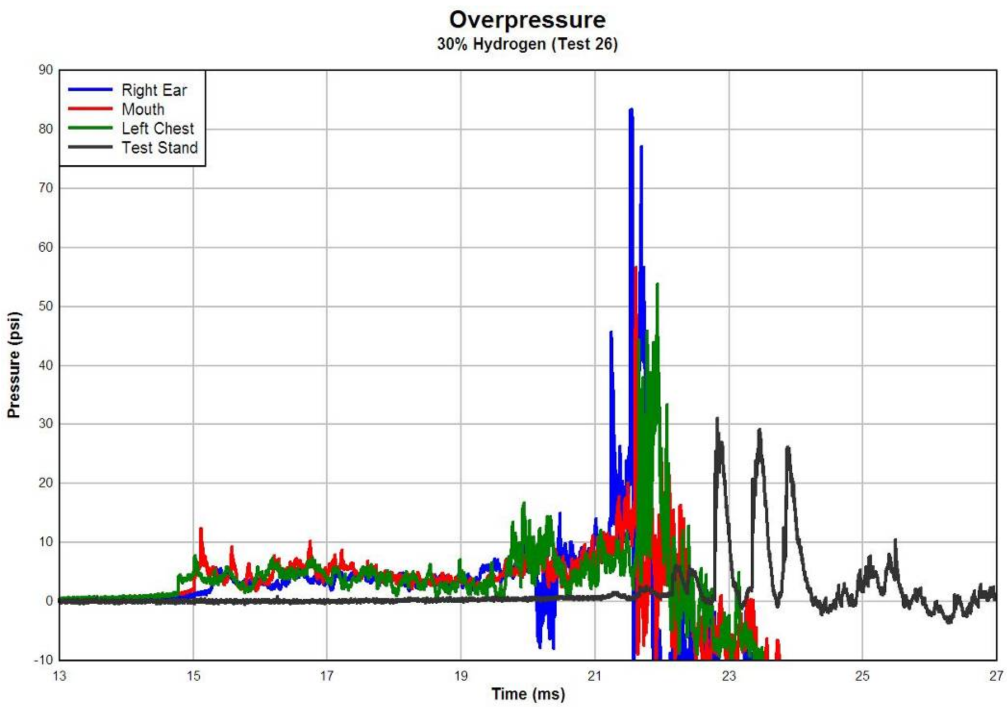

Figure II-40. Test 26 overpressure composite.

Stills from the high-speed imagery are shown in Figure II-41. The middle picture was recorded during the frame time of 20.2-25.2 msec. This time window correlates to the interval over which the rapid rise and elevated pressure were observed.

Test 26 resulted in the greatest extent of damage to the ACS panels. The manikin also was slightly damaged due to acceleration forces and the subsequent dislodgment of sensors. The damaged sensors were not available for further tests.

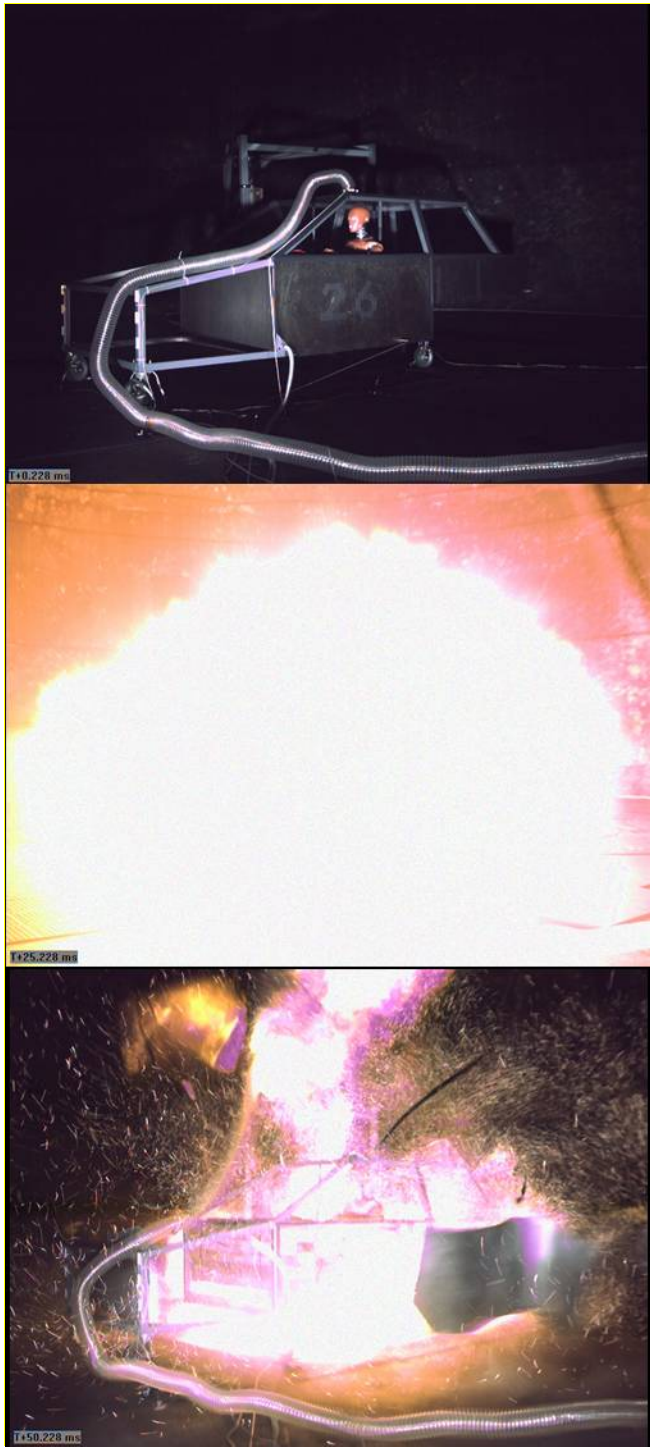

Figure II-41. High-speed stills showing detonation and separation of ACS panels in Test 26.

Test 28: 60 Percent Ignition, Passenger Leak. All panel seams were sealed with duct tape. Ten steel panels were used; six Lexan panels, for window locations and one for the driver front side panel. Two hydrogen panels were stationed at the 50 percent front passenger and trunk compartments. The ignition source was located on the dashboard. The right underarm sensor and right back knee sensor were not used in this test. A photograph of Test 28 is shown in Figure II-42.

Figure II-42. Test 28 ACS setup.

The ignition time was 24 min, 30 sec. A bar graph comparing the concentrations of the Task 2a test vehicle, ACS, and Test 28 is shown in Figure II-43.

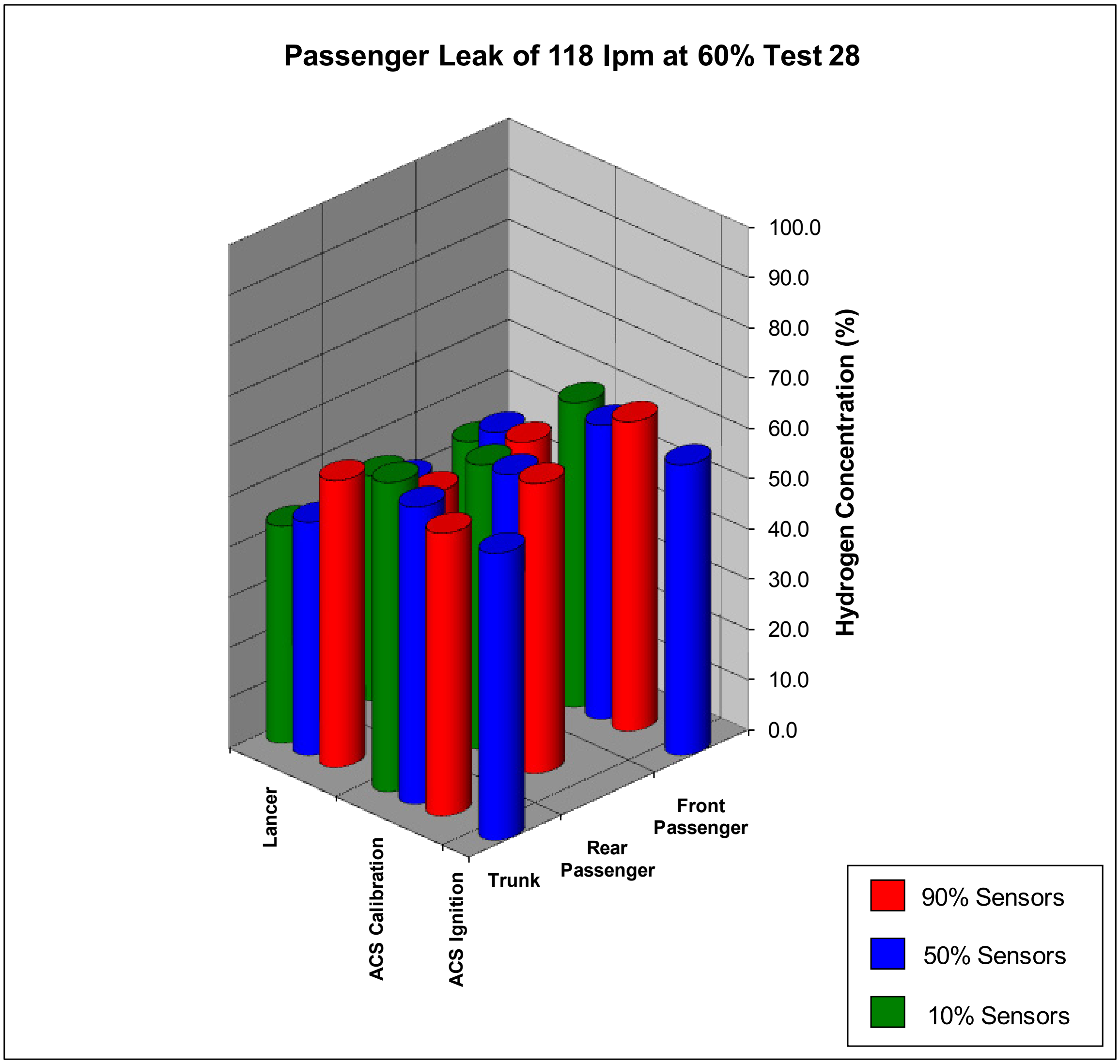

Figure II-43. Concentration in the Task 2a test vehicle and Task 22b ACS during calibration and at ignition (118 lpm and 60%).

Sensors in the right eye, left cheek, right cheek, right shoulder, left underarm, groin, left outer wrist, left hand between fingers, and left hand backside positions detected heat fluxes that could result in first- or second-degree burns. The complete data set is presented in Appendix G.

Burn injury predictions from BURNSIM are shown in Figure II-44. Table II-9 lists the maximum temperatures and burn threshold depths predicted for each active heat flux sensor. Personnel located at the test stand position could be exposed to significant thermal energy.

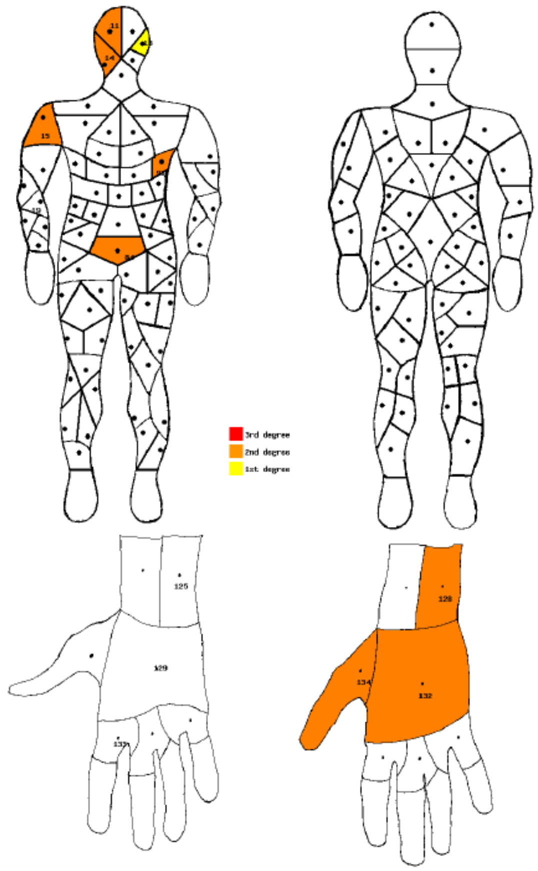

Figure II-44. BURNSIM results on manikin for Test 28 (60% hydrogen).

Table II-9. BURNSIM data for Test 28 (60% hydrogen).

Sensor Location	Degree of Burn	Maximum Temperature (^{o}C)	Burn Threshold Depth (µm)
Right Eye	2nd	260	527
Left Cheek	1st	95	0.53
Right Cheek	2nd	276	550
Right Shoulder	2nd	268	519
Left Underarm	2nd	170	511
Groin	2nd	226	631
Left Outer Wrist	2nd	83	202
Left Hand Backside	2nd	233	595
Left Hand between Fingers	2nd	256	574
Test Stand	2nd	117	181

A small overpressure resulted from combustion in this test. Figure II-45 shows peak pressures of ≈ 1.0 psi. Again, the negative trend observed on manikin sensors was the result of lowering ambient pressure (loss of slight positive pressure during leak), exceeding the discharge time constant of the piezoelectric circuit (a slow, long pressure for these types of transducers), and thermal effects from the long duration fireball. The overpressure in this test is very similar to Test 34, the 60 percent trunk leak.

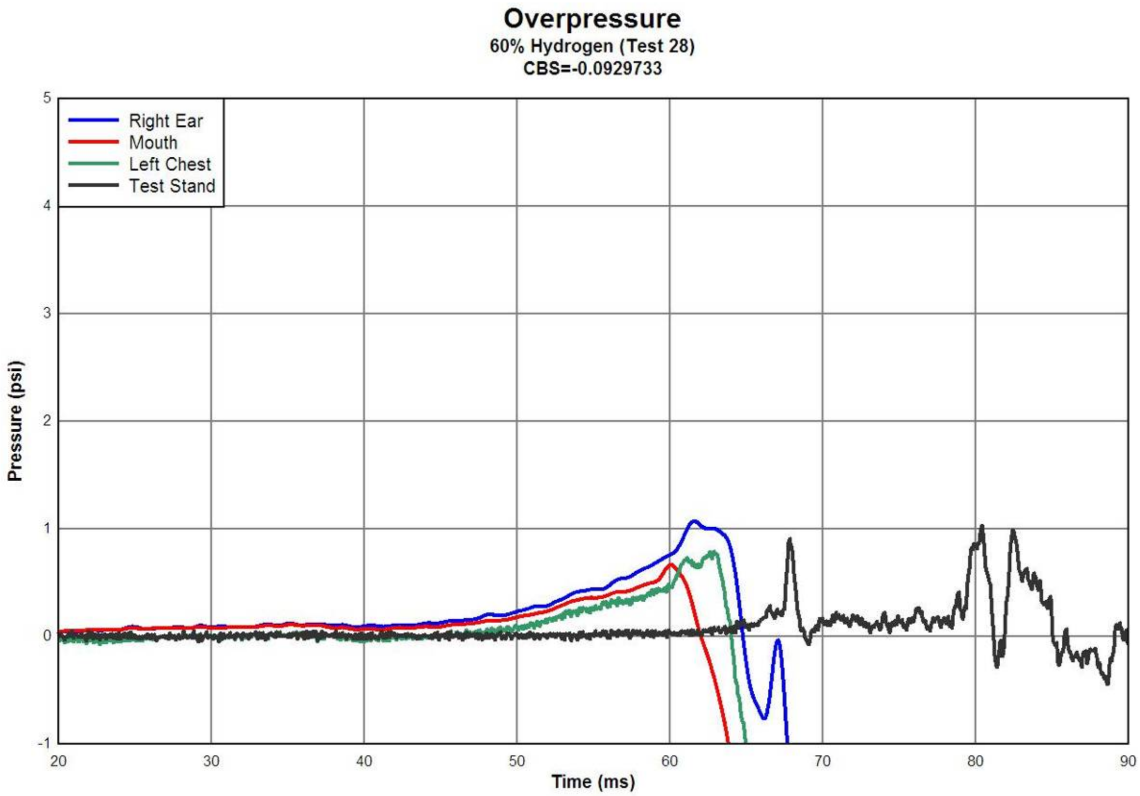

Figure II-45. Test 26 overpressure composite.

Stills from the high-speed imagery are shown in Figure II-46. Visible combustion is evident at approximately 51 msec. Two subsequent stills show the hydrogen/air fireball and the separation of the panels.

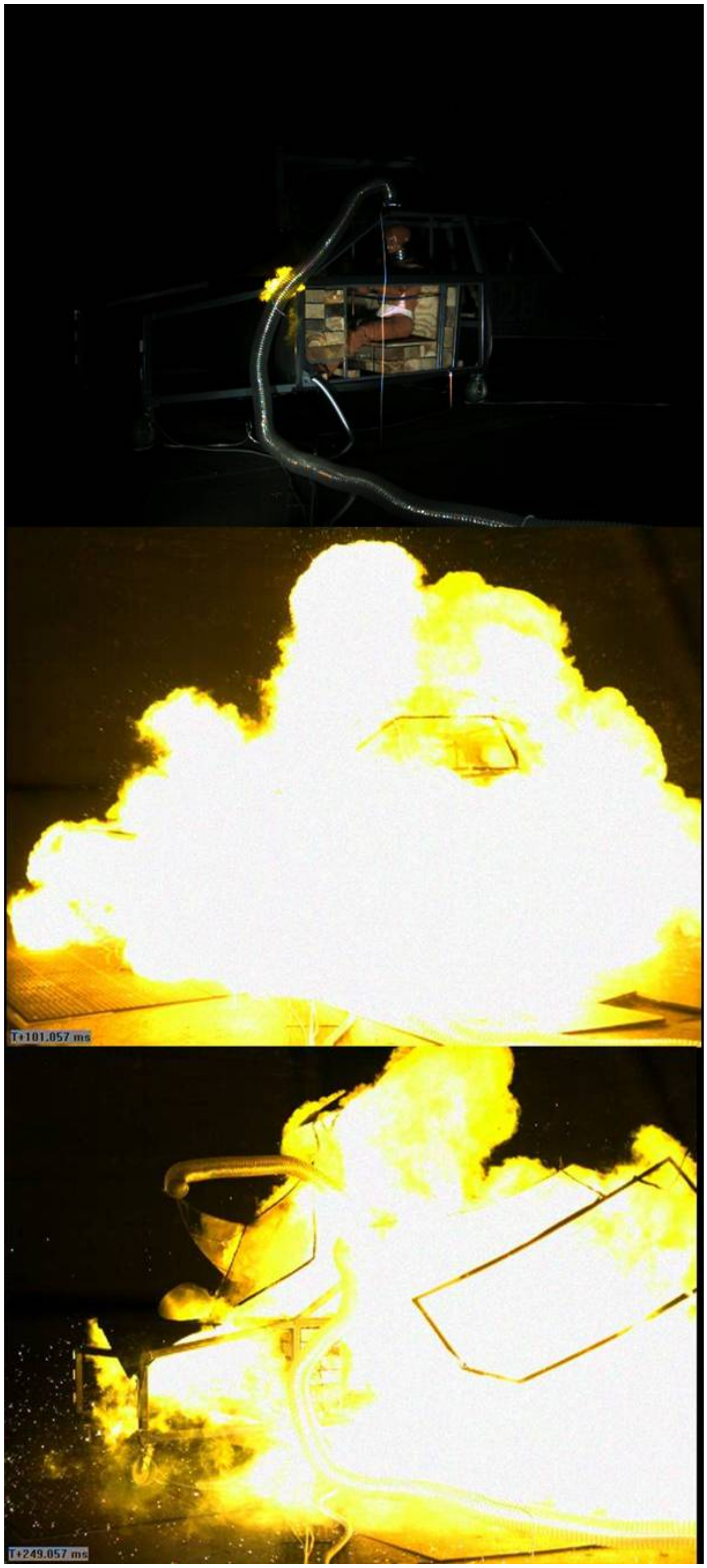

Figure II-46. High-speed stills showing combustion and separation of the panels in Test 28.

SUMMARY

Task 2b test data were used to estimate potential injuries to vehicle occupants from the flame and blast effects resultant from the combustion of different levels of accumulated hydrogen inside a simulated vehicle following a leak into the passenger compartment or trunk.

Appendix F is a reprint of a recent report that relates overpressure exposure to personal injury; data therein were used in this program to interpret threats from observed overpressure effects. The BURMSIM algorithm was used to convert heat-flux profiles into burn-injury predictions. BURNSIM uses the total heat flux impulse for its burn calculation. Appendix G contains all the heat-flux waveforms. Appendix H contains data on the peak hydrogen concentrations tested.

The most significant observation derived from Task 2b test data can be summarized as follows:

> At all levels of accumulated hydrogen inside the vehicle, ≈ 5 percent, ≈ 15 percent, ≈ 30 percent, or ≈ 60 percent, the most probable predicted consequence of a driver's exposure to the combustion of
> this hydrogen is second-degree burns to exposed skin (face and hands).

Ignition tests at 5 percent accumulated hydrogen in the ACS with leaks yielded the lowest temperatures and burn threats (some first-degree burns). This result was anticipated because the concentration is near the lower flammability limit of hydrogen (4%), which is known to yield cooler, slower burning fireballs than at the stoichiometric (≈ 30%) level[(7)].

Ignition tests at 15 percent, 30 percent, and 60 percent accumulated hydrogen resulted in higher exposure temperatures; 30 percent and 60 percent hydrogen yielded longer duration fireballs and higher temperatures than at 15 percent (all second-degree burns). Predictions for burn threshold depths indicate that 30 percent and 60 percent hydrogen combustion created the most severe threats. Ignition of 30 percent hydrogen was the expected worst-case (near-stoichiometric) concentration and yielded the hottest fireball. The maximum burn threshold depth value for 30 percent hydrogen was more than 1.5 times higher than other values measured.

No observable overpressure was detected at ≈ 5 percent or ≈ 15 percent hydrogen concentrations, but a slight overpressure was observed via high-speed imagery in the form of panel motion. No personal injury could be expected.

Ignition of ≈ 60 percent hydrogen generated about 1.0 psi of overpressure. The physiological consequence of exposure to ≈ 1.0 psi is the rupture of eardrums in 20 percent of the exposed population.

Overpressure posed a very serious threat during the combustion of ≈ 30 percent hydrogen: possible death. Blast pressures in excess of 80 psi peak overpressure were measured at the right ear.

Table II-10 displays the peak heat fluxes and overpressures recorded for each hydrogen concentration ignited. The purpose of presenting peak data is to show the relative threat potential increase near stoichiometric mixtures and to allow some comparison with relevant data from other studies on this topic.

Table II-10. Peak heat flux and overpressure for combustion of hydrogen at different concentration.

		Hydrogen Concentration						
		5%		15%		30%	60%	
		Trunk Leak	Passenger Leak	Trunk Leak	Passenger Leak	Passenger Leak	Trunk Leak	Passenger Leak
Peak Heat Flux (W/cm^2)	Occupant	14	14	261	260	675*	285**	306
	Bystander	4	0	16	113	340**	206	95
Peak Pressure (psi)	Occupant	0	0	0	0	83	0.9	1.1
	Bystander	0	0	0	0	31	1.3	1

* Peak values were estimated due to peak signal clipping – difference <15 percent.

** Peak values were estimated due to peak signal clipping – difference <40-80 percent.

Inspection of the as-recorded, raw data heat flux profiles revealed that in a few tests the peak amplitudes were clipped. The peaks in question are short in duration, and the missing information has no significant affect on the impulse. Estimates were attempted to determine the true peak value. In some cases, the amplitude was clipped only slightly, and the estimate was believed to be reasonably quantitative (denoted by * in Table II-10). In the 30 percent concentration test, the amplitudes were clipped significantly, making an estimate difficult (denoted by ** in Table II-10).

In any case, not knowing the actual peak heat flux did not alter the findings predicted by BURNSIM that uses the time dependence. The heat flux was sufficient to cause burn injuries to exposed skin at every level of accumulated hydrogen in the simulated test vehicle.

An important overall observation to be made from Task 2a and Task 2b tests is that the flow characteristics of hydrogen are complex, expectedly so as a result of its low density (high buoyancy) and high diffusivity. Large differences in hydrogen accumulations in the ACS could be observed after small test changes were made to the tightness of its structure, such as taping a few additional seams. In short, this experience indicates that different makes and models of automobiles are likely to exhibit significant differences in terms of hydrogen fill profiles and accumulation levels. Information from manufacturers can assist in determining the extent to which the data acquired in this program are vehicle-specific.

OBSERVATIONS

Data captured in Task 2b were compared with limited test results reported elsewhere by SAE technical papers[4,5]. In the earlier of these reports[4], hydrogen was leaked into the engine compartment from the outside of the vehicle and ignited at concentrations of about 23 percent. A heat flux sensor and a pressure transducer were placed outside the vehicle to assess the impact caused by the ignition. Tissue paper also was placed on the right and left sides of the intake manifold and the vehicle front grill to quantify the extent of burn damage imparted to the vehicle. The authors reported that burn damage to the vehicle and injuries to personnel from the pressure and heat flux created by the ignition event were minimal. The heat flux reported, recorded at approximately 1.0 m from the vehicle, was 0.15 kW/m^2 (0.015 W/cm^2) for ignition of the 23.7 percent hydrogen inside the engine compartment. This value is orders of magnitude lower than the heat flux measured on the Task 2b manikin (50–100 W/cm^2) for 15 percent or 30 percent hydrogen combustion inside the passenger compartment. Similarly, the other study[5] investigated the potential for injury to nearby personnel resulting from the ignition of a $\approx$ 20 percent hydrogen/air mixture. Heat flux and pressure data again were captured at positions approximately 1.0 m from the vehicle. Tissue paper again was placed on the vehicle to assess the potential for burn damage to the vehicle components. The authors reported that the ignition of this hydrogen mixture did not produce heat fluxes or pressures that could be considered injurious to personnel placed at the locations of these sensors.

The difference results from several factors. First is the volume of hydrogen ignited. The volume leaked in the technical paper was about half (131 lpm for 10 min = 1310 l) of that leaked in Task 2b (118 lpm for 20 m = 2360 l); overall hydrogen concentrations were somewhat comparable ~23 percent (JAR) or ~30 percent (Task 2b). More important, in these tests, hydrogen was leaked from outside the car and, therefore, was never *contained*, resulting in a much smaller volume of hydrogen involved in the ignition. In Task 2b tests, the leak was inside the car; a substantial portion of hydrogen remained because of seals. This containment resulted in the hydrogen volume in Task 2b tests being more than twice that in literature tests. These hydrogen volume and containment effects could be manifest in the size and intensity of the fireball, which affects the *view factor* or extent to which the sensor *sees* radiant heat flux. The size of the fireball also affects how far the surface of the fireball is away from the sensor. Radiant heat flux decays as a function of reciprocal distance squared. In both the JAR and Task 2b tests, the heat flux sensors (same vendor and comparable model) were about 1.0 m from a reference point on a vehicle. However, in JAR tests, the heat flux gage at 1.0 m likely was blocked almost completely by the vehicle structure. Last, in JAR tests, only a small flame *sprouted* from the grills and louvers; in Task 2b tests, the entire vehicle was engulfed in flame that extended well beyond the vehicle periphery. Hence, in Task 2b tests, the fireball was dramatically larger in surface area and shorter in the distance to the sensor compared to the JAR tests. As such, dramatically higher heat fluxes could be created and measured.

In summary, results from Task 2b ignition tests provide information on the personal burn and pressure injury during combustion. Task 2b data pertains to leaks in the trunk and passenger compartments of a vehicle; the JAR leaks were in the engine compartment.

VOLUME III: TASK 2C

The objective of Task Order 3, *Post-Crash Hydrogen Leakage Limits and Fire Safety Research*, was to conduct research on the fire safety of proposed hydrogen leakage limits, including calculations and experimental verification. This assessment provides technical data that correlate hydrogen fuel system leak rates to the accumulation of ignitable mixtures of hydrogen in trunk, passenger and engine enclosed compartments. Tasks conducted under Task Order 3 were:

Task 2a: Leak Rate vs. Hydrogen Concentration Tests on Intact Automobile;
Task 2b: Ignition and Combustion Tests on Simulated Automobile Compartments; and
Task 2c: Full-Scale Leak, Ignition and Fire Tests on Intact and Crashed Automobiles.

This report describes progress on Task 2c, the objectives of which were to quantify the effects of crash damage on hydrogen accumulation and hydrogen combustion characteristics for three leak parameters (location, rate, and duration); relate them to the extent of personal injury (physical trauma and burns); and assess the establishment of a minimum allowable post-crash hydrogen leak rate. Task 2c tests were conducted on four vehicles: intact and front-impact 2008 Mitsubishi Lancers; side-impact 2009 Mazda6 Sedan; and rear-impact 2008 Ford Taurus.

Altogether, 39 leak-accumulation tests were completed on four vehicles at seven leak rates (3, 6, 15, 30, 59, 118, or 236 liters per min, lpm) over 60 min, originating from three locations (trunk or rear-passenger compartment, or underneath the vehicle) and using up to 12 hydrogen sensors (Neodym Panterra, 0-100 percent; no endorsement implied) in three arrays at four positions (10%, 50%, 90%, and/or 100% compartment height). Hydrogen sensor performance was verified via calibration.

Observations from accumulation tests on the front-crashed vehicle were: (1) leaks as low as 30 lpm in trunk or passenger compartment resulted in detectable flammable levels in the other compartment; (2) leaks as high as 236 lpm underneath the vehicle did not result in detectable accumulation inside the vehicle; and (3) low leak rates resulted in random (inversions; local pockets), but sometimes detectably flammable, levels of hydrogen.

Observations from accumulation tests on the side-crashed vehicle were: (1) leaks ≥59 lpm in the passenger compartment resulted in detectable flammable levels, but leaks as high as 236 lpm in the trunk did not result in detectable flammable atmospheres in the passenger compartment; (2) leaks underneath the vehicle (near door seals) as high as 236 lpm did not result in detectable accumulation inside the vehicle; and (3) even with high leak rates, accumulations sometimes appeared random and elusive with respect to migrating to the highest locations.

Observations from accumulation tests on the rear-crashed vehicle were: (1) leaks as low as 30 lpm in the rear-passenger compartment resulted in detectable flammable levels much lower than those in intact or front-crashed cars; (2) leaks as high as 236 lpm underneath the vehicle did not result in detectable accumulation inside; and (3) leaks originating in passenger and trunk compartments resulted in somewhat random accumulations, all of which were flammable.

Overall observations from Task 2c hydrogen accumulation tests were: (1) at low leak rates (≤60 lpm), hydrogen did not mix well in air, resulting in its concentrations being random, exhibiting characteristics similar to a lava lamp in which slow motion causes media of different densities to remain unmixed, pocketing locally, varying and moving in random fashion, and inverting where higher-sensor locations register lower concentrations than do lower-sensors locations, or being absent at highest locations; (2) at high leak rates (≥118 lpm), hydrogen mixes more homogenously, resulting in more stratified levels, increasing more uniformly throughout the vehicle, being detectable nearest the leak source first, generally seeking higher elevations, and reaching more uniform and steady-state concentrations with time; and (3) door, window, and frame seals in front or rear-impact vehicles were not compromised to the extent of allowing hydrogen from leaks underneath to accumulate inside the vehicle. Such flow, mixing, and stratification behavior has been predicted by computational fluid dynamic modeling by Breitung.

Altogether, eight ignition tests were conducted on the intact or front, rear, or side-impact vehicles. Two types of ignition tests were conducted: (1) at the in-going potential standard leak rate of 118 lpm for a duration of 1.5 min, which introduced a just-flammable ~5 percent hydrogen inside the car if distributed evenly; and (2) at the lowest leak rate experimentally possible (3 lpm) over 60 min, which resulted in accumulated hydrogen (~5%) that could be ignited by sparking at the top of the passenger compartment (leaking 3 lpm for 60 min was near-equivalent to the volume of hydrogen leaking at 118 lpm for 1.5 min).

With regard to achieving the objective of determining a *minimum allowable* *post-crash leak rate*, tests indicated that leak rate is not defining metric. Instead, the critical information was whether hydrogen, if allowed to leak into a car compartment, could accumulate anywhere *locally* to ~5 percent, just above the lower flammability limit of hydrogen (~4%). Tests indicated that flammable concentrations of hydrogen could accumulate in different locations within passenger compartments, either at low leak rates after long times or at high leak rates after short times.

Fire effects varied in terms of peak thermal flux, overpressure, and internal vehicular damage. Aftereffects ranged from window fogging (condensation from hydrogen combustion) to structural damage (deformed doors, broken windows) to second-degree burns and eardrum rupture.

One additional significant finding was a propensity for secondary fire after sparking and hydrogen ignition, which was replicated. These secondary fires, that consumed flammable material inside the vehicles, occurred in the intact and front and side-impact cars. The origin of these secondary fires, that erupted within minutes after initial sparking and severely damaged the vehicles, appeared to be flammable material inside the trunk (spare tire) or cabin (headliner).

Significant overall observations and recommendations from Task 2c tests were as follows:

- All accumulation of hydrogen should be avoided in passenger compartments.
- More than one sensor in various locations is needed for passenger-alarm purposes.
- Vehicle devices that vent passenger compartments upon impact may be warranted.
- New flammability tests on fabrics exposed to hydrogen (not air) have merit.
- On-board vehicle fire-suppression systems could be revisited.

TASK SCOPE AND OBJECTIVE

This report describes the work performed and results obtained under Task Order 3 Task 2c: *Full-Scale Leak, Ignition and Fire Tests on Intact and Crashed Automobiles*. The objectives of Task 2c tests were to quantify hydrogen combustion effects, relate them to the extent of personal injury, and use these data to assess the establishment of a minimum allowable post-crash hydrogen leak rate.

Combustion properties were quantified with heat flux and overpressure measurements subsequent to ignition and evaluated in terms of their potential for personal injury (physical trauma and burns).

Tests were completed using the following test automobiles: intact and front-impact 2008 Mitsubishi Lancers; side-impact 2009 Mazda 6 Sedan; and rear-impact 2008 Ford Taurus.

The scope of Task 2c was accomplished in two types of tests, one on accumulation and the other on ignition. Accumulation was quantified by measuring hydrogen concentrations created by a leak in the trunk or passenger compartments of crashed vehicles, as done in Task 2a in an intact vehicle. Accumulated hydrogen was documented at leak rates of 30, 60, 118, and 236 lpm. Additional accumulation tests were performed in the intact vehicle at ultra-low leak rates of 3, 6, and 15 lpm originating in the trunk and rear passenger compartments. These tests were designed to determine the minimum allowable hydrogen leak rate that caused a fire hazard, which was the overall objective of the program.

The purpose of the ignition series of tests was to spark and attempt to ignite specific hydrogen leakage conditions and to measure the resulting heat flux and overpressure. These results could be used to gain insight into the likely possibilities of different leak conditions igniting and to quantify the level of injury received by vehicle occupants as well as damage sustained by the automobile and surroundings. Injury assessments were to be made with respect to burns (first-, second, or third-degree) using a burn-injury algorithm (BURNSIM) and to overpressure (blast) exposure.

This Task 2c Test Report completes the series on Task Order 3, *Post-Crash Hydrogen Leakage Limits and Fire Safety Research*. Test Reports for Tasks 2a and 2b were issued separately [1, 2].

TEST FACILITY, INSTRUMENTATION, AND HARDWARE

Test Facility. Tests were conducted at the Battelle High Energy Research Laboratory Area inside JS-10 (Figure III-1), a 40-ft. diameter, steel-reinforced, concrete domed chamber capable of containing up to 50 lbs of TNT explosive or equivalent flammable materials, including hydrogen. Conducting tests inside this large blast containment chamber precluded the influence of variable meteorological conditions, which could affect the dispersion and ignition properties of hydrogen. Parameters such as ventilation, temperature, and relative humidity were recorded during testing (quiescent, within a controllable range). JS-10 can accommodate a vehicle and allows both leak and ignition-fire tests to be conducted inside.

Figure III-1. JS-10 blast chamber used for indoor testing of hydrogen leaks into vehicles and ignitions.

Vehicles. Vehicles used in Task 2c tests included intact and front-impact 2008 Mitsubishi Lancers, side-impact 2009 Mazda6 Sedan, and rear-impact 2008 Ford Taurus. These vehicles, shown in Figure III-2, were shown by the client to Battelle as government-furnished equipment. Prior to all tests, all fluids were drained and batteries were removed. Window and door seals in the front and rear-crashed vehicles appeared intact, but those in the side-crashed car appeared compromised (driver's side door and window). To the extent possible, windows were put back into their upright condition. If windows had been ejected from impact (front, rear, and side), thin plastic film was taped over the openings.

Figure III-2. Task 2c vehicles (clockwise, top left): intact Mitsubishi Lancer, front-impact Mitsubishi Lancer, rear-impact Ford Taurus, and side-impact Mazda (no endorsement implied).

Hydrogen Sensors. Two types of hydrogen sensors were used during testing. Neodym Panterra sensors with remote heads were used to measure hydrogen levels from 0–100 percent. These sensors have a reported rise time of approximately 1.5 sec and were employed to measure hydrogen levels inside the vehicles and near the top of the blast chamber ceiling.

Neodym HydroKnowz sensors equipped with alarms were placed on the ceiling in the blast chamber and in the control room to monitor the presence of hydrogen during testing as a safeguard against the accumulation of potentially dangerous (flammable) hydrogen while personnel were present. These sensors have higher resolution, but measure only 0–4 percent hydrogen levels. Their alarms were set to activate when hydrogen levels reached 1 percent (10,000 ppm) in air. Figure III-3 shows the two sensor types in their respective housings.

Figure III-3. Neodym Panterra (left) and HydroKnowz (right) hydrogen sensors (no endorsement implied).

Hydrogen Sensor and Leak Locations. During hydrogen accumulation tests, crashed vehicles were instrumented with Neodym Panterra sensors in the trunk and passenger compartments. Each compartment typically contained an array of hydrogen sensors positioned as follows:

- 3 in the trunk compartment (except rear impact vehicle),
- 3 in the rear passenger compartment,
- 3 in the front passenger compartment, and
- 3 in the engine compartment.

Each compartment contained sensors positioned at 10 percent, 50 percent, and 90 percent of the vertical compartment dimension. The sensor suites were aligned on the centerline of the vehicle. These sensor positions essentially replicated positions employed in the Task 2a intact test vehicle. The face of each sensor was oriented downward to aid in the detection of rising hydrogen. Sensor positions were referenced to the leading edge of the front of each vehicle, subsequently referred to in this report as the sensor reference point.

In a limited series, accumulation tests were conducted with sensors located at 100 percent height. These details are noted in the next section and in accumulation plots in Appendix J.

The flow of hydrogen originated from a specific location either directly into or underneath the vehicle. Leak locations were as similar as possible given the dimensional differences among the different automobile models. The end of the leak tube was open, representing a sheared fuel line. No diffusers or nozzles were employed during any of Task 2c testing. Figure III-4 displays the typical positions of the hydrogen sensors and Figure III-5 shows representative leak locations. Detailed positions for sensors in each test vehicle are shown in Appendix I.

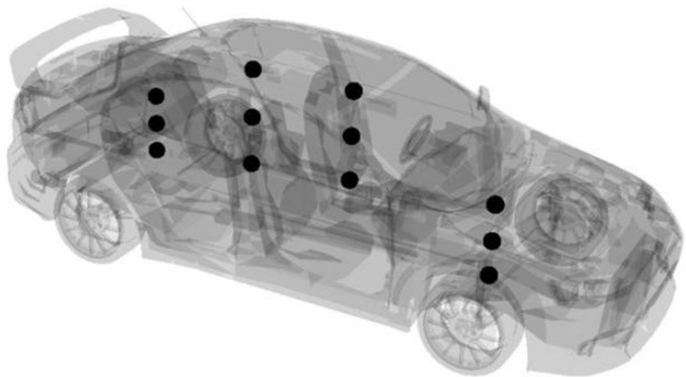

Figure III-4. Locations of hydrogen sensor arrays in trunk, rear-passenger, front-passenger, and engine compartments.

Figure III-5. Hydrogen leak locations in trunk floor (left), rear-passenger compartment floor (center), and underneath vehicle (right).

The majority of tests were conducted using the trunk leak location and employed some modified sensor configurations. The common sensor arrangement employed a 10 percent-50 percent-90 percent-100 percent height array in the vehicle interior, the same as in earlier tests, but with the addition of the sensor at the 100 percent height.

A second arrangement consisted of all sensors at the 100 percent compartment height along the vehicle ceiling centerline. Trunk sensors were positioned along a transverse line extending 3 in. to the left and right of the vehicle centerline. Sensor faces were oriented towards the origin of the flow. Photographs in Figure III-6 show this setup; detailed dimensions are shown in Appendix I.

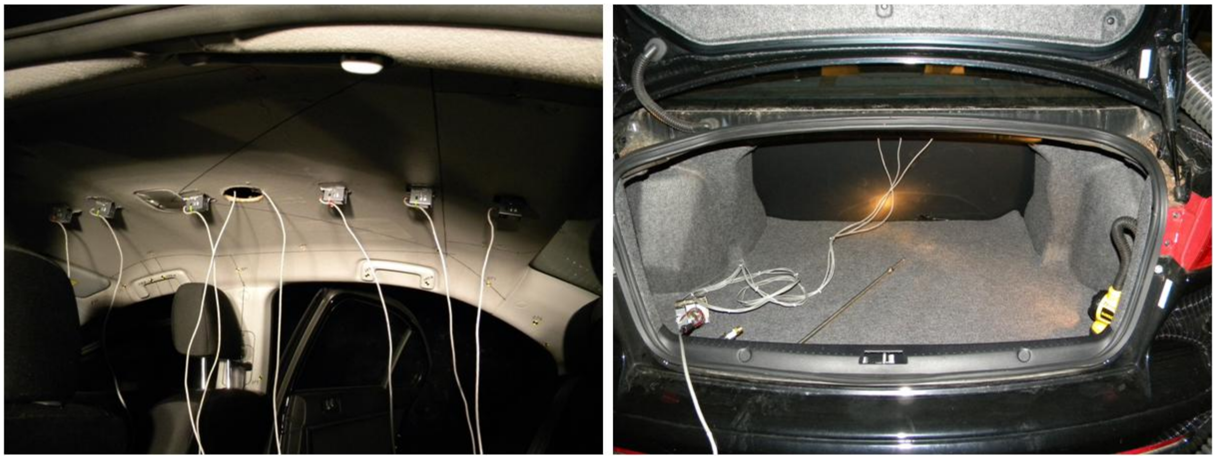

Figure III-6. 100 percent sensor-height arrangement in intact vehicle front and rear-passenger compartments (left) and in trunk compartment (right).

Ignition. Standard gasoline-engine spark plugs were employed as the ignition source. These spark plugs were connected to a 100-joule Cordin 640 pulser. The pulser's energy delivery circuitry consisted of a charged capacitor and spark gap trigger. The charging voltage was 5,000 V, and the discharge time a few microseconds. Figure III-7 shows the typical hydrogen sensor and spark plug arrangement used during ignition tests. Several variations were used and are documented in Appendix I.

Figure III-7. Typical arrangement of hydrogen sensors (circled in yellow) and spark plugs (circled in red) deployed in ignition tests.

Heat Flux Sensors. Vatell HFM7-E/L sensors with modified housings were used for acquiring heat flux data during ignition testing. The sensors have a reported response time of 17 μsec and were calibrated for about 100 $\mu V/W/cm^2$ (no endorsement is implied).

Overpressure Transducers. PCB ICP Model 102A16 sensors captured blast overpressure data during ignition testing. The reported response time (reflected shock) of the pressure sensors was $\leq$ 1.0 µsec. The sensors were calibrated to ~50 mV/psi (no endorsement implied).

Heat Flux and Transducer Locations. The interior of the vehicle was monitored at the driver's head location and outside the vehicle. The first ignition test employed sensors at a rear-passenger head location. The number of sensors and monitor positions was reduced after the first secondary fire occurred. Interior sensors were mounted in plastic cylinders and secured to the seat headrest with nylon straps. Exterior sensors were mounted in a steel housing on a steel test stand.

Cameras. Still photographs were taken to capture test setup preparation, sensor installation, and alignment. Photographs also were taken to document each test.

A standard-speed video camera was used to capture any unexpected events during accumulation tests and to record real-time data during ignition tests. This camera was placed in one of the chamber viewing ports. A translucent Lexan panel was used to protect the camera from damage. The real-time feed from this camera was captured, monitored, and temporarily recorded using a television and DVD recorder located inside the JS-10 control room.

A Vision Research Phantom v7.3 or v710 high-speed imager was used to capture the ignition event and subsequent hydrogen combustion. The imager was mounted in the same port as the standard video camera. The v7.3 model was setup to record at a rate of 800 frames per second (fps) with a 600 × 800 pixel resolution and 1.1 msec exposure time. The v710 model was setup to record at a rate of 1,000 fps with an 800 × 1,280 pixel resolution and 0.99 msec exposure time.

Burn Injury Prediction. Heat flux data were processed using an algorithm called BURNSIM to predict potential burn injury.[6] BURNSIM uses heat flux data to compute tissue temperature as a function of exposure time and skin depth and then estimates the tissue damage at a particular depth by integrating an Arrhenius rate equation (damage integral). The value of the damage integral determines the burn depth and, by extension, the degree of injury. The threshold depth is the maximum depth a burn achieves during an exposure. The extent of injury, or burn degree, is determined by the burn threshold depth. If this depth is less than the depth of the epidermal/dermal interface (approximately 100 microns), the injury is considered a first-degree burn. The result is the reddening of skin. Second-degree burns are injuries in which the threshold depth lies between the epidermal/dermal and dermal/subcutaneous (approximately 1,500 microns) interfaces. The result is blistering. In third-degree injuries, the skin tissue is completely damaged, i.e., the burn threshold depth exceeds the dermal/subcutaneous interface. The result is charred and destroyed tissue.

Overpressure Injury Prediction. Physical trauma, in the form of the extent of eardrum rupture, was predicted using empirical data reported by Altman on the auditory effects of blast waves on humans.[8]

RESULTS AND DISCUSSION

Task 2c Accumulation Tests

Test Matrix. Hydrogen accumulation data were collected in two types of tests (Table III-1).

In the first test series, *high* leak rates of 30, 59, 118, or 236 lpm were administered for 60 min in the front-, rear-, or side-impact vehicles. Hydrogen levels were measured at the same sensor positions used during Task 2a (10%, 50%, and 90% compartment height in trunk, rear-passenger, and engine compartments), except for rear-impact vehicle tests as no trunk sensors could be installed because this compartment had been crushed. In some of these tests, sensors also were deployed at the 100 percent compartment-height location.

In the second test series, hydrogen accumulation data were measured in the intact vehicle. The objective of these tests was to use ever lower leak rates to identify the rate that resulted in hydrogen levels accumulating at the lower flammability limit of hydrogen in air (~4%). Low rates of 3, 6, or 15 lpm were leaked into the trunk or 3 lpm from the rear-passenger compartment. In both cases, the duration of the leak was 60 min. Hydrogen sensors were arranged in either a 10 percent-50 percent-90 percent-100 percent compartment-height setup or all at 100 percent compartment-height setup.

The matrix for both series of Task 2c accumulation tests is listed in Table III-1. The sensor array types employed in these 39 tests were categorized as follows:

- Setup A: Array at 10 percent-50 percent-90 percent compartment height;
- Setup B: Array at 10 percent-50 percent-90 percent-100 percent compartment height; and
- Setup C: Array all at 100 percent compartment height.

Table III-1. Matrix for Task 2c hydrogen accumulation tests.

Task 2c Accumulation Tests					
Vehicle	**Leakage Location**	**Leak Rate (lpm)**	**Test #**	**Sensor Setup**	**Ignitable Mixture Present in Passenger Compartment? (Y/N)**
Front-Impact	Trunk	30	42	B	Y
		59	37	A	Y
		118	36	A	Y
		236	38	A	Y
	Rear Passenger	30	41	B	Y
		59	39	A	Y
		118	35	A	Y
		236	40	A	Y
	Underneath	30	43	A	N
		59	44	A	N
		118	45	A	N
		236	46	A	N
Side-Impact	Trunk	30	60	A	N
		59	59	A	N
		118	65	A	N
		236	64	A	N
	Rear Passenger	30	58	A	N
		59	57	A	Y
		118	56	A	Y
		236	66	A	Y
	Underneath	30	61	A	N
		59	67	A	N
		118	62	A	N
		236	63	A	N
Rear-Impact	Rear Passenger	30	49	B	Y
		59	48	B	Y
		118	47	A – no trunk sensors	Y
		236	54	B	Y
	Underneath	30	50	B	N
		59	51	B	N
		118	52	B	N
		236	53	B	N

Task 2c Accumulation Tests					
Vehicle	**Leakage Location**	**Leak Rate (lpm)**	**Test #**	**Sensor Setup**	**Ignitable Mixture Present in Passenger Compartment? (Y/N)**
Intact	Trunk	3	72	B	N
		3	73	B	N
		3	77	C	N
		6	78	C	Y
		15	79	C	Y
	Rear Passenger	3	74	B	N
		3	75	B	N

***High* Leak Rates into Crashed Vehicles.** *High* leak rates were defined as 30 to 236 lpm.

Plots of hydrogen concentration as a function of time were created for each sensor in each test to document accumulation rates and any *steady-state* levels achieved. Yellow-shaded displays of hydrogen levels at 10 percent intervals from 0 percent to 100 percent were generated for each test to illustrate when and where hydrogen appeared and how long its level persisted between 4 percent to 75 percent. Each plot contains a yellow band between 4 percent to 75 percent hydrogen, representing the flammability regime. The darker yellow band from 28 percent to 32 percent represents hydrogen/air mixtures near or at the stoichiometric level (~30%). A complete compilation of plots is given in Appendix J.

As observed in Task 2a tests on the intact car, hydrogen did not leak into the trunk or passenger compartments of the crashed vehicles even when the leak was underneath and even though their seals could have been compromised (Figure III-8). Additional plots (Appendix J) also show minimal accumulation is typical with this below-vehicle leak location, even at high leak rates.

Leaks into trunk or passenger compartments resulted in significant accumulations of hydrogen (as observed in Task 2a for the intact car), reaching steady-state levels at all but the lower leak rates (Appendix J).

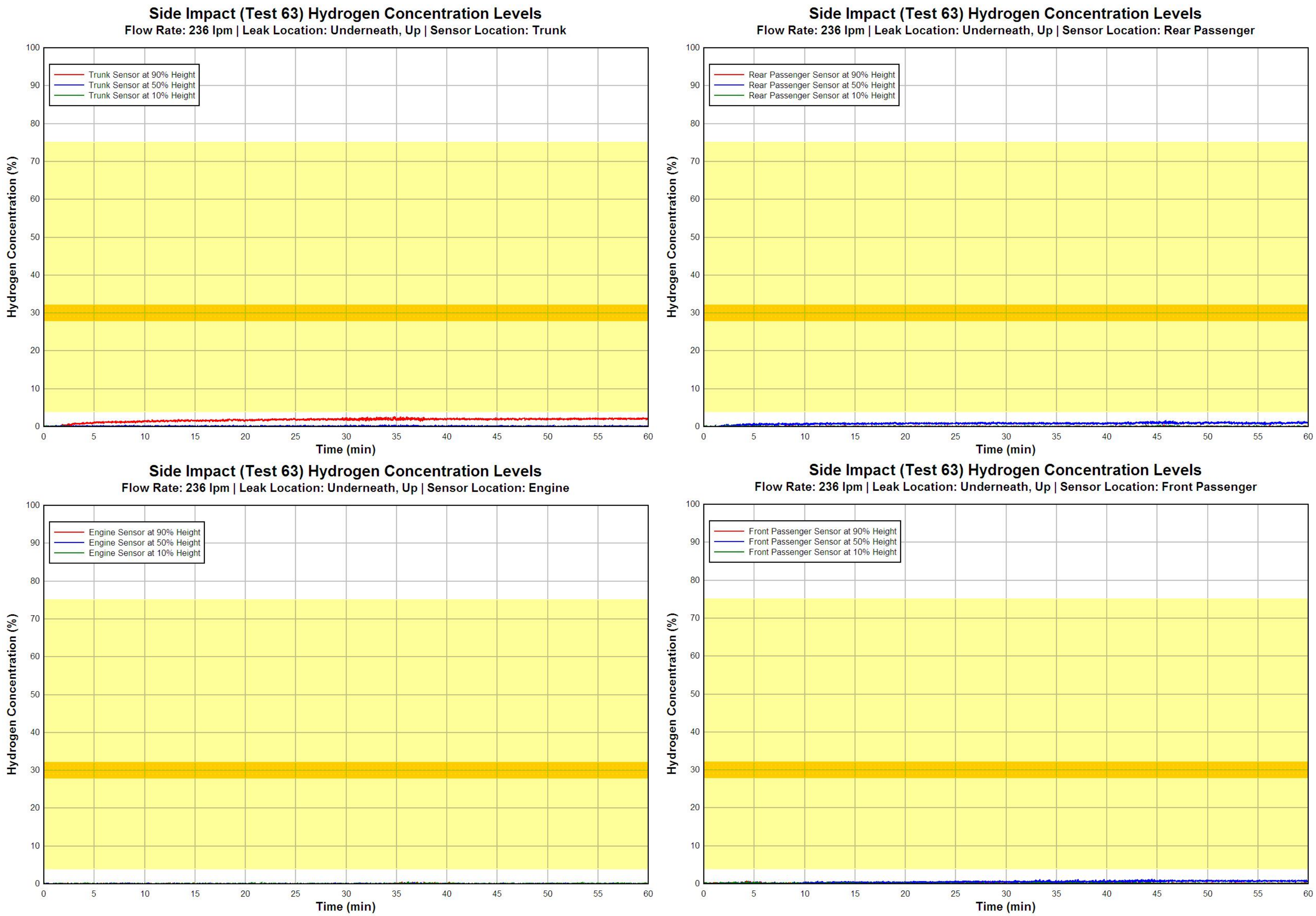

Figure III-8. Typical hydrogen accumulation data for 236 lpm leak underneath side-impact.

Leaks into trunk or passenger compartments of the crashed cars, when the sealing integrity of the vehicle could have been compromised, resulted in different accumulations, probably because hydrogen could vent through gaps. Figure III-9 shows that a *local inversion* occurred (highest hydrogen concentration not at the highest location) over narrow (inches) sensor separations. This behavior was observed for rear and side-impact vehicles. These data reveal that hydrogen migration and accumulation within crashed vehicles are complex phenomena.

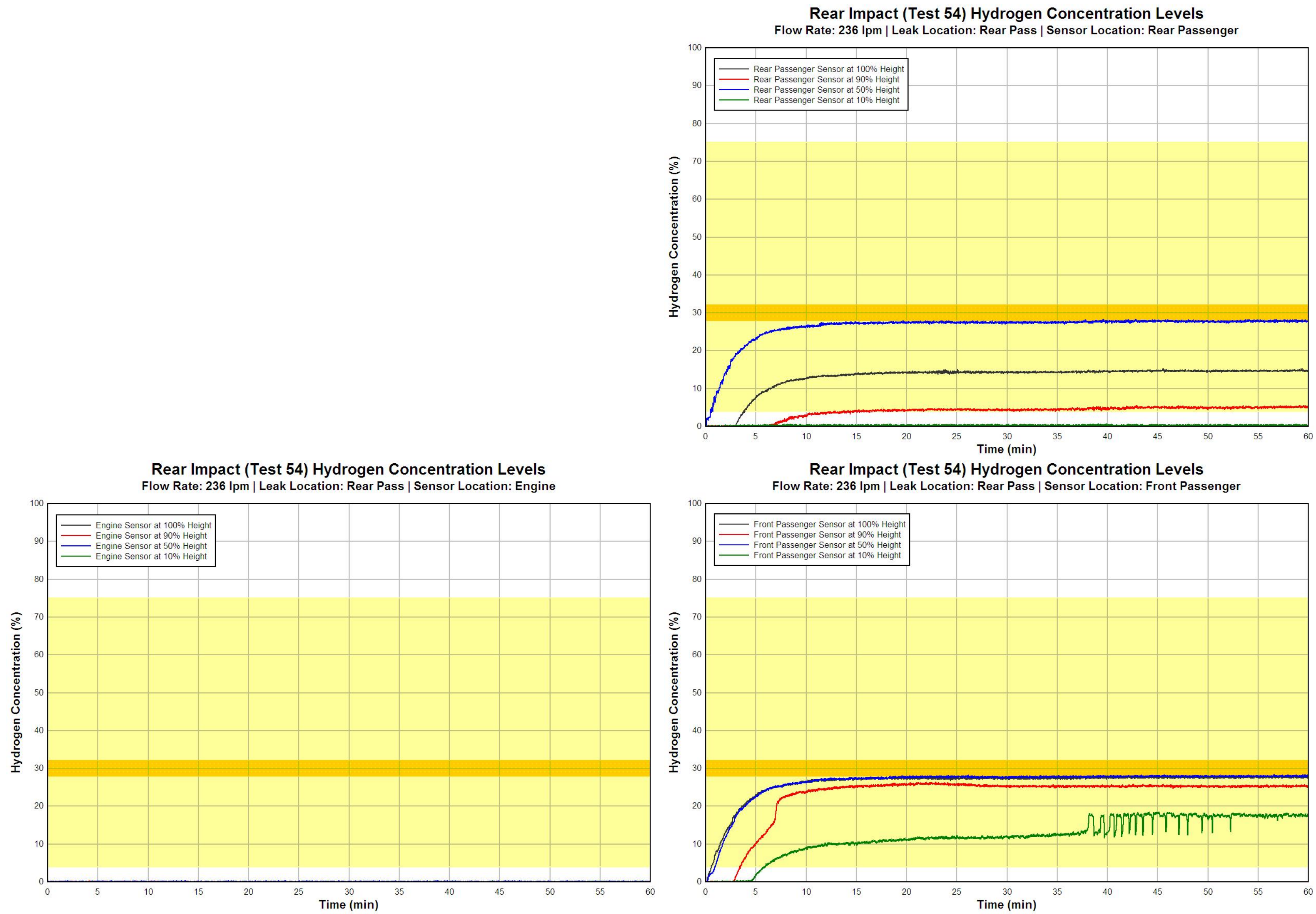

Figure III-9. Hydrogen accumulation data for 236 lpm leak into rear-passenger compartment of rear-impact vehicle for Test 54.

In addition to the effects witnessed as a function of seal integrity (intact vs. crashed vehicles), several other interesting characteristics associated with hydrogen accumulation were observed when slower (≤ 59 lpm) leak rates were employed. In general, slower leaks appeared to limit the mixing of hydrogen with air, making *movement* of hydrogen somewhat irregular and random. Higher leak rates appeared to cause better mixing of hydrogen with the surrounding air, making hydrogen movement more regular and predictable. This trend is demonstrated clearly in the next series of accumulation plots for the front-impact vehicle (Figure III-10 – Figure III-13). Plots are presented starting with the lowest leak rate, then increasing. As the leak rate increased, accumulation curves behaved in a more logical and expected manner, which was not true when the passenger compartment seals were compromised.

When leaked into a vehicle-sized volume, the rate at which the hydrogen is injected dictates where and to what extent it accumulates. Leak rates above 118 lpm from an open-ended tube appear to provide sufficient turbulence to achieve adequate mixing, such that the mixture moves predictably throughout the vehicle volume. Thus, hydrogen is detected first by sensors nearest the leak source; later, higher sensor locations eventually register the highest concentrations and, as time progresses, at steady-state levels.

Lower leak rates did not appear to induce sufficient mixing, making the hydrogen migration appear complex and unpredictable. A crude visual analogy is a lava lamp. Slow motion within allows the two media of different densities to remain separate and flow in random fashion as localized pockets.

Witnessed accumulation characteristics of slow hydrogen leak rates included:

- Rapid changes - concentrations rapidly increase at various times;
- Inversion – higher-level sensors register lower concentrations; and
- Dead zones – no hydrogen detected, even at high sensor locations.

From a macro perspective, higher leak rates appeared to generate more uniform concentrations front-to-back with some bias towards highest elevations. Lower leak rates appeared to generate multiple, random concentrations. Slower leaks appeared to produce pockets of higher concentration that are more dangerous and could have a higher potential for causing injury if ignited.

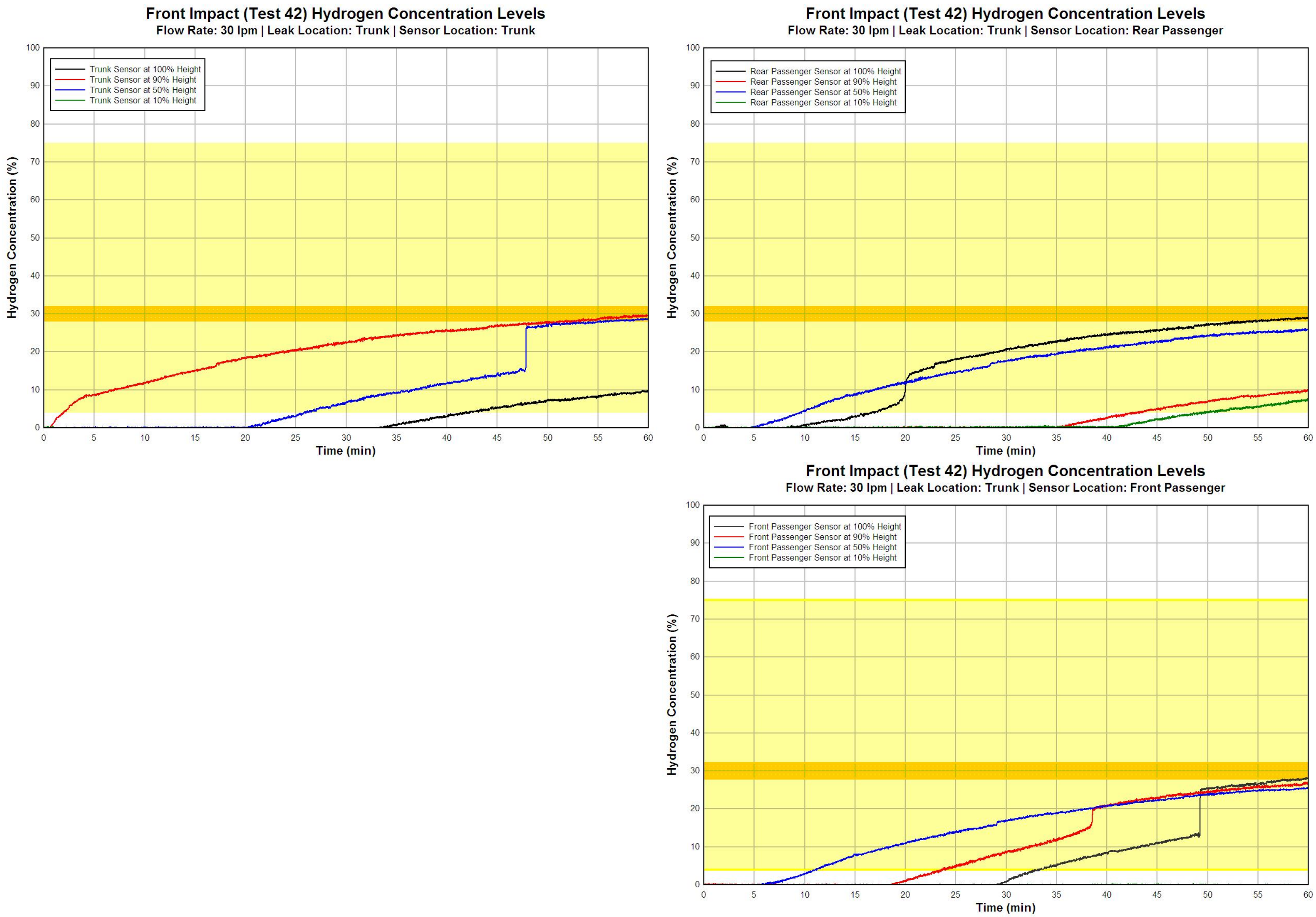

Figure III-10. Hydrogen accumulation data for 30 lpm leak into trunk of front-impact vehicle for Test 42.

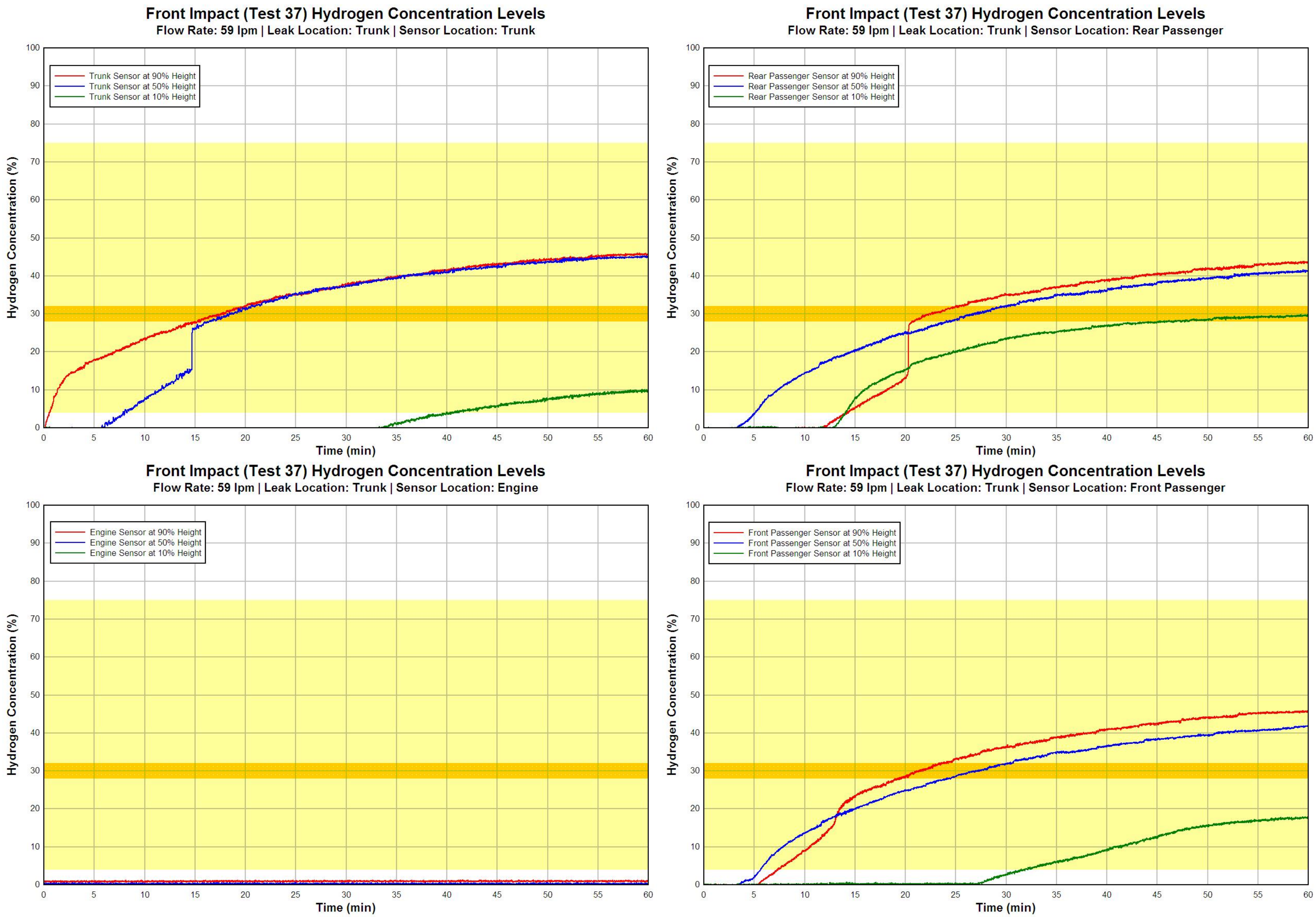

Figure III-11. Hydrogen accumulation data for 59 lpm leak into trunk of front-impact vehicle for Test 37.

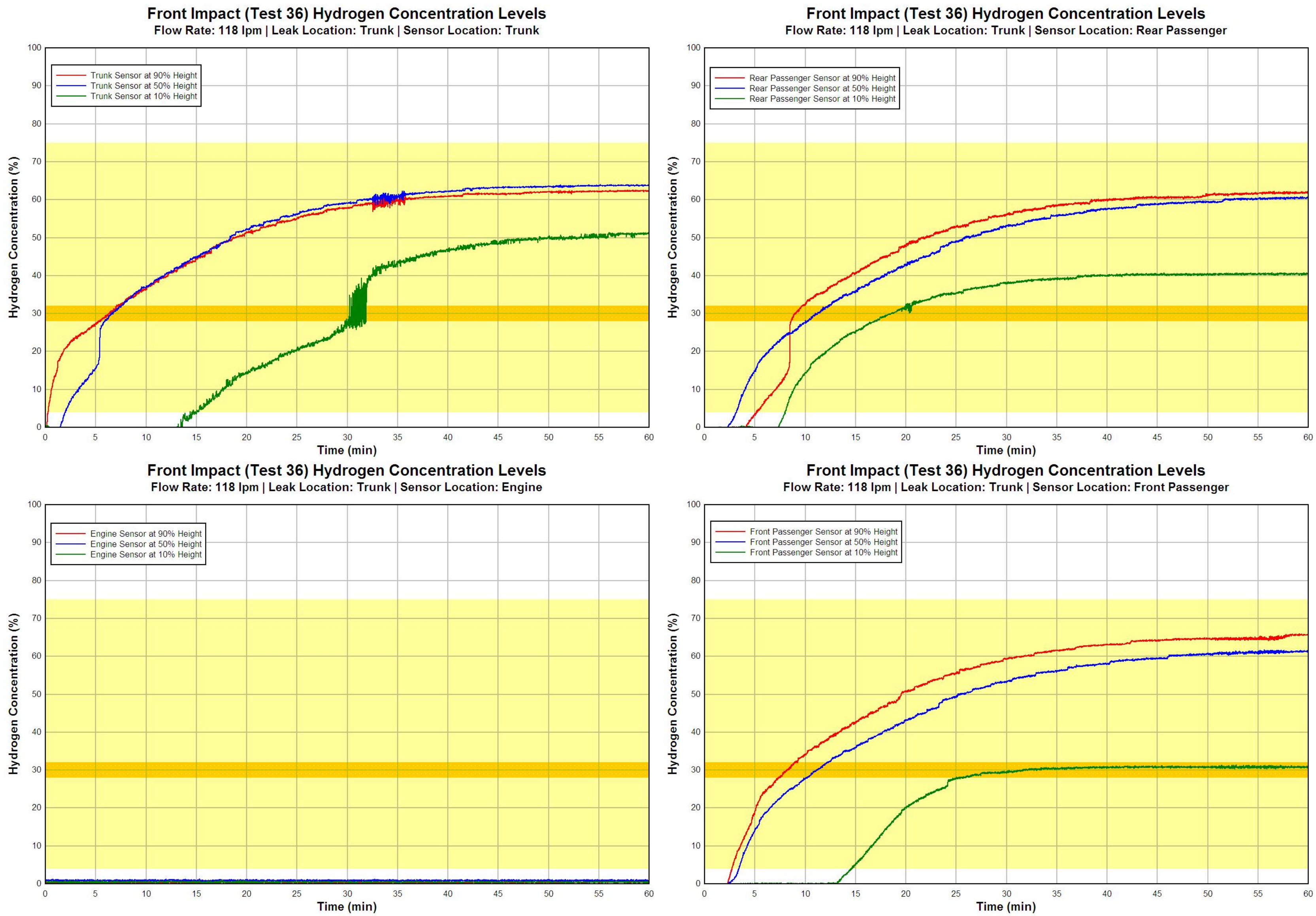

Figure III-12. Hydrogen accumulation data for 118 lpm leak into trunk of front-impact vehicle for Test 36.

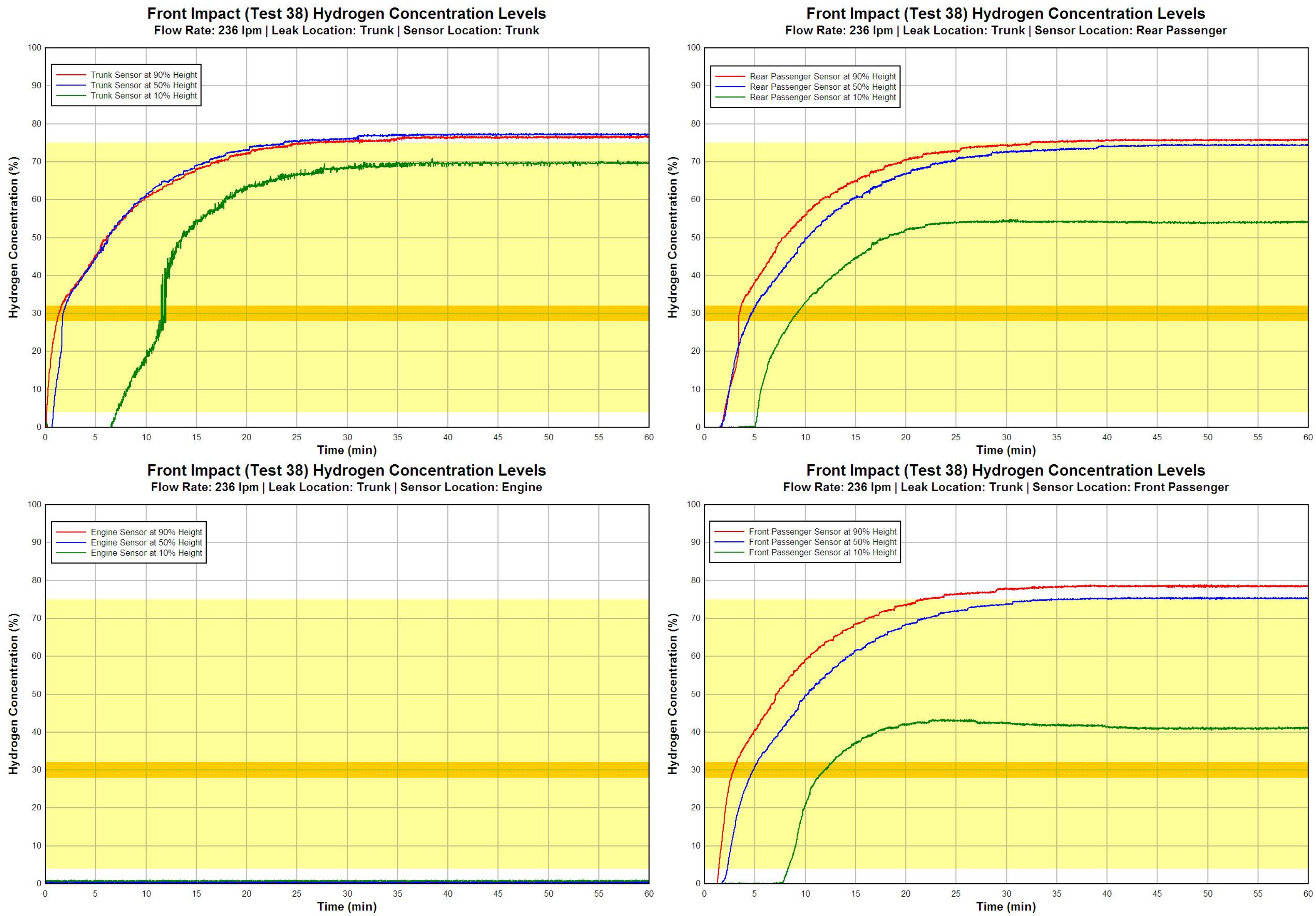

Figure III-13. Hydrogen accumulation data for 236 lpm leak into trunk of front-impact vehicle for Test 38.

Low Leak Rates into Intact Vehicle. *Low* leak rates were defined as ≤30 lpm; *ultra-low* as 3 lpm.

Hydrogen accumulation characteristics were evaluated further using low leak rates in the intact test vehicle that had sealed passenger and trunk compartments. Plots of hydrogen concentration as a function of time were recorded for each sensor in each test to document accumulations and steady-state behavior (see Intact Section, Appendix J). As before, the following plots contain a yellow band to illustrate when the mixture was within the flammable regime and a darker yellow band to show when the mixture was at or near the stoichiometric.

The lowest leak rate tested was 3 lpm, the lowest flowrate the mass flowmeter was certified to deliver reliably. A 3lpm leak rate over 60 min (180 l) is near-equivalent to ~5 percent of the volume of the passenger compartments as was 118 lpm for 1.5 min leaked in Task 2b. First tests had the leak in the trunk and the 10 percent-50 percent-90 percent-100 percent hydrogen sensor arrangement. About 1-3 percent hydrogen was detected at the 50 percent and 100 percent rear-passenger sensors (Figure III-14). These levels of hydrogen are nonflammable. No other sensors detected hydrogen. Similar results were obtained for leaks into the rear-passenger compartment.

Accumulation tests indicated that hydrogen was measurable at the 50 percent and 100 percent sensors, but not at the 90 percent sensor in the same compartment. Hydrogen was also not detected in the trunk near the leak outlet or in the front-passenger compartment separated by a collapsible rear seat that appeared to be an ineffective barrier to flow between the compartments in higher flow rate tests. To validate these "no hydrogen detected" data, and those indicating an apparent "randomness" in hydrogen accumulation at low leak rates, additional accumulation tests were conducted at ultra-low flowrates. First, informal checks were performed on each sensor to verify its operation by using it near the leak outlet while flowing hydrogen. All sensors were always found to be functioning as indicated by the detection of very high levels of hydrogen. Second, formal checks were performed by recalibrating the sensors against a certified standard (5% hydrogen; balance nitrogen) and 100 percent hydrogen (Appendix L). All sensors were determined to be *in calibration*. Therefore, all accumulation data presented in this report accurately depict where and to what extent hydrogen accumulates in the intact car at ultra-low leak rates.

To attempt to locate other locations in which hydrogen might be accumulating, the decision was made to reposition all hydrogen sensors to the 100 percent height along the centerline of the roof of the trunk. The logic was that if buoyancy dominated laminar/turbulent flow mixing at ultra-low leak rates, ultra-light hydrogen (compared to air) could migrate to the highest elevations inside the vehicle. Such behavior has been observed in modeling studies[9].

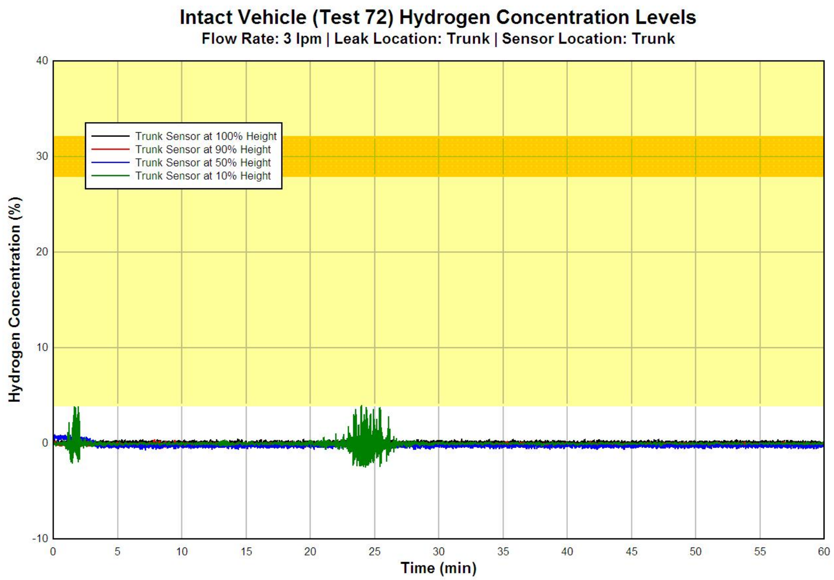

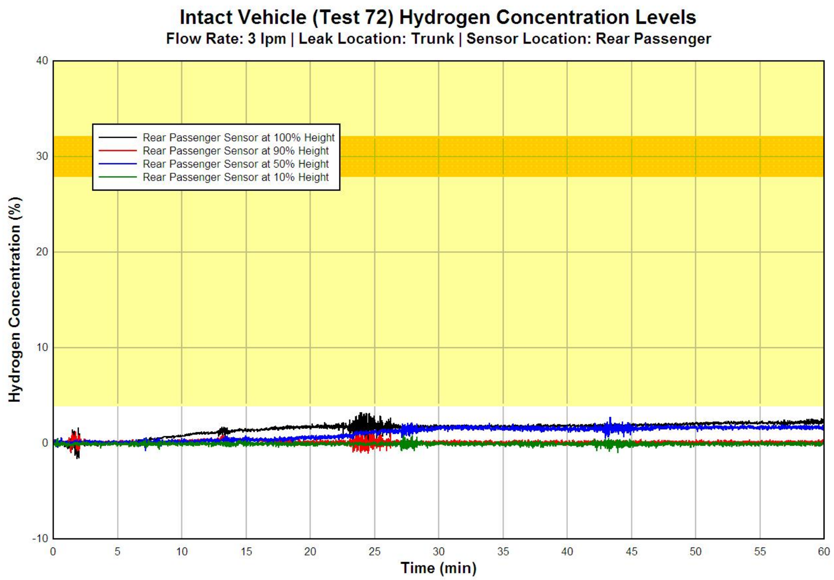

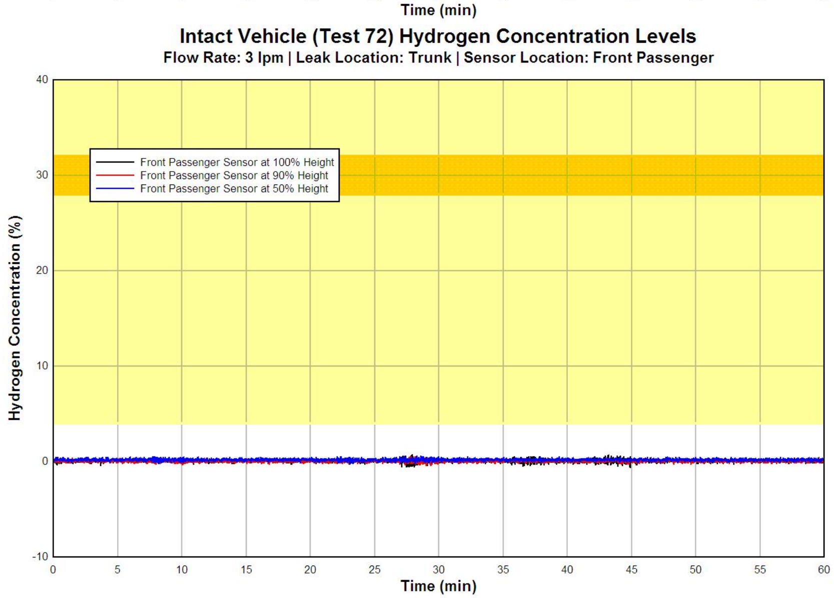

Figure III-14. Hydrogen accumulation data for 3 lpm leak into trunk of intact vehicle using 10 percent-50 percent-90 percent-100 percent-height hydrogen sensor setup for Test 72.

Data obtained for the 3 lpm flowrate after reconfiguring to the all-100 percent sensor setup are shown in Figure III-15. Slight accumulations are revealed at or near the rear window and near a possible location for an overhead light.

To confirm that 60 min was a sufficient *time constant* for accumulation near the inside roof of the vehicle to reach a static condition, tests were extended for 30 min after leakage had been ceased. No significant increases in hydrogen concentration at any of the sensors were observed, implying that accumulations measured after 60 min were effectively *steady-state*.

To verify that hydrogen was accumulating in the vehicle and not leaking, the leak rate was increased systematically from 3-to-6-to-15 lpm in an attempt to achieve richer accumulations, or the absence of same. The resulting data are shown in Figure III-15, Figure III-16, and Figure III-17, respectively. Systematically higher hydrogen accumulations were observed at the same two sensor positions as flowrate was increased from 3-to-6-to-15 lpm, with no hydrogen accumulation again observed at the other sensors positions. Hydrogen concentrations at each location did reach flammable levels at flowrates above 6 lpm.

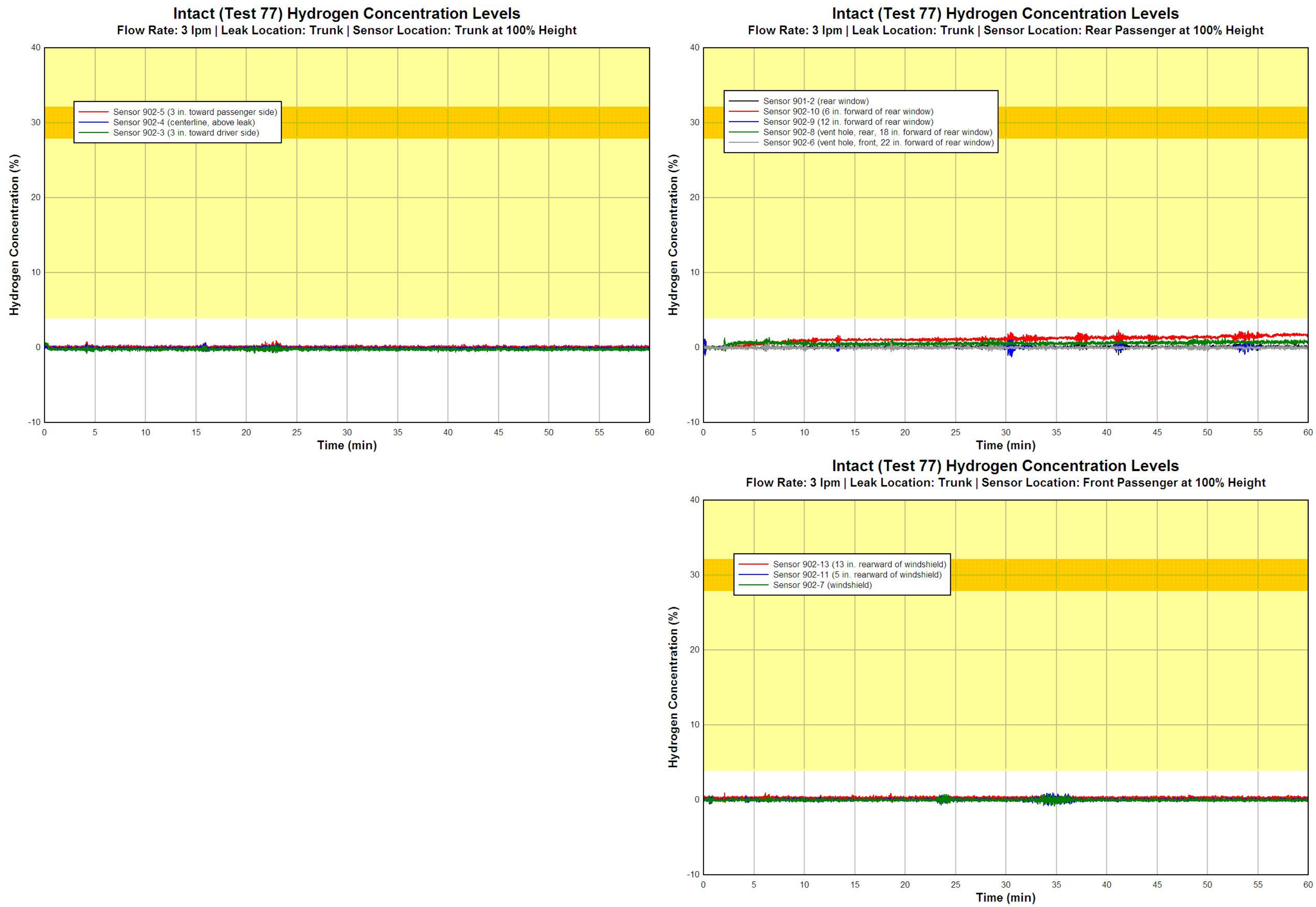

Figure III-15. Hydrogen accumulation data for 3 lpm leak into trunk of intact vehicle using all-100 percent-height hydrogen sensor setup for Test 77.

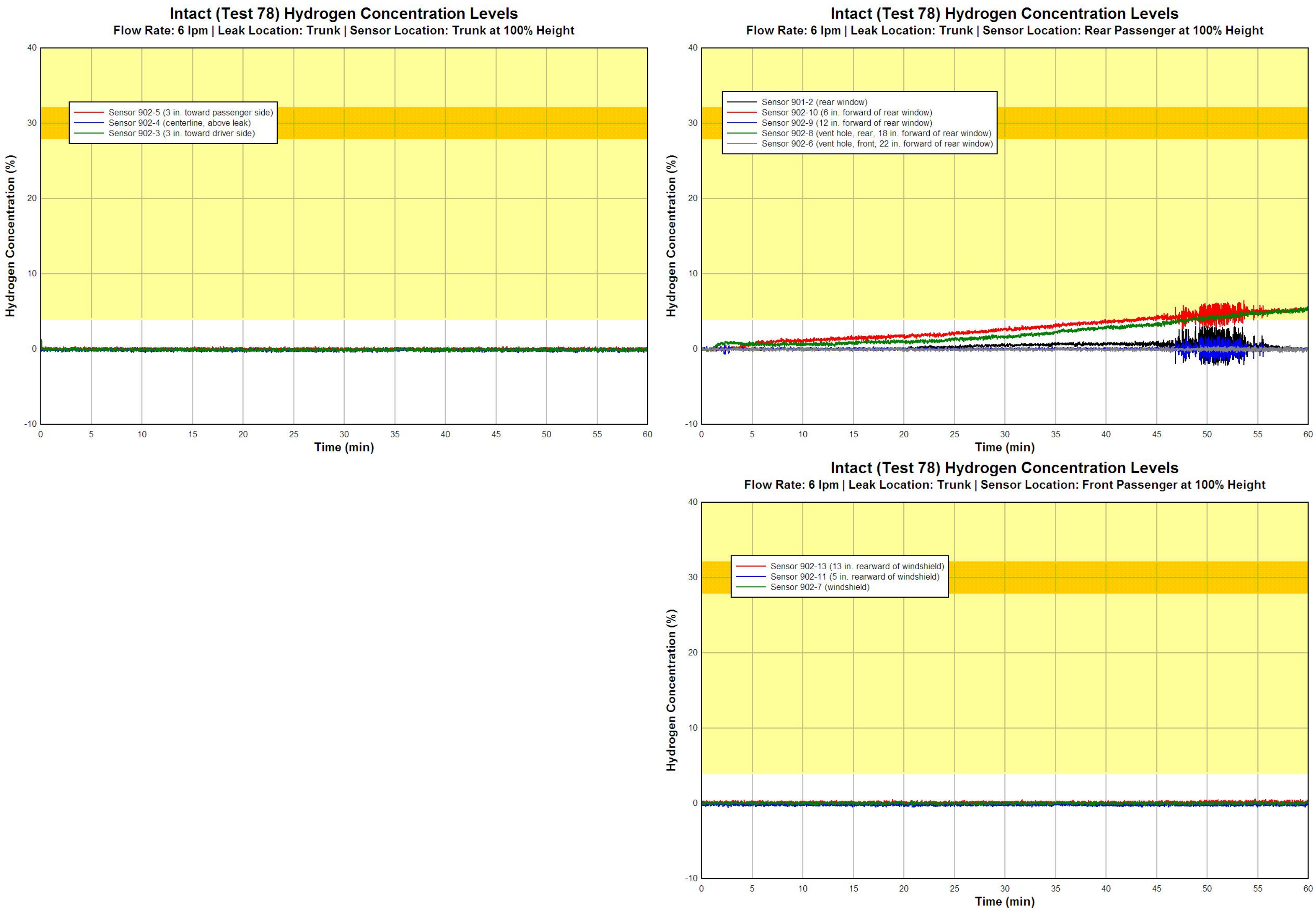

Figure III-16. Hydrogen accumulation data for 6 lpm leak into trunk of intact vehicle using all-100 percent-height hydrogen sensor setup for Test 78.

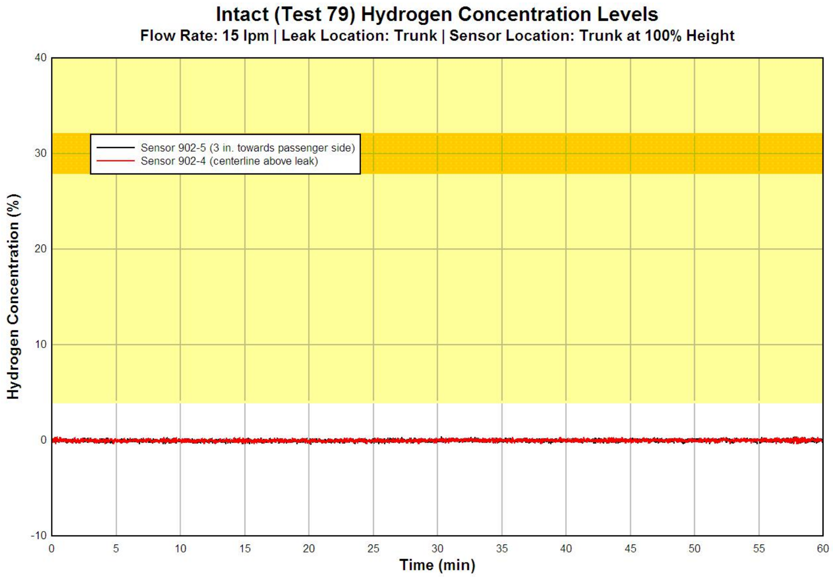

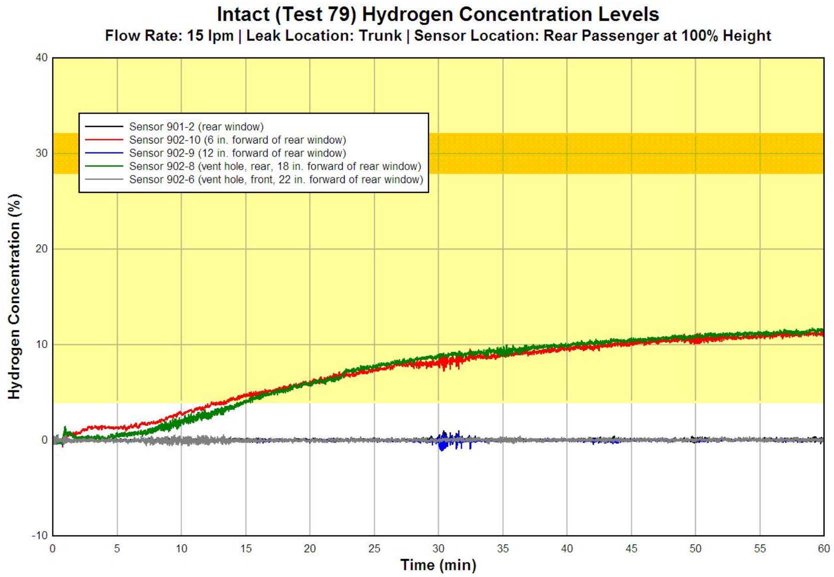

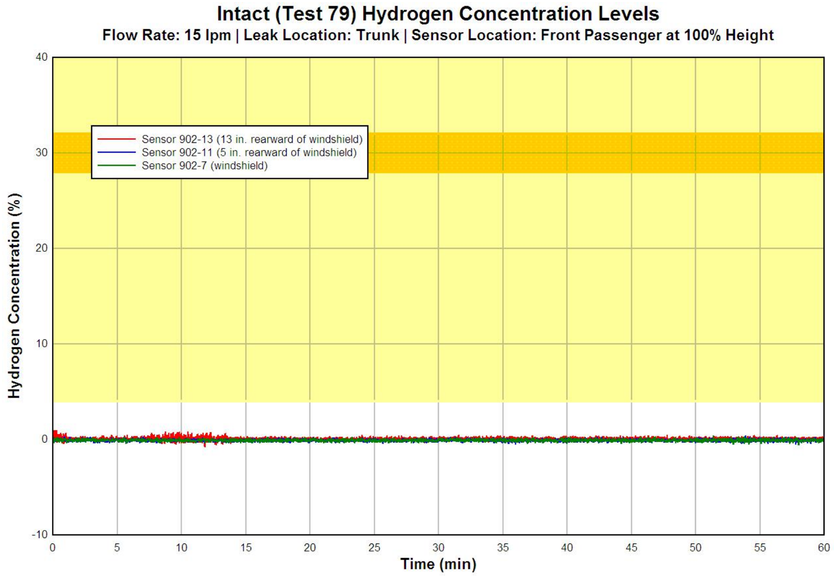

Figure III-17. Hydrogen accumulation data for 15 lpm leak into trunk of intact test vehicle using all-100 percent-height hydrogen sensor setup for Test 79.

Summary of Task 2c Leak-Accumulation Data. In view of these efforts, hydrogen accumulation data in intact and crashed vehicles at ultra-low (3 lpm) to ultra-high (236 lpm) levels have been acquired to the most reliable extent possible.

Observations specific to leak tests on the front-crashed vehicle were as follows:

- Leaks in the trunk or passenger compartment always resulted in detectable accumulation in the other compartment, comparable to that measured in Task 2a (intact car).
- Leaks underneath the vehicle did not result in detectable accumulation inside.
- Low leak flowrates into the trunk or passenger compartment resulted in random detectable hydrogen flow patterns and levels (inversions and localized pockets).

Observations specific to leak tests on the side-crashed vehicle were as follows:

- Leaks in trunk or passenger compartment resulted in significantly lower detectable accumulations in the other compartment compared to the intact or front-crashed cars.
- Leaks underneath the vehicle (near door seals) still did not result in detectable accumulation inside the vehicle.
- Leaks even at high flowrates into trunk or passenger compartment resulted in detectable accumulations that were random and irregular (concentration inversions).

Observations specific to leak tests on the rear-crashed vehicle were as follows:

- Leaks in passenger compartment resulted in significantly lower detectable accumulations than in other compartments, compared to intact or front-crashed cars.
- Leaks underneath the vehicle did not result in detectable accumulation inside.
- Leaks originating in passenger and trunk compartments resulted in random, but detectable accumulations, which were flammable.

Overall observations on Task 2c hydrogen leak accumulation tests are as follows:

- At low leak rates ($\leq$60 lpm), hydrogen does mix well with air, resulting in its accumulation being randomized, exhibiting characteristics similar to a lava lamp in that slow motion causes media of different densities to remain unmixed, pocketing locally, inverting where higher-sensor locations register lower concentrations than lower-sensor locations, and being absent at high locations.
- At high leak rates ($\geq$118 lpm), hydrogen mixes more homogenously, resulting in more distinct stratified levels, increasing more uniformly throughout the vehicle, being detected first nearest leak, generally seeking higher elevations with time, and reaching more uniform and steady-state concentrations.
- Door, window, and frame seals in front or rear-impact vehicles were not compromised to the extent of allowing hydrogen outside and below the vehicle to accumulate inside the vehicle, behavior indicative of an intact vehicle. Moreover, hydrogen outside and underneath the side impact vehicle also did not leak and accumulate inside, even though its window and door seals were compromised.

The implications of these accumulation data to a minimum allowable post-crash leak rate were:

- Although accumulation data at the 3 lpm leak rate in the intact car did not detect a region within the passenger compartment that was flammable, this ultra-low leak rate cannot be considered as the minimum allowable because of the distinct possibility that hydrogen might be accumulating at flammable levels in pockets away from sensor locations.
- The finding that hydrogen migration and accumulation in vehicles was random and localized has significance in efforts to determine the number and locations of on-board hydrogen sensors to signal an alarm about the presence of a flammable atmosphere in passenger compartments following a crash. One hydrogen sensor in one *logical* or expected location cannot be sufficient to know that a flammable condition exists.

Computational fluid dynamic (CFD) modeling data, albeit for a hydrogen release into a garage not a vehicle, suggest that hydrogen accumulations measured here might not be unusual.(6) The aforementioned accumulation characteristics are portrayed in these CFD-predictions: (1) hydrogen can appear and disappear rapidly at one location and (2) hydrogen levels can be higher at lower positions than at higher positions.

Task 2c Ignition Test Results

The scope of Task 2c ignition tests was the measurement of the heat flux and overpressure created upon ignition of flammable levels of hydrogen accumulated in the trunk and passenger compartments of intact and crashed vehicles following plausible leak rates from a post-crash hydrogen fuel system. The objective was to quantify hydrogen combustion effects, relate them to the extent of personal injury, and use these data to establish a minimum allowable post-crash hydrogen leak rate. Similar tests were conducted in Task 2b using the ACS, that allowed multiple ignition tests to be conducted on the same vehicle-like system in a relatively short period of time via the use of replacement compartment panels.

Table III-2 summarizes the vehicle condition, flowrate leaked, test number, ignition event, and the occurrence of a secondary fire.

Table III-2. Matrix and critical data from Task 2c ignition tests.

Task 2c Vehicle Ignition Tests					
Vehicle	**Leak Rate (lpm)**	**Leak Duration (min)**	**Test #**	**Ignition?**	**Secondary Fire?**
Front Impact	**118**	**1.5**	**68**	**Yes**	***Yes***
Intact	3	60	82	No	No
	6	**60**	**83**	**Yes**	***Yes***
Rear Impact	6	60	84	No	No
	12	60	85	No	No
	24	**60**	**86**	**Yes**	**No**
	48	60	87	Yes	No
Side Impact	**60**	**60**	**88**	**Yes**	***Yes***

As evident in Table III-2, some vehicles underwent multiple ignition tests. These multiple tests were possible only because ultra-low leak rates were used first and were expected to result in low damage levels upon sparking. When either the test did not result in an ignition or only a *mild*, nondestructive reaction that did not affect the visual integrity of the vehicle (i.e., seals or physical structure), a second ignition test was conducted on the same vehicle.

Table III-2 indicates that not one, but two *events* occurred in three of the four tests; the first was called *ignition* and the other, *secondary fire*. For clarity of presentation, the next section first presents information on the ignitions and then information on secondary fires.

Task 2c Ignition Test Results: Ignition

Test 68. The first ignition test was conducted with the front-impact vehicle (Figure III-18). The leak was located in the trunk and flowed at a rate of 118 lpm for 90 sec. The total hydrogen volume delivered was ≈ 177 l into ≈ 3,012 l, or ≈ 5 percent of the trunk and passenger compartment volumes. A hydrogen sensor was located at 50 percent height in both the front-passenger and trunk compartments. The ignition source was a spark plug (100 J), located a few inches between the leak in the trunk and the 50 percent sensor location. Heat flux and overpressure sensors were located at the front driver side at head height, rear passenger side at head height, and outside the driver side *B* pillar (outside vertical support between driver and passenger compartments) at a standing head height (4 ft).

Figure III-18. Heat flux gauges and pressure transducers mounted in plastic cylinders at driver's and rear passenger's head locations and exterior (first responder) test stand (right) in Test 68.

Although neither hydrogen sensor detected a flammable hydrogen concentration, sparking resulted in a combustion event more damaging than expected based on Task 2b testing. The increased confinement of the vehicle, albeit after impact (front), compared to that of the ACS that was sealed with magnets and tape, appears to have held pressure generated longer after ignition and allowed it to build to significantly higher levels. Figure III-19 shows the effects.

Figure III-19. High-speed imagery stills for showing first observed light (41 msec), rear headliner motion (43.5 msec), glass fracture/door bulge (58.5 msec), and glass ejection (110.5 msec) in Test 68.

The resulting overpressure (Figure III-20) peaked at ≈ 9 psi in the back seat, significantly higher (same flow conditions and transducers) than generated in the Task 2b ACS ignition tests. In contrast, heat flux (Figure III-21) was similar for tests in both tasks.

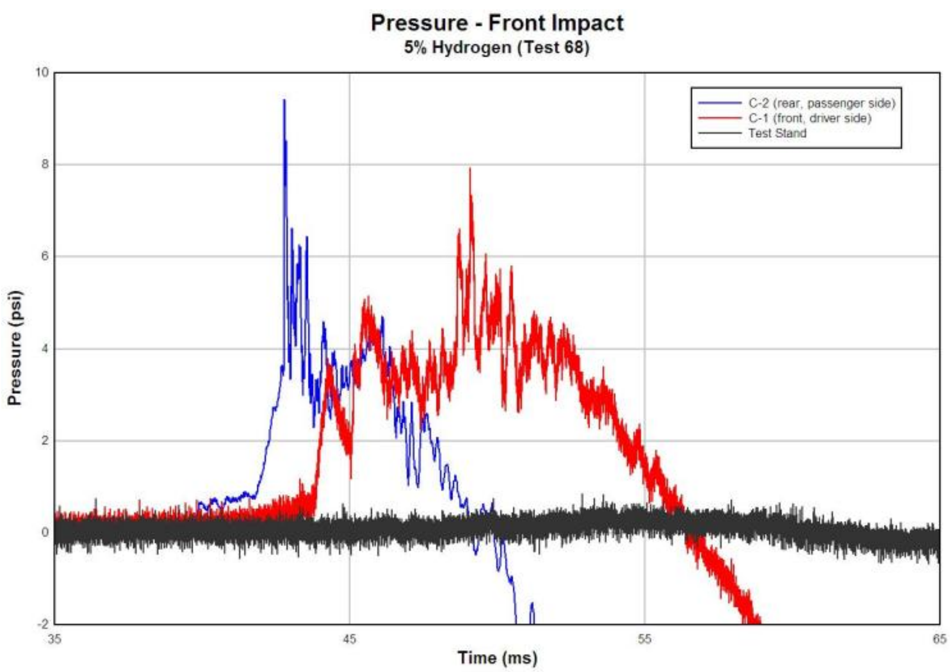

Figure III-20. Post-ignition overpressure data for 5 percent hydrogen injected volume into front-impact vehicle in Test 68.

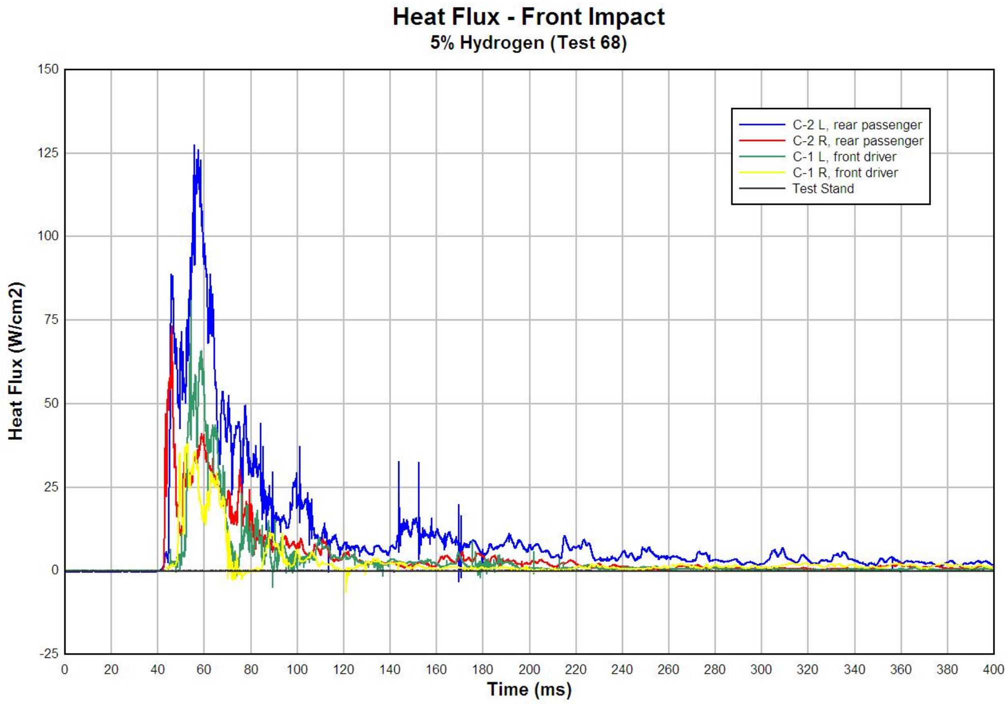

Figure III-21. Post-ignition heat flux data for 5 percent hydrogen injected volume into front-impact vehicle in Test 68.

Heat flux data were processed using the BURNSIM algorithm to predict the burn injury threat posed to personnel in the driver or rear passenger seats, or outside (first responder) the vehicle[6]. Physical trauma, in the form of the extent of eardrum rupture, was predicted using empirical data reported by Altman on the auditory effects of blast waves on humans.[8]

Predictions listed in Table III-3 indicate that in Test 68 first-degree burns are likely for the driver and that second-degree burns are expected for a passenger seated in the rear-passenger compartment. No burn injury was predicted at the test stand location where a first responder could be standing.

Table III-3. Prediction of skin burn injuries from heat flux in Test 68.

Thermal Injury Prediction (BURNSIM)			
Sensor Location	**Degree of Burn**	**Maximum Temperature (°C)**	**Burn Threshold Depth (µm)**
C1-L Front Driver	1st	87	0.8
C1-R Front Driver	None	68	0
C2-L Rear Passenger	2nd	128	151
C2-R Rear Passenger	1st	85	25
Test Stand	None	34	0

Table III-4 presents the results for the prediction of potential injury to the eardrum of the driver, rear passenger, and first responder. Both the driver and rear passenger could be expected to experience some degree of eardrum rupture from the blast overpressure associated with the ignition of the hydrogen accumulation. No eardrum injury was predicted to result from overpressure at the first responder location (outside the vehicle test stand).

Table III-4. Prediction of ear injuries from overpressure in Test 68.

Overpressure Injury Prediction		
Sensor Location	**Peak Pressure (psi)**	**Eardrum Injury**
C1 Front Driver	7.9	≈ 20% Rupture
C2 Rear Passenger	9.4	≈ 30% Rupture
Test Stand	0	None

Because Test 68 was a first-of-its-kind vehicle-ignition test, its outcome was analyzed to confirm or upgrade procedures for subsequent tests. Of particular concern was the lack of response of the hydrogen sensors. Just prior to sparking, neither sensor in the trunk or passenger compartment detected hydrogen after 90 sec of flow. However, the result of sparking after injecting hydrogen equivalent to ≈ 5 percent of the volume of the trunk and passenger compartments was a definite ignition, implying a flammable level of hydrogen somewhere near the spark. The ignition caused window glass to be shattered, windshield to be blown out (in one piece), and doors and trunk to be buckled and breached.

The fact that no hydrogen was detected at either sensor, yet ignition occurred after spark discharge, implied that the local hydrogen level was between 4 percent and 75 percent. After consulting with NHTSA staff, the consensus was that additional tests were required on the hydrogen sensors used in order to determine their responses and response times to hydrogen concentrations of ~5 percent. A very slow response time could explain why hydrogen could be ignited, but not detected as flammable in proximity with the hydrogen sensor.

The object of this exercise was to determine if hydrogen sensor response time was a function of hydrogen concentration. Response times of about 1-2 sec, given by the vendor, reportedly were determined at 100 percent hydrogen. If the response time at ~5 percent hydrogen was different from that at 100 percent hydrogen, additional response time tests could be conducted at 10 percent to 15 percent hydrogen. Appendix L provides details on conducting these tests, along with their results.

Response times (10% to 90% full scale) for the sensors (Neodym Panterra; no endorsement) at 5±1 percent hydrogen (certified) were ~10±5 sec; however, at 95±5 percent hydrogen, the response times were ≤ 5 sec. Although response times were somewhat longer at 5 percent than at 100 percent, the failure of these sensors to detect hydrogen after 90 sec of flow was not because of very slow response time, but because of ≤ 4 percent hydrogen in the vicinity. The hydrogen sensor and spark plug were merely inches apart.

Tests 82-83. A revised procedure was used for the next Task 2c ignition test. The original procedure leaked hydrogen into the passenger compartment from the trunk at a rate of 118 l for 90 sec to achieve an effective volume of 5 percent. Because the objective of this program was to establish a *minimum* allowable post-crash hydrogen leak rate, the next logical test was to recreate the same ~5 percent total hydrogen volume condition, not at 118 lpm, but at the slowest rate possible. Because FMVSS 303 requires a 60 min test duration, the slowest the flowrate could be was ~3 lpm. The objective of testing at this *ultra-low* leak rate was to confirm if a low leak rate created the same fire threat as 118 lpm, proposed at the outset of this program. NHTSA reviewed and approved this proposal, along with the following other procedures:

- Use the intact car as the next test vehicle.
- Locate the origin of the leak in the trunk compartment.
- Conduct leak and accumulation tests before ignition tests.
- Locate hydrogen sensor arrays in the front and back passenger compartments.
- Mount hydrogen sensors not only at 10 percent, 50 percent, and 90 percent heights, but also at 100 percent.
- Locate one hydrogen sensor in the trunk compartment near the hydrogen leak inlet.
- Use data from accumulation tests to locate pockets of flammable levels of hydrogen.
- Remove hydrogen sensors; install spark plugs near flammable hydrogen pockets.
- Install one heat flux and one pressure sensor at driver face location in the vehicle.
- Leak hydrogen into trunk and attempt to spark ignite after 5 percent car volume was leaked.
- If ignition did not occur, spark again at the same or multiple locations until ignition occurs.
- If still no ignition, increase leak rate by a factor of two until ignition is achieved.
- If explosion damage did not compromise the intact car, continue ignition tests with it.
- Conduct the same procedures and sequence on the rear and side-crashed vehicles.

The objectives of these next Task 2c ignition tests were to confirm: (1) if the ignition and injury threat posed by 5 percent hydrogen from post-crash hydrogen leakage was dependent upon leak rate or was dependent only upon the presence of a flammable level of hydrogen in the passenger compartments, and (2) that ignition could be achieved by sparking in the passenger compartment and not in the trunk near the hydrogen leak outlet. These test procedures also were designed to allow conducting as many tests as possible on any of the intact or remaining impact vehicles, which would increase realism in the determination the minimum allowable leak rate.

Based on data from accumulation tests with the intact vehicle, an initial flowrate of 3 lpm was chosen for the first ignition tests with the intact car. The plan was to increase the hydrogen leak rate, attempt to ignite, and retest until ignition was achieved. If the vehicle was not damaged (breaches or broken glass), another test could be conducted using it.

Test 82 consisted of introducing a 3 lpm leak into the intact vehicle for 60 min, followed by up to three spark ignition attempts, as needed. Figure III-22 shows the hydrogen concentrations measured near two of the spark plugs, which were below the lower flammability limit (4%). As expected, the result of sparking was no ignition of the hydrogen mixture.

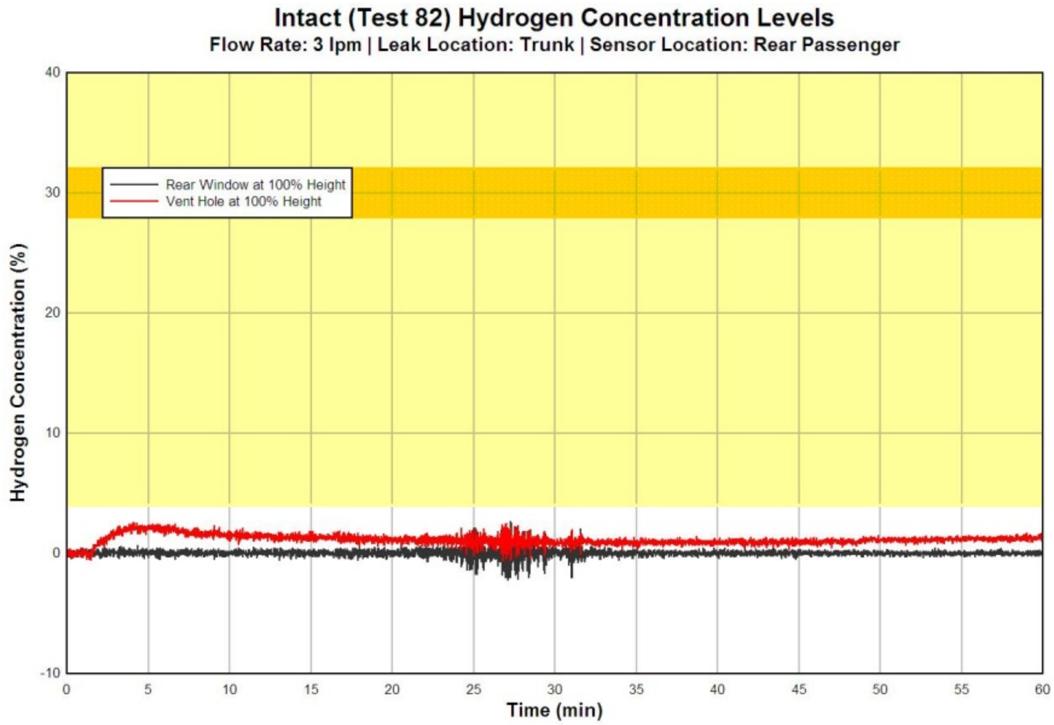

Figure III-22. Hydrogen accumulation data for 3 lpm leak into trunk of intact vehicle in Test 82.

In Test 83, in an attempt to create a flammable atmosphere, the hydrogen leak rate was doubled to 6 lpm. Upon sparking, ignition occurred (Figure III-23). Figure III-24 – Figure III-26 respectively show data on hydrogen accumulation, heat flux, and overpressure. In this test, the hydrogen sensor detected flammable hydrogen levels in the vent hole (Figure III-24).

Figure III-23. High-speed imagery stills showing intact vehicle at moment of first spark (left at T = 0 sec) and when windows fogged (right at T = 1.4 sec, note displacement of string) in Test 83.

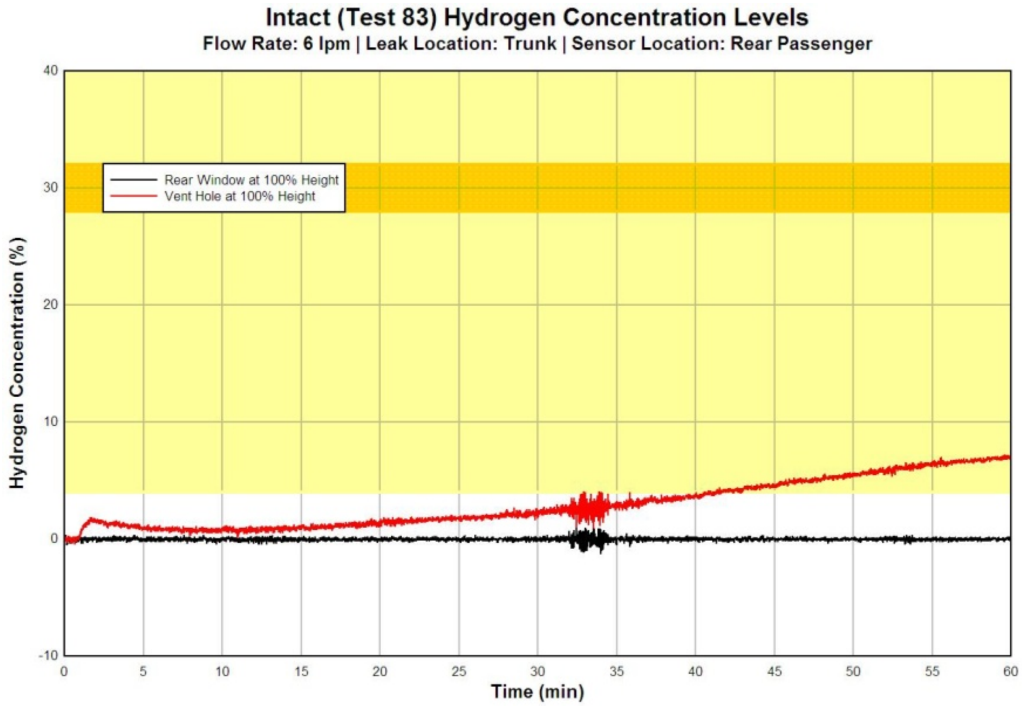

Figure III-24. Hydrogen accumulation data for 6 lpm leak into trunk of intact vehicle in Test 83.

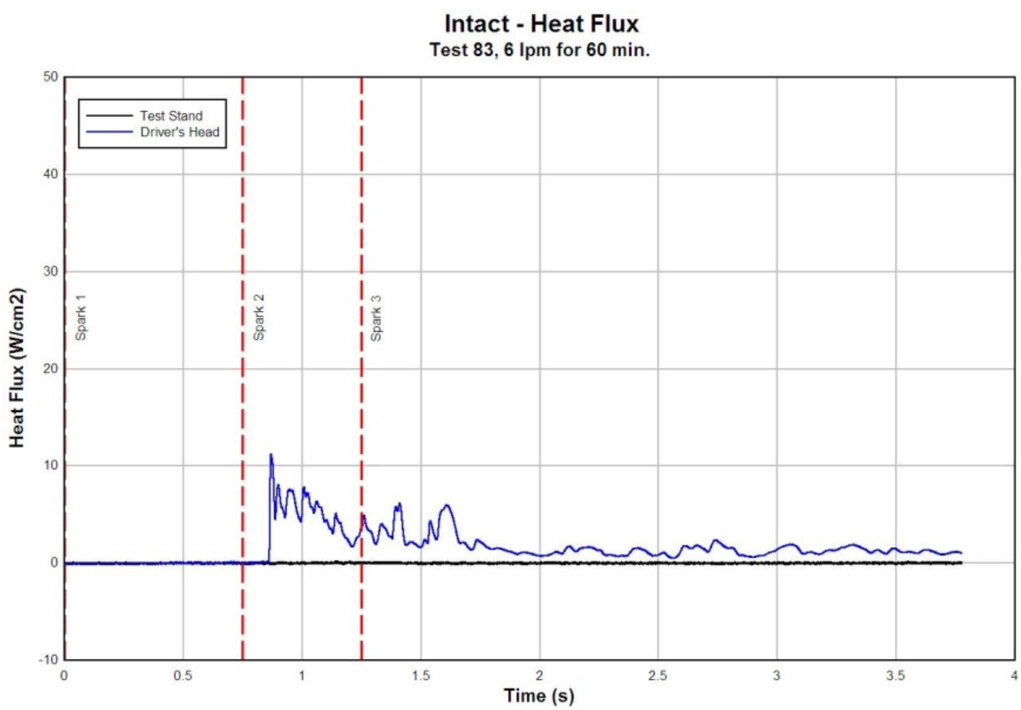

Figure III-25. Post-ignition heat flux data for 6 lpm leak into trunk of intact vehicle in Test 83.

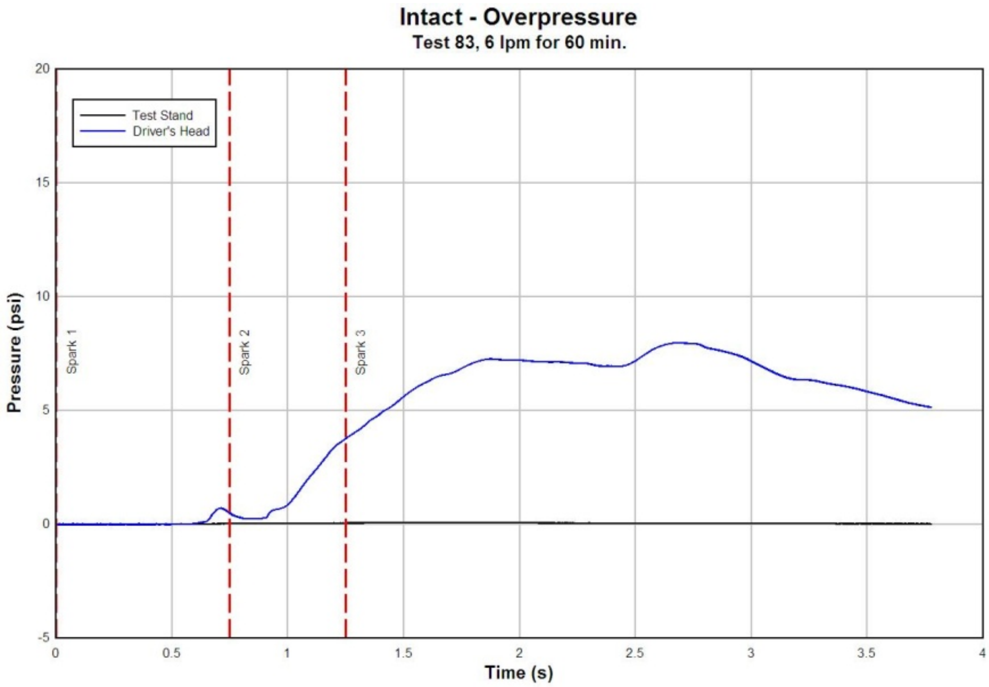

Figure III-26. Post-ignition overpressure data for 6 lpm leak into trunk of intact vehicle in Test 83.

Ignition originated in the vehicle headliner from Spark #1 in the vent hole near the hydrogen sensor. Damage consisted of the front driver door window frame being bent out slightly (about 0.25 in. at the top rear corner). This test also produced a secondary fire, to be discussed later.

Combustion effects observed in ignition Test 83 had somewhat different properties as compared to ignition Test 68. Inspection of the data revealed a *delay time* until thermal energy and overpressure were detected, indicating a *slow* hydrogen burn. Although peak pressures were comparable, the thermal output was drastically different. These differences can be attributed to the location and extent to which hydrogen accumulated differently in the vehicle.

This slowness of combustion and the evolution of its aftereffects were significant in regard to predictions on the extent of injury. Results for heat-flux-induced, burn-injury predictions, listed in Table III-5, indicated that the driver could experience first-degree burns, but no burn injury could be predicted for the nearby first responder (at the outside test stand location).

Table III-5. Prediction of skin burn injuries from heat flux in Test 83.

Thermal Injury (BURNSIM)			
Sensor Location	**Degree of Burn**	**Maximum Temperature (^oC)**	**Burn Threshold Depth (µm)**
Driver's Head	1st	69	50.3
Test Stand	None	34	0

Table III-6 presents the results for the potential injury to the eardrum of the driver. The eardrum injury potential in Test 63 was significantly less than that for Test 68, probably because the ear could compensate for pressure differential, given the much slower rate of pressure rise.

Table III-6. Prediction of ear injuries from overpressure in Test 83.

Overpressure Injury Prediction		
Sensor Location	**Peak Pressure (psi)**	**Eardrum Injury**
Driver's Head	8.0	≈ 20% Rupture
Test Stand	0.1	None

Tests 84-86. Ignition tests continued using the crashed vehicles. Visually knowing that seals had been compromised on the rear-impact vehicle, an initial hydrogen leak rate of 6 lpm, instead of 3 lpm, was selected in Test 84. Sparking did not result in an ignition. The leak rate then was doubled to 12 lpm in Test 85; again sparking did not result in ignition. The leak rate was doubled again to 24 lpm in Test 86. Upon sparking, an ignition occurred that can be described as a *mild thermal reaction*, manifested by a lazy blue flame (Figure III-27). The integrity of the vehicle was not compromised, i.e., seals did not fail, vehicle body had no physical damage, and windows remained intact. Figure III-28 shows that flammable levels of hydrogen were not detected by the sensors. However, low-level thermal and pressure pulses were measured, as shown in Figure III-29 and Figure III-30. Window fogging observed was a result of water vapor forming as the natural product of hydrogen combustion and condensing.

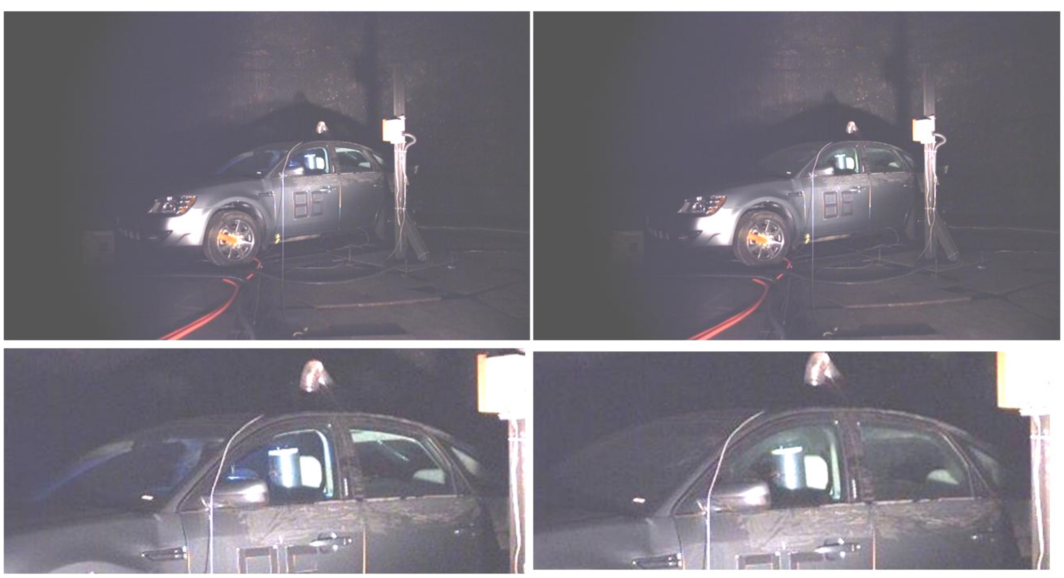

Figure III-27. High-speed imagery stills showing rear-impact vehicle at moment of first spark (top left, bottom left close-up at T = 0 sec) and window fogging (top right, bottom right close-up at T = 3 sec in Test 86.

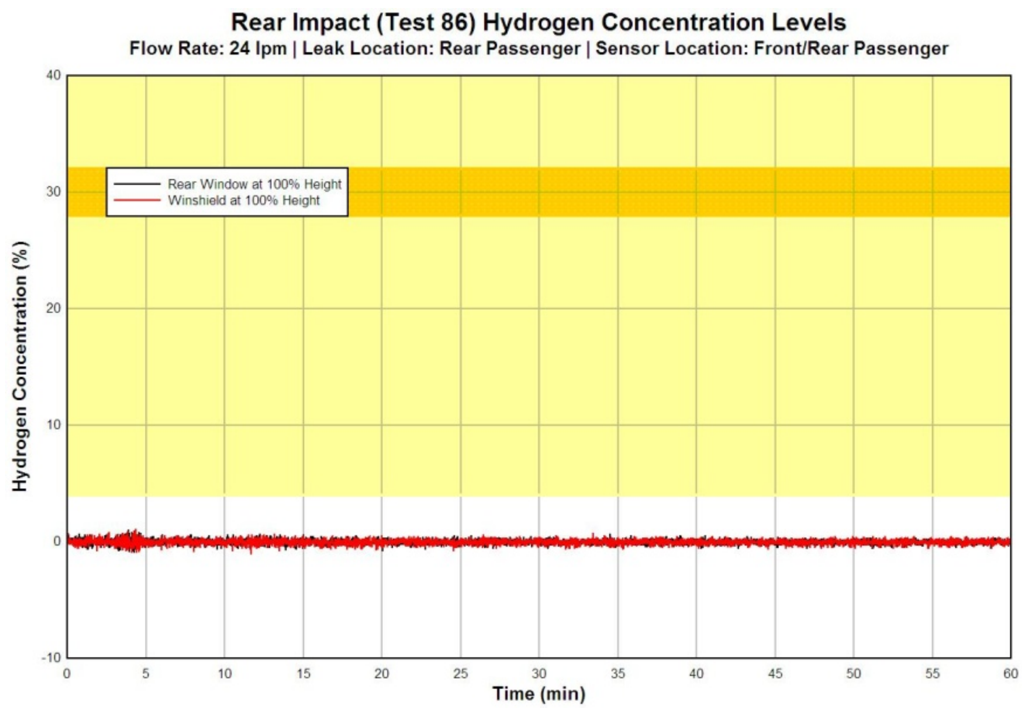

Figure III-28. Hydrogen accumulation data for 24 lpm leak into rear passenger compartment of rear-impact vehicle in Test 86.

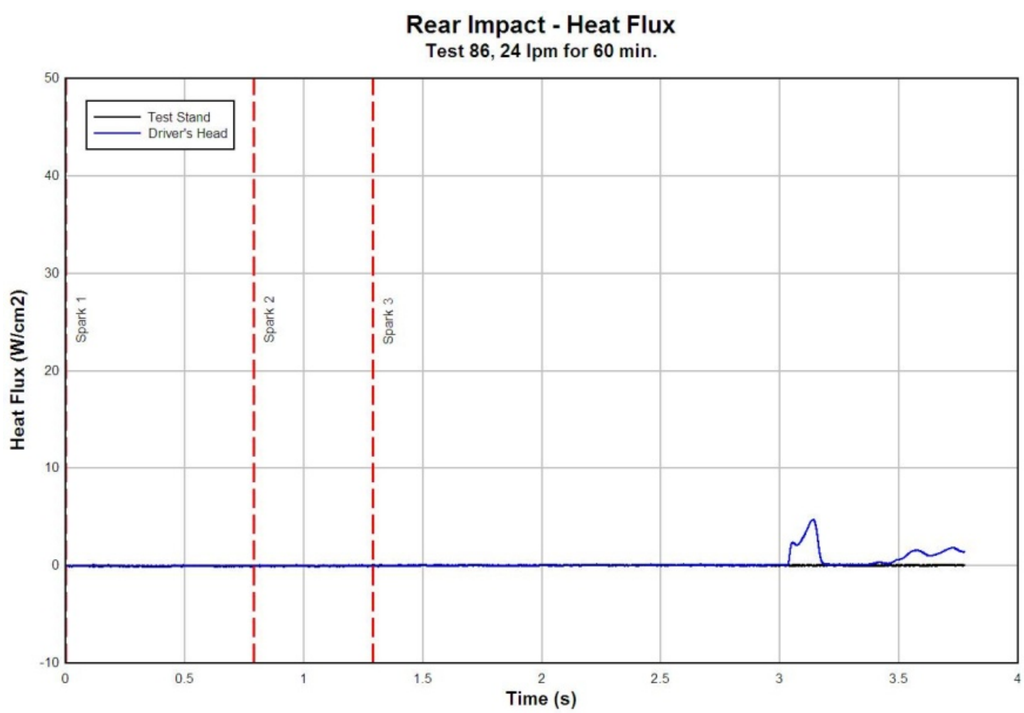

Figure III-29. Post-ignition heat flux data for 24 lpm leak into rear-passenger compartment of rear-impact vehicle in Test 86.

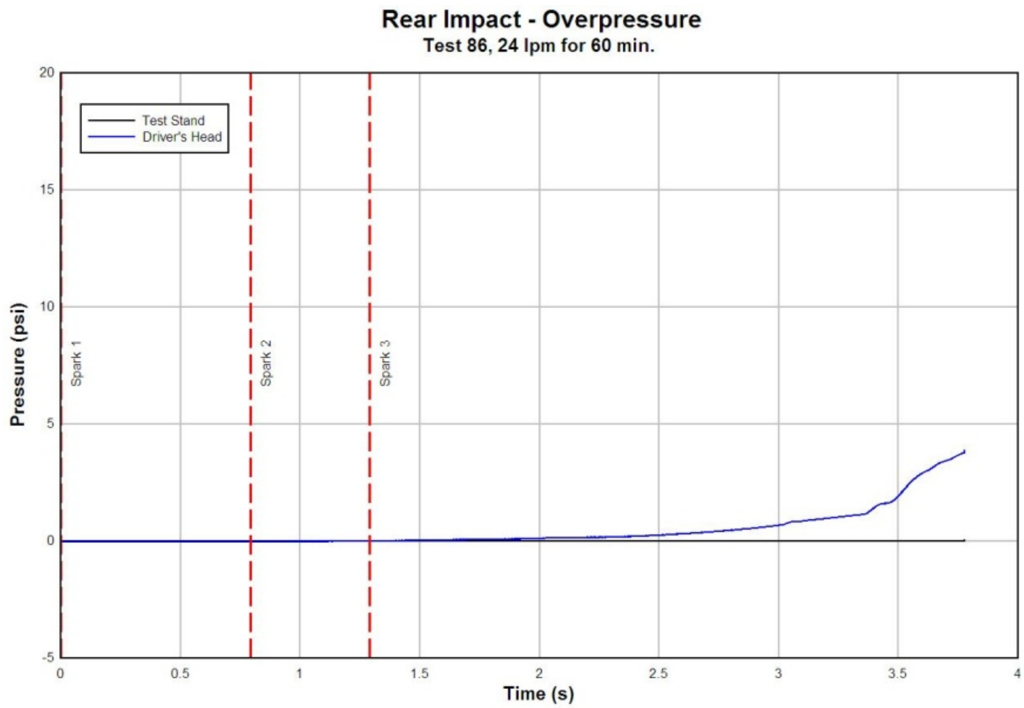

Figure III-30. Post-ignition overpressure data for 24 lpm leak into rear-passenger compartment of rear-impact vehicle in Test 86.

One other observation was that the aftereffects of ignition displayed a long induction time. Pressure was not detected until approximately 2 sec after sparking, but thermal energy was observed 3 sec after the first spark. Sensors were located 1 in. away from Spark Plugs 1 and 3. It was not evident which spark or sparks initiated the combustion event.

Results for the heat flux predictions, listed in Table III-7, indicated that no burn injury was predicted for either the vehicle driver or the first responder

Table III-7. Prediction of skin burn injuries from heat flux in Test 86.

Thermal Injury Prediction (BURNSIM)			
Sensor Location	**Degree of Burn**	**Maximum Temperature (^oC)**	**Burn Threshold Depth (µm)**
Driver's Head	None	47	0
Test Stand	None	34	0

Table III-8 presents the results for potential injury to the eardrum of the driver and first responder. Although peak pressure data were not captured because of the very long duration of the overpressure event (data acquisition system limitation), the even slower rise in pressure as compared to Test 83 (in which minimal or no ear injury was predicted), could suggest that no eardrum injury could have resulted from exposure to these overpressures.

Table III-8. Prediction of ear injuries from overpressure in Test 86.

Overpressure Injury Prediction		
Sensor Location	**Peak Pressure (psi)**	**Eardrum Injury**
Driver's Head	≥3.9	≥ 2% Rupture
Test Stand	0	None

Test 87. Because no visible damage occurred, the rear-impact vehicle was used in another ignition test, this time with the hydrogen flow doubled to 48 lpm. Upon sparking, a much more energetic combustion event was observed (Figure III-31) despite neither hydrogen sensor detecting measurable hydrogen (Figure III-32). The stills from high-speed imagery show the driver-side and rear-passenger doors bulging from the internal overpressure. Post-test visual inspection of the vehicle revealed that all four vehicle doors were bulged. The deformation at the top of the window frames was measured as ≈ 1–1.25 in. No secondary fire occurred. Heat flux and pressure effects were measured and are displayed in Figure III-33 and Figure III-34, respectively.

Figure III-31. High-speed imagery stills showing rear-impact vehicle at moment of first spark (top left at T = 0 sec); deformation of vehicle doors (top right at ~T = 0.28 sec); noticeable smoke accumulation (bottom left at ~T = 0.34 sec); and fireball inside vehicle (bottom right at ~T = 0.61 sec) in Test 87.

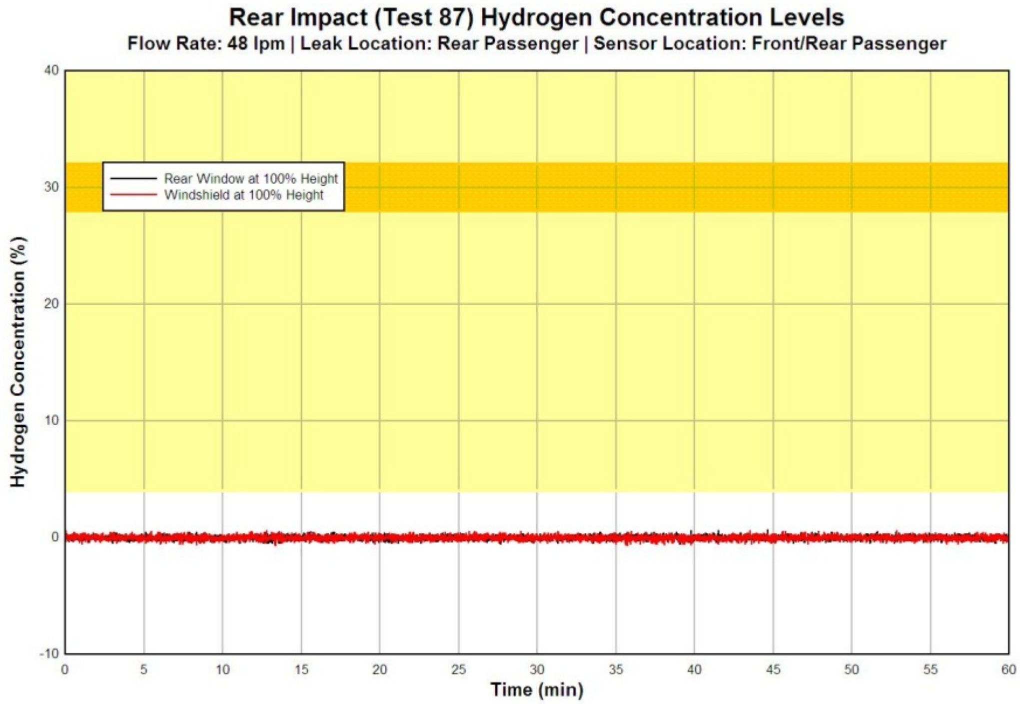

Figure III-32. Hydrogen accumulation data for 48 lpm leak into rear-passenger compartment of rear-impact vehicle in Test 87.

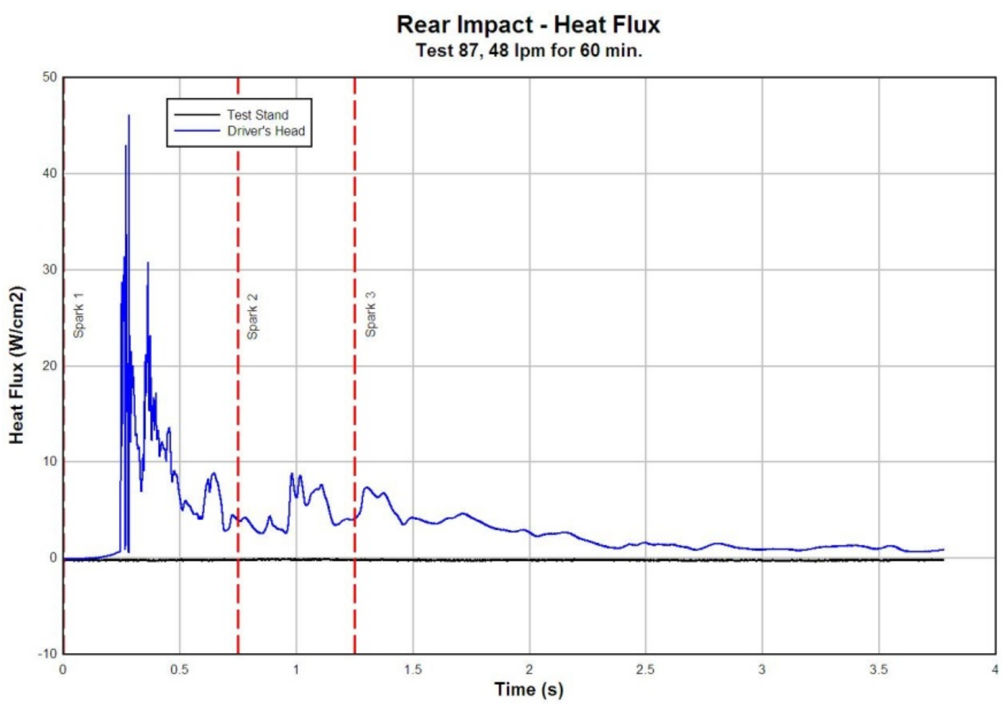

Figure III-33. Post-ignition heat flux data for 48 lpm leak into rear-passenger compartment of rear-impact vehicle in Test 87.

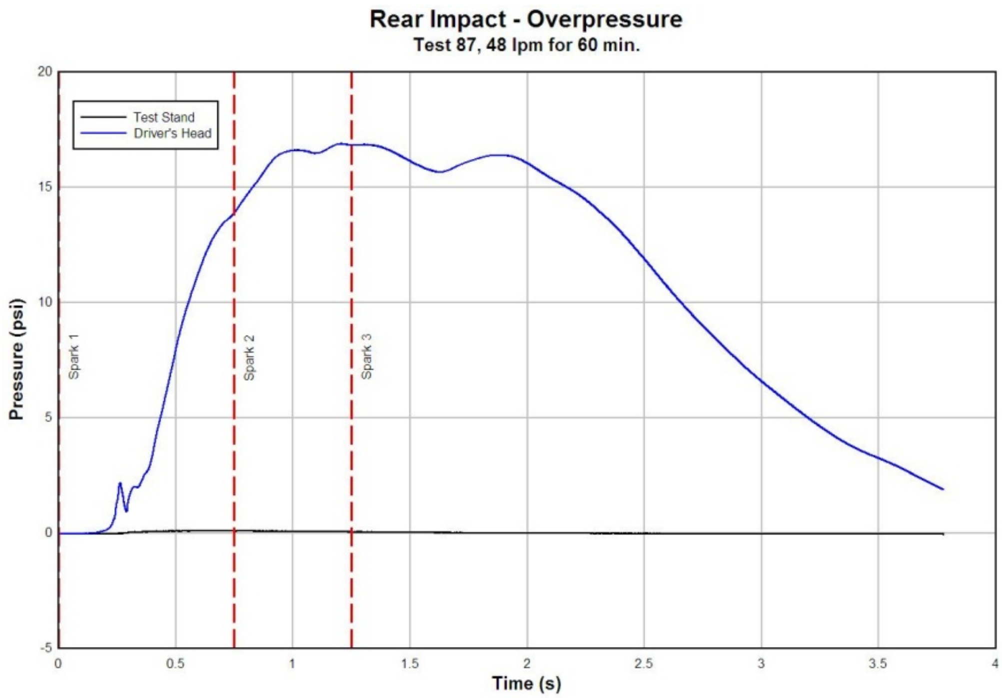

Figure III-34. Post-ignition overpressure data for 48 lpm leak into rear-passenger compartment of rear-impact vehicle in Test 87.

The induction time was much shorter than in Test 86 and Spark 1 clearly was the source. None of the window glass fractured even with the sustained overpressure above 15 psi. Results for the heat flux predictions, listed in Table III-9, indicate that second-degree burns could be predicted for the vehicle driver, but no burn injury was predicted for the first responder.

Table III-9. Prediction of skin burn injuries from heat flux in Test 87.

Thermal Injury (BURNSIM)			
Sensor Location	**Degree of Burn**	**Maximum Temperature (^{o}C)**	**Burn Threshold Depth (µm)**
Driver's Head	2nd	102	354.4
Test Stand	None	33	0

Table III-10 presents the results for potential injury to the eardrum of the vehicle driver and first responder. Some degree of eardrum rupture was expected for the driver because the rate of pressure rise and timeframe approach/exceed those at which an eardrum could not compensate. Again, no injury from overpressure was predicted at the first responder location.

Table III-10. Prediction of ear injuries from overpressure in Test 87.

Overpressure Injury Prediction		
Sensor Location	**Peak Pressure (psi)**	**Eardrum Injury**
Driver's Head	16.9	≈ 50% Rupture
Test Stand	0.1	None

Test 88. The final ignition test was conducted on the side-impact vehicle, which, by visual inspection, had the worst seal damage of all the vehicles. Thus, a leak rate of 60 lpm was selected as a starting point. Accumulation tests detected no flammable levels of hydrogen in the passenger compartment for trunk leaks as high as 236 lpm (Appendix J). To characterize better any hydrogen accumulation, sensors and spark plugs were repositioned along the driver side roof centerline line instead of the compartment centerline (Appendix I).

Upon sparking, ignition occurred. Analysis of the high-speed images (Figure III-35) showed displacement of the rear driver-side plastic window covering shortly after sparking, indicating that internal combustion of hydrogen had occurred. Blue flame was observed. Hydrogen accumulation, heat flux, and pressure data are displayed in Figure III-36 – Figure III-40, respectively. Figure III-36 reveals that a flammable level of hydrogen was detected at the sensor located approximately 0.5 in. forward of the first spark plug. This sensor was near the vehicle headliner in the gap because of the deformation of the damaged driver-side door. Accumulation tests on this vehicle, in which hydrogen sensors were located along the compartment centerline, detected no appreciable hydrogen levels, even at 236 lpm. These results suggested that hydrogen migrated rapidly and escaped through the gaps created as a result of impact.

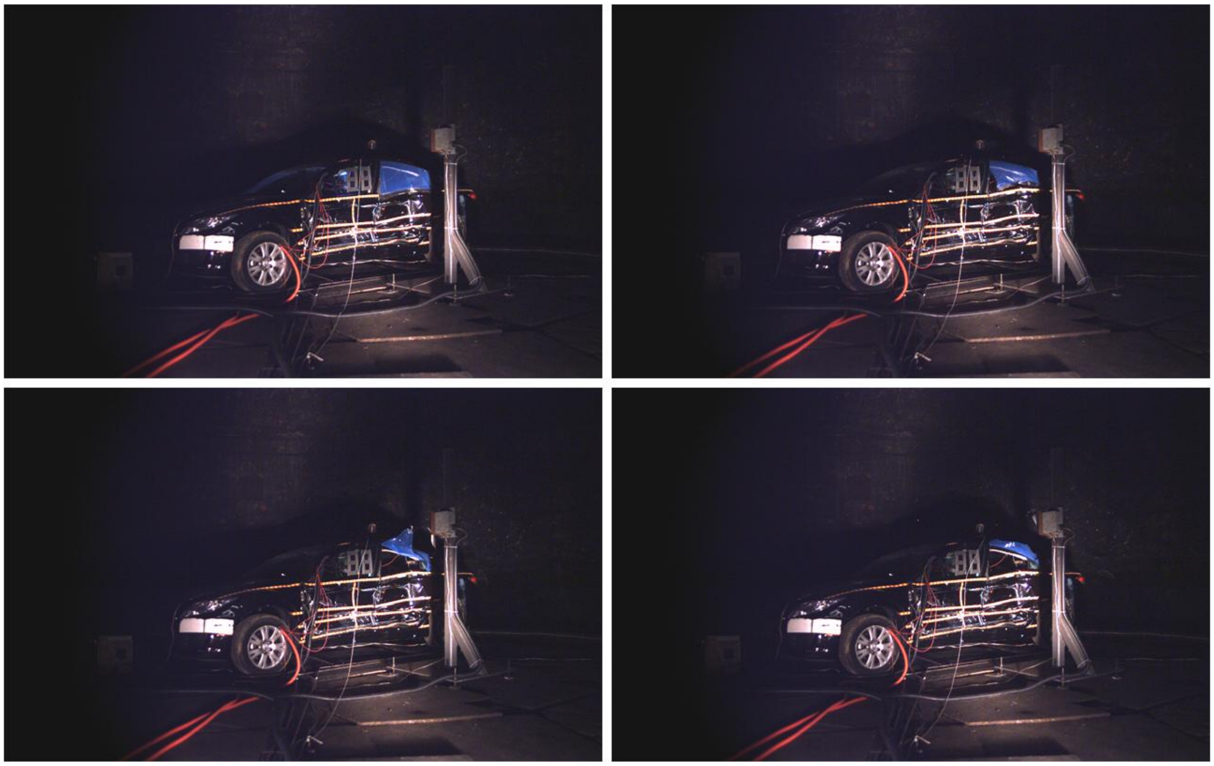

Figure III-35. High-speed imagery stills showing side-impact vehicle at moment of first spark (top left at T = 0 sec) and displacement of rear driver-side plastic window covering (top right at ~T = 0.58 sec, bottom left at ~T = 0 0.61 sec, and bottom right at ~T = 0.68 sec) in Test 88.

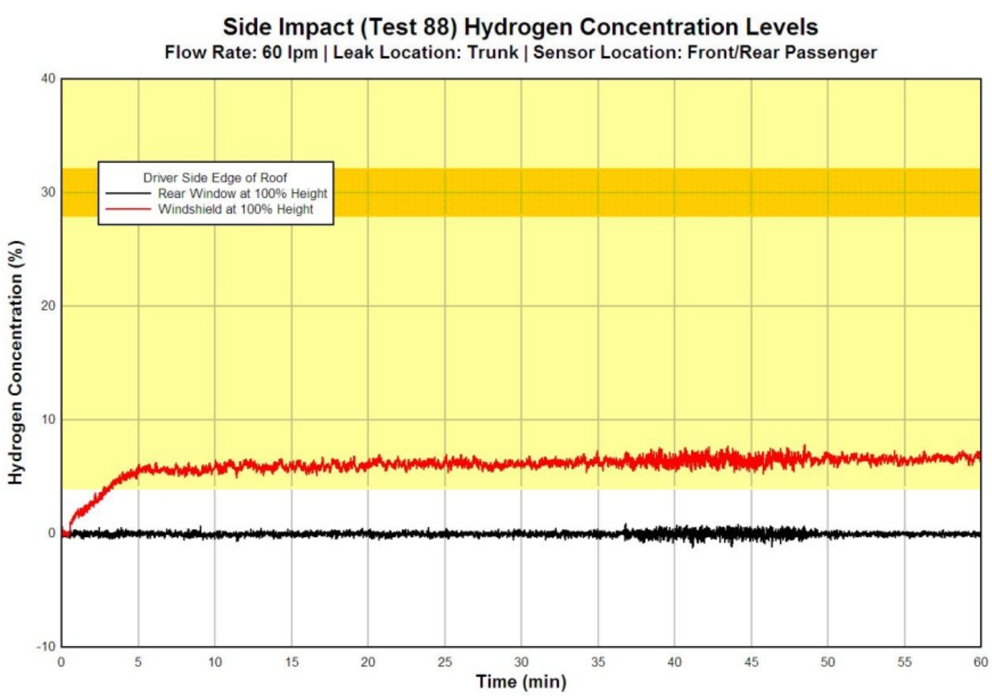

Figure III-36. Hydrogen accumulation data for 60 lpm leak into trunk of side-impact vehicle in Test 88.

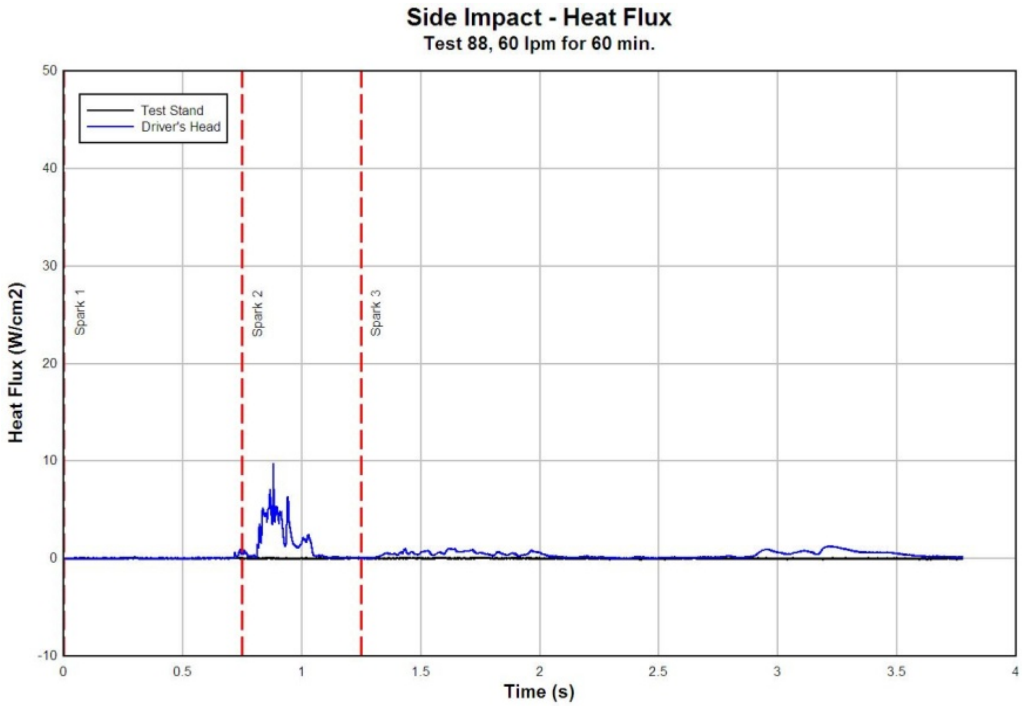

Figure III-37. Post-ignition heat flux data for 60 lpm leak into trunk of side-impact vehicle in Test 88.

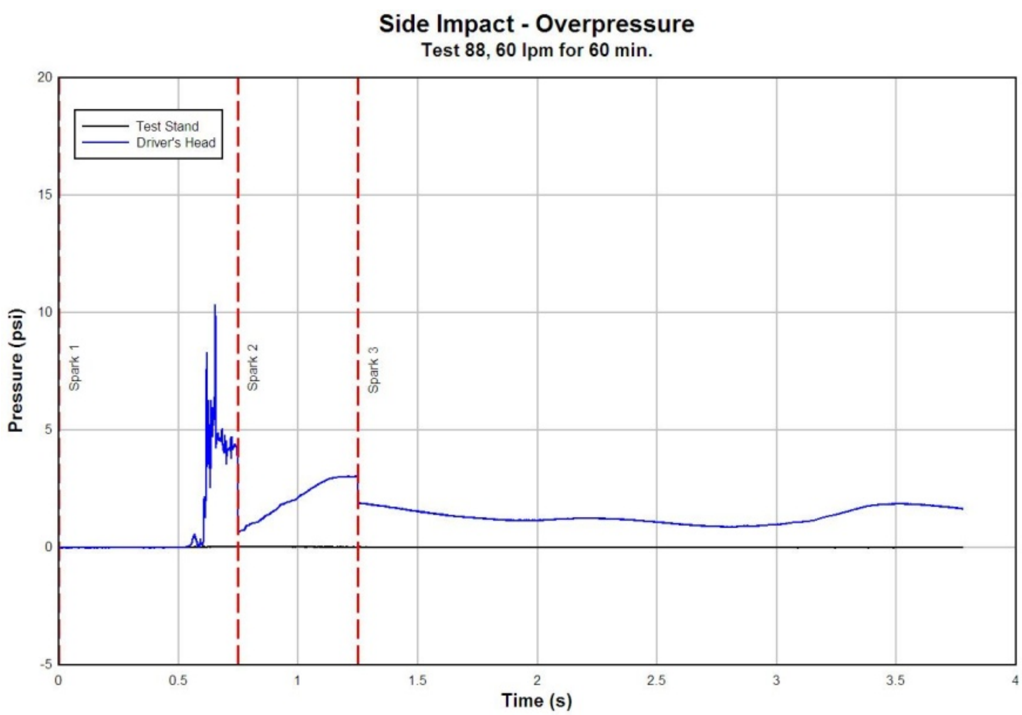

Figure III-38. Post-ignition overpressure data for 60 lpm leak into trunk of side-impact vehicle in Test 88.

Heat flux and pressure data showed relatively short induction times, with both appearing prior to activation of the second spark. The pressure generated by the event was only enough to cause displacement of the rear driver-side plastic sheet window covering.

One experimental artifact was that the pressure trace appeared electrically coupled to the second and third spark attempts (Figure III-38). The setup was the same as used in previous ignition tests; the source of the noise problem remains unknown.

Results for the heat flux predictions, listed in Table III-11, indicate that no burn injury was predicted for the vehicle driver or first responder.

Table III-11. Prediction of skin burn injuries from heat flux in Test 88.

Thermal Injury (BURNSIM)			
Sensor Location	**Degree of Burn**	**Maximum Temperature (^oC)**	**Burn Threshold Depth (µm)**
Driver's Head	None	50	0
Test Stand	None	33	0

The alteration in the pressure trace (Figure III-38), because of possible electrical interference from the spark discharge, did not mask the higher and more damaging overpressures at times later in the combustion event. This pressure behavior was consistent with the pressure being vented as it was being generated, indicative of open vent area. This vent area could have been created by the impact.

Table III-12 presents the prediction for potential injury to the eardrum of the vehicle driver and first responder. In Test 88, although the peak pressure was not as high as in Test 87, its rise time was shorter. Because of these offsetting properties, exposure to the conditions in Test 88 could be predicted to cause about the same degree of ear rupture potential as in Test 87, ≈ 50 percent eardrum rupture to the driver and none for the first responder.

Table III-12. Prediction of ear injuries from overpressure in Test 88.

Overpressure Injury Prediction		
Sensor Location	**Peak Pressure (psi)**	**Eardrum Injury**
Driver's Head	10.4	≈ 30% Rupture
Test Stand	0.1	None

Task 2c Ignition Test Results: Secondary Fires.
As Table III-2 listed, *secondary fires* occurred in three of five ignition tests (Tests 68, 83, and 88). The first ignition, Test 68, was unexpected. As a result, Tests 83 and 88 were conducted differently.

After ignition was observed in Tests 83 and 88, a 20-min waiting period was exercised before the hydrogen exhaust system was activated. Activation of this exhaust system coincided with the secondary fire in Test 68. Delaying this step could reveal if a secondary fire could occur under quiescent conditions. The main chamber exhaust also was activated after an additional 20 min wait to confirm that its action did not influence the propensity for a secondary fire.

As will be detailed, the secondary fires were different in nature, likely because of the individual vehicle pretest condition, severity of the ignition event, and post-ignition event condition. These hydrogen-ignition induced fires were difficult to extinguish after flames were observed. Only one secondary fire was extinguished before the entire inside of the vehicle was consumed and destroyed.

Test 68 Secondary Fire. Figure III-39 shows the timeline of events. After ignition and the chamber had been exhausted, the vehicle was inspected visually to check for damage and fire potential. At that time, the observations were that: (1) no glowing embers or smoke appeared anywhere inside the vehicle, (2) the rear seat back was forced forward against the backs of the front seats, (3) the headliner was torn loose, and (4) the trunk lid was forced open. Direct viewing into the trunk was possible, and it was noted that the trunk carpet was formed around the spare tire. The floor of the trunk is comprised of hardboard with a carpet cover that rests on the top of the spare tire. Apparently, the pressure pulse from the ignition fractured the hardboard spanning the gap between the spare tire and vehicle structure, forcing carpet into the gap. No embers or smoke were noted at the time of vehicle inspection (4+ min); fire appears to have started in this general area. The secondary fire spread fast throughout the passenger compartment and was very intense.

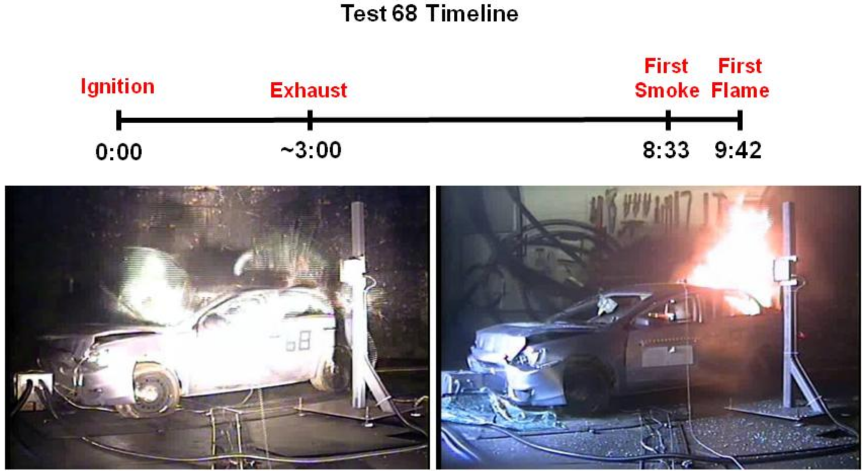

Figure III-39. Timeline of events after ignition (left) and secondary fire (right) in Test 68.

Two 15-pound carbon dioxide fire extinguishers were used to extinguish the fire. Preplumbed nozzles, one on the dashboard and one in the trunk aimed directly across the top of the spare tire, were insufficient. The fire totally consumed the car including all instrumentation (Figure III-40).

Figure III-40. Damage to front-impact vehicle after secondary fire burned to completion in Test 68.

Test 83 Secondary Fire. Figure III-41 shows the timeline of events. In Test 83, the possibility of a secondary fire was anticipated. No fire was observed during the first 20 min wait period after ignition although smoke was generated nearly the entire time. First flame was observed shortly after the hydrogen exhaust system was activated, probably caused by the forced ventilation of air around and inside the vehicle.

The fire was small and appeared near the front edge of the headliner, directly above the front passenger seat. This smaller (than Test 68) secondary fire was extinguished with a Halotron fire suppression system (no endorsement implied). Scorching was noted above the headliner in the vent hole. A relatively large area on the top side of the headliner must have been burning given the amount of smoke produced during the wait period (Figure III-42).

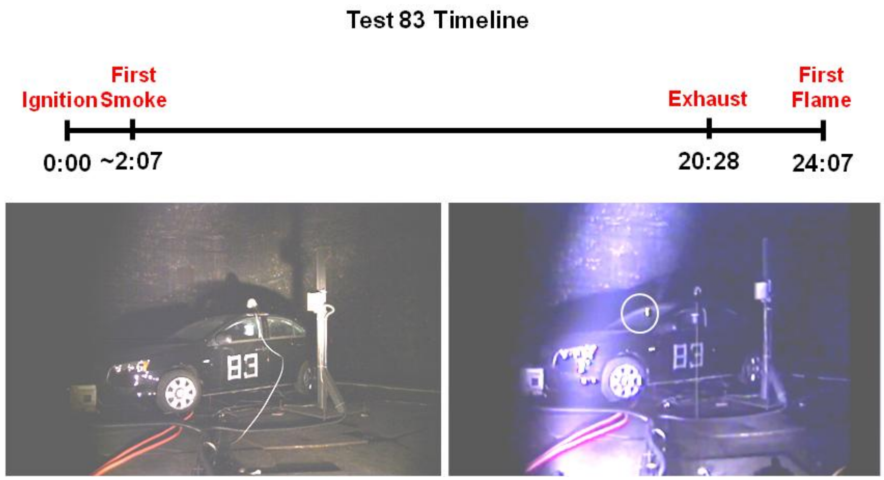

Figure III-41. Timeline of events after ignition (left) and secondary fire (right; circled) in Test 83.

Figure III-42. Damage to headliner above front-passenger seat after secondary fire was extinguished in Test 83.

Test 88 Secondary Fire. Figure III-43 shows the timeline of events. First smoke was observed about 5.5 min after ignition. First flame was observed in the rear seat area and then at the driver-side rear light cluster. Thick smoke was also evident, assumed to be from the spare tire. The smoke in the video gives the impression that the origin also could have been the passenger-side rear tire.

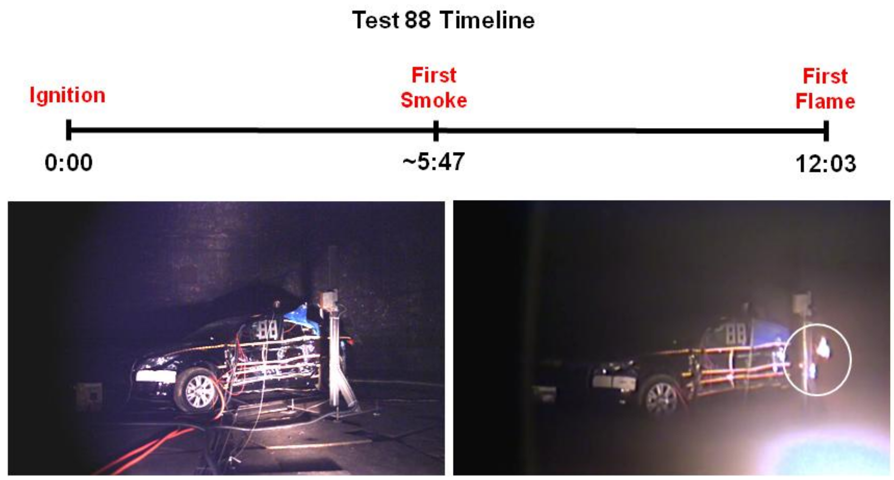

Figure III-43. Timeline of events after ignition (left) and secondary fire (right; circled) in Test 88.

Two 15-pound Halotron fire extinguishers were used to extinguish the fire. Preplumbed nozzles, one on the dashboard and one in the trunk aimed directly across the top of the spare tire, were insufficient to extinguish the fire, which consumed the interior of the car, including all instrumentation (Figure III-44).

Figure III-44. Damage to front-impact vehicle after secondary fire burned to completion in Test 88.

Based on these results, it is recommended that future tests involving the ignition of hydrogen in vehicles include a fire suppression system that can deploy aqueous foam rapidly to fill the entire vehicle. Although this foam possibly could damage sensors and instrumentation, extinguishing the fire could save ancillary test equipment from worst damage (i.e., hydrogen exhaust system and static dissipative matting).

SUMMARY

The objective of Task Order 3, *Post-Crash Hydrogen Leakage Limits and Fire Safety Research*, was to conduct research on the fire safety of proposed hydrogen leakage limits, including calculations and experimental verification. This assessment provides technical data that correlate hydrogen fuel system leak rates to the accumulation of ignitable mixtures of hydrogen in trunk, passenger and engine enclosed compartments and quantifies hydrogen combustion effects, including the potential for personal injury. Tasks conducted under Task Order 3 were:

Task 2a: Leak Rate Versus Hydrogen Concentration Tests on Intact Automobile;
Task 2b: Ignition and Combustion Tests on Simulated Automobile Compartments; and
Task 2c: Full-Scale Leak, Ignition, and Fire Tests on Intact and Crashed Automobiles.

This report describes progress on Task 2c, the objectives of which were to quantify the effects of crash damage on hydrogen accumulation and hydrogen combustion characteristics for three leak parameters (location, rate, and duration); relate them to the extent of personal injury (physical trauma and burns); and assess the establishment of a minimum allowable post-crash hydrogen leak rate. Task 2c tests were conducted on four vehicles: intact and front-impact 2008 Mitsubishi Lancers, side-impact 2009 Mazda6 Sedan, and rear-impact 2008 Ford Taurus.

Altogether, 39 leak-accumulation tests were completed on four vehicles at seven leak rates (3, 6, 15, 30, 59, 118, or 236 liters per min, lpm) over 60 minutes (min) originating from three locations (trunk or rear-passenger compartment, or underneath the vehicle) using up to 12 hydrogen sensors (Neodym Panterra, 0-100%) in three arrays at four positions (10%, 50%, 90%, and/or 100% compartment height). Hydrogen sensor performance was verified via calibration.

Observations from accumulation tests on the front-crashed vehicle were: (1) leaks as low as 30 lpm in trunk or passenger compartment resulted in detectable flammable levels in the other compartment; (2) leaks as high as 236 lpm underneath the vehicle did not result in detectable accumulation inside the vehicle; and (3) low leak rates resulted in random (inversions; local pockets), but sometimes detectably flammable, levels of hydrogen.

Observations from accumulation tests on the side-crashed vehicle were: (1) leaks ≥59 lpm in the passenger compartment resulted in detectable flammable levels, but leaks as high as 236 lpm in the trunk did not result in detectable flammable atmospheres in the passenger compartment; (2) leaks underneath the vehicle (near door seals) as high as 236 lpm did not result in detectable accumulation inside the vehicle; and (3) even with high leak rates, accumulations sometimes appeared random and elusive with respect to migrating to the highest locations.

Observations from accumulation tests on the rear-crashed vehicle were: (1) leaks as low as 30 pm in the rear-passenger compartment resulted in detectable flammable levels much lower than those in intact or front-crashed cars; (2) leaks as high as 236 lpm underneath the vehicle did not result in detectable accumulation inside; and (3) leaks originating in passenger and trunk compartments resulted in somewhat random accumulations, all of which were flammable.

Overall observations from Task 2c hydrogen accumulation tests were: (1) at low leak rates (≤60 pm), hydrogen did not mix well in air, resulting in its concentrations being random,

exhibiting characteristics similar to a lava lamp in which slow motion causes media of different densities to remain unmixed, pocketing locally, varying and moving in random fashion, inverting where higher-sensor locations register lower concentrations than do lower-sensors locations, or being absent at highest locations; (2) at high leak rates (≥118 lpm), hydrogen mixes more homogenously, resulting in more stratified levels, increasing more uniformly throughout the vehicle, being detectable nearest the leak source first, generally seeking higher elevations, and reaching more uniform, steady-state concentrations with time; and (3) door, window, and frame seals in front or rear-impact vehicles were not compromised to the extent of allowing hydrogen from leaks underneath to accumulate inside the vehicle.

Altogether, eight ignition tests were conducted on the intact or front-, rear-, or side-impact vehicles. Two types of ignition tests were conducted: (1) at the in-going potential standard leak rate of 118 lpm for a duration of 1.5 min, which introduced a just-flammable ~5 percent hydrogen inside the car if distributed evenly; and (2) at the lowest leak rate experimentally possible (3 lpm) over 60 min, which resulted in accumulated hydrogen (~5%) that could be ignited by sparking at the top of the passenger compartment (leaking 3 lpm for 60 min was near-equivalent to the volume of hydrogen leaking at 118 lpm for 1.5 min).

With regard to achieving the objective of determining a *minimum allowable post-crash leak rate*, tests indicated that leak rate is not defining metric. Instead, the critical information was whether hydrogen, if allowed to leak into a car compartment, could accumulate anywhere *locally* to ~5 percent, just above the lower flammability limit of hydrogen (~4%). Tests indicated that flammable concentrations of hydrogen could accumulate in different locations within passenger compartments, either at low leak rates after long times or at high leak rates after short times.

Fire effects varied in terms of peak thermal flux, overpressure, and internal vehicular damage. Aftereffects ranged from window fogging (condensation from hydrogen combustion) to structural damage (deformed doors, broken windows) to second-degree burns and eardrum rupture.

One additional significant finding was a propensity for secondary fire after sparking and hydrogen ignition, which was replicated. These secondary fires, that consumed flammable material inside the vehicles, occurred in the intact and front and side-impact cars. The origin of these secondary fires, that erupted within minutes after initial sparking and severely damaged the vehicles, appeared to be flammable material inside the trunk (spare tire) or cabin (headliner).

OBSERVATIONS

Significant overall observations and recommendations from Task 2c tests were as follows:

- All accumulation of hydrogen should be avoided in passenger compartments.
- More than one sensor in various locations is needed for passenger-alarm purposes.
- Vehicle devices that vent passenger compartments upon impact may be warranted.
- New flammability tests on fabrics exposed to hydrogen (not air) have merit.
- On-board vehicle fire-suppression systems could be revisited.

REFERENCES

1. Battelle Memorial Institute. (2009, April). *Leak Rate vs. Hydrogen Concentration Tests on an Intact Vehicle*. Test Report Task 2a for National Highway Traffic Safety Administration.

2. Battelle Memorial Institute. (2009, August). *Ignition and Combustion Tests on Simulated Automobile Compartments*. Test Report Task 2b for National Highway Traffic Safety Administration.

3. Battelle Memorial Institute. (2010, April). *Full-Scale Leak, Ignition, and Fire Tests on Intact and Crashed Vehicles*. Test Report Task 2c for National Highway Traffic Safety Administration.

4. Maeda, Y., Takahashi, M., Tamura, Y., Suzuki, J., & Watanabe, S. (2006). *Test Vehicle Ignition Due to Hydrogen Leakage.* SAE Technical Paper Series 2006-01-0126. SAE 2006 World Congress & Exhibition, April 3, 2006, Detroit, Michigan.

5. Maeda, Y., Itoi, H., Tamura, Y., Suzuki, J., & Watanabe, S. 2007). *Diffusion and Ignition Behavior on the Assumption of Hydrogen Leakage from a Hydrogen-Fueled Vehicle*. SAE Technical Paper Series 2007-01-0428. SAE World Congress & Exhibition, April 16, 2007, Detroit, Michigan.

6. Knox, T., Mosher, S., & McFall, M. (2008, August). BURNSIM Version 3.0.2 USER Guide. (Document Number WPAFB88ABW-2009-0309). Bonney Lake, WA: BlastZone Technology Services.

7. Kuchta, J. M. (1985). *Investigation of Fire and Explosion Accidents in the Chemical, Mining, and Fuel-Related Industries-A Manual*. Bulletin 680. Washington, DC: Bureau of Mines. Available at www2.galcit.caltech.edu/EDL/public/flammability/USBM-680.pdf

8. Altman, J. (2001). *Acoustic Weapons-A Prospective Assessment*. In Science and Global Security: The Technical Basis for Arms Control, Disarmamanet, and Nonproliferation Initiatives, Volume 9, pp. 165-234. Princeton, NJ: Princeton University.

9. Breitung, W., Necker, G., B. Kaup, B., & Veser, A. (2001). Numerical Simulation of Hydrogen Release in a Private Garage. *Proceedings of Hypothesis IV*, p. 368-377.

10. Hirsch, F. (1968). Effects of Overpressure on the Ear - A Review. *Annals of the New York Academy of Sciences, 152*. No. 1. p. 147-162.

DOT HS 811 816
October 2013

U.S. Department
of Transportation
National Highway
Traffic Safety
Administration

NHTSA
www.nhtsa.gov

9047-102213-v3